332-8
P567

U.S. DEPT. OF AGRICULTURE
LIBRARY
SEP 12 1962
RECORDS

SPSE

Photographic SCIENCE AND ENGINEERING

Some Characteristics of Panoramic Cameras for Aerial Surveillance
K. G. Leistner and D. P. Paris 257

Circuit for Adjusting Automatic Color Printer Response • *R. K. Rickard* 263

Film Response as a Function of Exposure • *Frank Scott and M. D. Rosenau, Jr.* 266

A Quantitative Study of the Influence of Tone-Reproduction Factors on Picture Quality • *J. L. Simonds* 270

On the Spatial Stability of Photographic Plates • *J. H. Altman and R. C. Ball* 278

Nomenclature for Fourier Transforms of Spread Functions • *Erik Ingelstam* 282

The Adsorption of Development-Restrainers to Silver and Their Effects on Physical Development • *R. J. Newmiller and R. B. Pontius* 283

Test Methods for Rating Abrasion Resistance of Photographic Film
J. F. Carroll and J. O. Paul 288

Dependence of Covering Power and Spectral Absorption of Developed Silver on Temperature and Composition of the Developer • *T. H. James and L. J. Fortmiller* 297

Effect of Development Temperature on Covering Power of a Developed Silver Image • *D. A. Nepela* 305

Short Communication: Rapid Processor for the KA-30 Camera • *J. S. Goldhammer* 311

Short Communication: The Camera Calibrator, Model III • *G. T. McNeil* 312

Book and Journal Reviews 315

New Products and Developments • *Frank Smith* 319

SPSE Journal Award • *Citation* 277

Coming Technical and Scientific Meetings 296

Volume 5 • Number 5

SEPTEMBER-OCTOBER • 1961

Editorial Policy

Photographic Science and Engineering is dedicated to the advancement of the knowledge and application of photography and other directly related sciences. Its pages are open to all who wish to report on new studies dealing with the theory of photosensitive systems, the design of photographic instruments and apparatus useful in the treatment of photographic materials, photographic optics and illuminants, the use of photography for scientific or engineering measurement or recording, and photographic instrumentation and data recording. Only original papers should be submitted except on special invitation.

Manuscripts should be typed double-spaced on white bond paper with 1½-inch margins all around. Literature references should be exact, and should include titles of journals, names of authors, numbers of volumes and pages, and year of publication. Book references should include title of volume, names of authors, publisher, number of edition, year of publication, and chapter and pages cited.

Graphs, charts, and other line illustrations should conform to good usage such as given in the American Standards Association Document Y-15, "A Guide for Preparing Technical Illustrations for Publication and Projection." Continuous-tone photographs should be made on 8 by 10-inch glossy paper and should show pertinent image detail sufficiently clearly to permit reduction to fit a 3-inch column in this journal. All illustrations should be numbered in soft blue pencil on the back to correspond with captions typed on a separate page. Tables should also be submitted on separate pages appropriately identified. An abstract should accompany each manuscript.

Papers intended for publication (two copies) and books for review should be submitted to the editor, T. H. James, Research Laboratories, Eastman Kodak Co., Rochester 4, N.Y. Correspondence regarding proofs and reprints should be directed to Jennie H. Allen, 94 Hastings Ave., Croton-on-Hudson, N.Y. All papers submitted for publication will be reviewed by members of the Editorial Review Board and if not accepted will be returned to the author. Published papers become the property of the Society and are protected by appropriate copyrights. Each author receives one copy of the issue in which his contribution appears. Authors may order reprints of their papers at the time they return the galley proofs. The Society does not assume responsibility for material in transit, nor guarantee publication of unsolicited material.

Photographic
SCIENCE AND ENGINEERING

official publication of the
Society of Photographic Scientists and Engineers

SEPTEMBER-OCTOBER 1961

Volume 5, Number 5

EDITORIAL STAFF

T. H. James, *Editor*
Jennie H. Allen, *Managing Editor*
H. F. Nitka, *Associate Editor*
Norman A. Exley, *Assistant Editor*
S. C. Goddard, *Feature Editor*
Frank Smith, *Feature Editor*

EDITORIAL REVIEW BOARD

J. H. Altman	K. G. Leistner
R. S. Barrows	Marilyn Levy
Richard L. Bent	C. S. McCamy
Fordyce M. Brown	J. A. Maurer
B. R. Harriman	F. W. H. Mueller
John H. Jacobs	W. S. Shoemaker
R. Clark Jones	Thos. D. Smith
Peter Krause	William West
John H. Ladd	Deane R. White

Photographic Science and Engineering is published six times a year by the Society of Photographic Scientists and Engineers.

• Address remittances, orders for subscriptions and for single copies, claims for missing numbers, and notices of change of address to the Society at Box 1609, Main Post Office, Washington, D.C. Subscription to nonmembers of the Society, $12.00 per year; subscription cost to members included in $10.00 annual dues; single copies, $2.00 each.

• The publication office is at 20th and Northampton Streets, Easton, Pa. Second-class mail privileges authorized at Easton, Pa. This publication is authorized to be mailed at the special rates of postage prescribed by Section 132.122.

• The Society is not responsible for the accuracy of statements made by authors and does not necessarily subscribe to their views.

© Copyright 1961 by the Society of Photographic Scientists and Engineers, Inc. Permission to reprint any part of the contents, except in reviews and abstracts, must be obtained in writing from the Editorial Vice President.

SPSE

RING

of the
raphic
ineers

1961
ber 5

Editor
Editor
Editor
Editor
Editor
Editor

ARD
eistner
n Levy
Camy
Maurer
Mueller
maker
Smith
n West
White

ering is
by the
sts and

or sub-
claims
ices of
at Box
hington,
bers of
ubscrip-
$10.00
0 each.
0th and
. Sec-
ized at
thorized
ates of
32.122.
for the
authors
tribe to

ciety of
eers, Inc.
of the
bstracts,
rom the

PHOTOGRAPHIC SCIENCE AND ENGINEERING
Volume 5, Number 5, September-October 1961

Some Characteristics of Panoramic Cameras for Aerial Surveillance

KARL G. LEISTNER AND DIETER P. PARIS,* *U.S. Army Signal Research and Development Laboratory, Fort Monmouth, N.J.*

Similarities and differences between modern panoramic cameras for aerial photography and the stationary panoramic cameras of old are discussed, and advantages of panoramic systems over wide-angle- and multiple-camera arrangements are pointed out. Images taken by panoramic cameras from airplanes are not geometrically similar to the objects they depict. Some of the deformations inherent in panoramic photography from the air are described, and proof is given that they cannot be avoided.

Panoramic cameras had quite an appreciable market in the amateur field up to the late Twenties, and then disappeared almost completely. Interest in this type of camera has been revived in recent years because of a new and important application in aerial photography. For this application the camera had to be refined, and a number of features had to be added, but the basic design is still the same as that shown in Fig. 1, which is a reproduction from the oldest patent found in the literature.[1] A lens rotates around its rear nodal point, and the film is held in an arc, the radius of which equals the focal length of the lens. In a different embodiment, also dating back to the Nineties,[2] the film moves in a plane behind a slit, in synchronism with the movement of the optical image. The image moves in this case because the whole camera body rotates around an axis.

The differences in the modes of operation between old and new cameras required new developments and modifications of this basic design. Briefly, these changes are as follows:

The optical axis of the old panoramic cameras swung in a mostly horizontal plane. The camera position was fixed. A trace of the optical axis on a distant object plane was a horizontal line. Objects were located in a large range of distances from infinity to very close, all around the camera, and all objects located on concentric circles around the camera station were imaged at the same scale. An observer, looking at a print of this panoramic picture (especially if he bends it in an arc), receives an impression essentially equivalent to that which he would get if he were looking around from a position at the camera station.

Present-day panoramic cameras are used in fast-moving airborne vehicles. The swing axis of the lens is essentially horizontal and parallel to the line of flight. The optical axis of the lens swings through barely more than 180°, and the surface which the axis generates during each swing is not a plane, but a rather complex form. The objects are located on an essentially horizontal plane, and the trace of the optical axis of this plane is not a straight line. The object distance changes continuously during each sweep of the lens; therefore, the image scale is also changing continuously. The impression which an observer gets looking at a print is different from the one he receives if he is in an airplane and looking from horizon to horizon. This seems surprising, because the same laws of optics and perspective apply to vision and to photography. But when an observer looks from an airplane, he interprets by an automatic mental process the signals from the eye nerves, and his mind perceives the object plane as a plane. Looking at a print, the observer lacks the stimulus which turns on this interpretation process, and he gets the impression that the objects are located on a cylindrical surface. To make full use of these pictures, a panoramic image rectifier is frequently needed, an auxiliary device which was never used with the old cameras. Image motion compensation (IMC) is another very important capability which has had to be devised for the airborne camera and which was not needed in its predecessor.

Advantages of Panoramic Cameras

Before analyzing some of the aforementioned characteristics, it seems worth discussing briefly the arguments in favor of a panoramic camera as compared to a wide-angle camera or an array of wide-angle cameras such as that known as the "Tri-Metrogon" arrangement. It is mainly the freedom in choice of focal length and aperture of the lens which gives the panoramic design its advantage. Wide-angle lenses have been made to cover almost

Presented at the Annual Conference, Binghamton, N.Y., 24 May 1961. Received 22 May 1961.

* Present address: Dieter P. Paris, Boeing Airplane Co., Seattle, Wash.

1. German pat. 55,660 (21 March 1891).
2. German pat. 56,515 (12 May 1891).

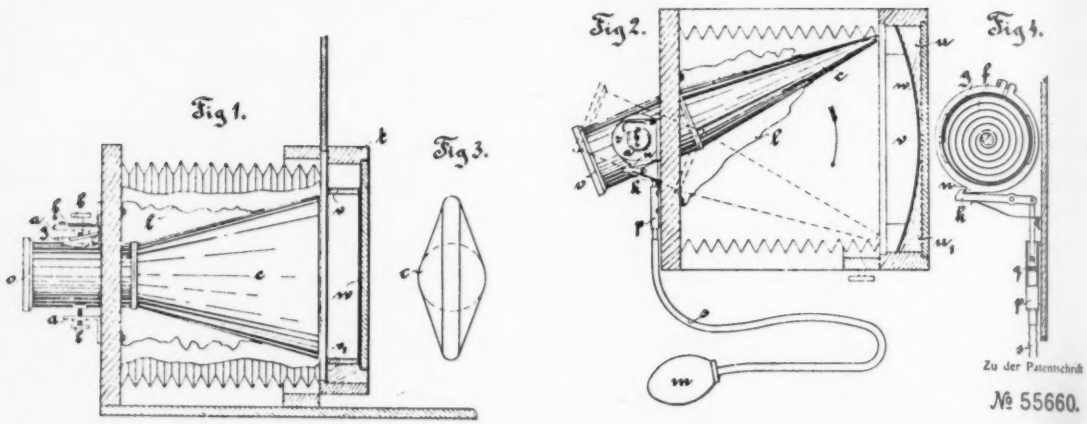

Fig. 1. Basic design of panoramic camera with swinging lens cone and stationary film. From German patent No. 55,660, dated 21 March 1891.

180°, but their relative aperture is very small, and for a given format size of the film the focal length must of necessity be very short. The image scale, therefore, will be too small for useful reconnaissance photography. Wide-angle lenses, covering up to about 120° field angle, can be made free of distortion, i.e., can have the same image scale everywhere in the field of view, but lenses of larger field angles will have large amounts of distortion, and this distortion probably will not follow as simple a law as that applicable to panoramic pictures. Rectification equipment for such wide-angle pictures requires lenses which match the distortion characteristics of the camera lens. With a panoramic camera, any lens covering at least the width of the film strip can be used.

Another advantage of the panoramic system, not very important perhaps, is a saving of film. For a given half-angle of view, the film used in a wide-angle camera is proportional to the tangent of this angle; that in a panoramic camera is proportional to the arc.

The "Tri-Metrogon" arrangement, where one camera axis is vertical and those of the adjacent cameras are inclined, also can cover a large angle across the flight line. For example, if the oblique cameras are inclined 33° against the vertical, the angle is 140°. In a wide-angle fixed-lens oblique camera, the film must move at an average IMC rate, correct only for a narrow strip of film. In the panoramic camera, however, the IMC rate at each angular position of the swinging lens axis can be adjusted to the image motion prevailing at this angle.

Dissimilarity between Object and Image

The characteristics, pointed out above as peculiar to the operation of a panoramic camera from an airplane, make it fairly obvious that true geometric similarity between image and object cannot be expected. A complete analysis of the object/image relationship, and of the factors limiting the resolution of a panoramic camera, is beyond the scope of this paper. Only the most fundamental relations will be mentioned, as a basis for the discussion of a distortion, the existence of which apparently is not generally realized.

Figure 2 shows the geometry of object, lens, and image, at an instant during which the camera is

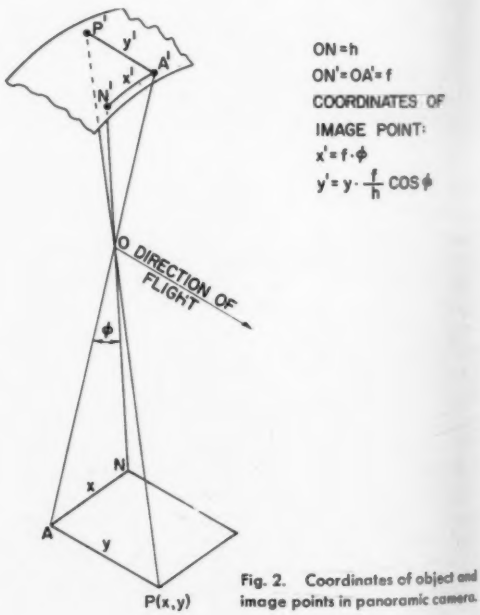

Fig. 2. Coordinates of object and image points in panoramic camera.

considered to be stationary. It gives the coordinates x' and y' for the image P' of an object point P having the coordinates x and y on the ground. The points of origin of the coordinate system are the nadir N on the ground and the image nadir N' on the film. The point P' is being exposed when the lens axis includes an angle ϕ with the vertical. As pointed out before, the scale of the image changes continuously with the scan angle of the lens. The rate of change is different in a direction parallel and perpendicular to the direction of flight, and is also a function of the coordinates of the object point. The magnifications parallel ($M\|$) and perpendicular ($M\perp$) to the flight direction at an object point $P_{x,y}$ are as follows:

$$M\| = \frac{f \cos \phi}{h} \quad (1)$$

$$M\perp = \frac{f}{h} \cos^2\phi \quad (2)$$

A camera presently under development by the Signal Corps has a scan angle of $\pm 70°$. Therefore, the scale at the edge of the field, parallel to the flight line, is 2.9 times less than at the nadir, and 8.5 times less perpendicular to this direction.

It is hard to visualize the significance of these figures. Published panoramic pictures of natural terrain show, of course, in different areas of the field, different objects which are hard to compare. Reproduced in Fig. 3 are photographs, made in this

Fig. 3. Image of terrain model, simulating panoramic photographs at nadir, and at 45° and 70° off vertical, from 1500 ft with $f = 3$ in. Prints enlarged 15.25 ×.

Laboratory, of a model of a piece of terrain, arranged on a turntable. The exposures were made with 0°, 45°, and 70° inclination of the axis of a 35mm camera from a line perpendicular to the terrain model. The distance of the camera was changed between exposures to obtain the scales corresponding to these angles. The image size of the film is that of real terrain taken from 1,500 ft with a 3-in. focal-length lens. The prints are magnified 15.25 times.

The sharpness of the 70° picture is reduced because it was taken with a very small aperture to obtain sufficient depth of field. At this aperture, resolution deteriorates because of diffraction effects. Exposures were made in pairs, to simulate the two overlapping panoramic scans that would be made for stereo viewing. It is interesting to note that with the stereo-viewer the observer no longer gets the impression that the slightly fuzzy objects of the 70° pictures lack sharpness. This observation can be taken as another indication of the usefulness of the stereoscopic presentation.

As mentioned above, the trace of the optical axis on the ground is not a straight line. It is the resultant of the uniform forward motion of the airplane and the uniform angular-scan motion of the lens across the flight line. Such a trace is shown in Fig. 4A. The points indicate the location of the lens axis for 10° intervals of a 140° scan. V is the ground speed of the plane and T the total scan time for 140°. Also shown are the coordinates for the ith forward motion interval, and the kth scan-angle position. Line D represents an imaginary grid line on the ground, perpendicular to the flight line, and passing through the nadir N at the time when the scan starts. FL is the projection on the ground of the path of the plane moving in the direction of the arrow.

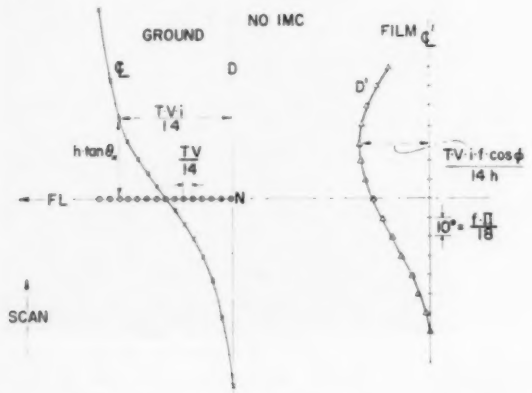

Fig. 4. A (*left*). Trace of optical axis of lens on ground, when lens is scanning through 140°. B (*right*). Image of straight line on ground, produced by panoramic camera without image motion compensation.

Assuming an exposure without IMC, the lens axis in the camera scans along the center line CL′ of the film, and the trace of the ground can be considered an image of the center line CL′ of the film, and vice versa. From this diagram, the image D′ of the straight grid line D can be derived. It is shown on the right side. Since the grid line on the ground recedes behind the plane, its image on film moves forward in the flight direction. The coordinates of the image points at 10° intervals are easily obtained: Along the CL′ axis, they are spaced at equal intervals because of the uniform angular motion of the scan. In the flight direction, they are obtained by dividing the ground coordinates by the magnification $M_{\parallel}$ applicable to the angle ϕ.

The belief seems to be widely held that the deformation shown in this diagram will be eliminated by the image-motion-compensation movement of the film which is necessary to ensure sharp imagery, unblurred by the relative motion of ground and camera.

The motion-compensating movement of the film has, at any particular instant, a speed of $(Vf \cos \phi)/h$ inches·sec^{-1} (if h and f are in inches, and V in inches·sec^{-1}). The *accumulated* amount of film movement at any instant of the scan can be represented by a trace of the swinging lens axis on the forward-moving film. The trace is shown in Fig. 5A. It is, of course, not a straight line since the film moves more slowly when the lens axis points towards larger angles. In Fig. 5B, this trace (IMC) is repeated, as is also Curve D′ of the previous figure. Combined, they yield the image D″ of the straight line D on the ground. Thus it may be seen that the maximum deviation in the flight direction occurs in the center, along the flight line. It becomes zero again at approximately one-half the maximum excursion angle, and increases with opposite sign towards the end of the scan.

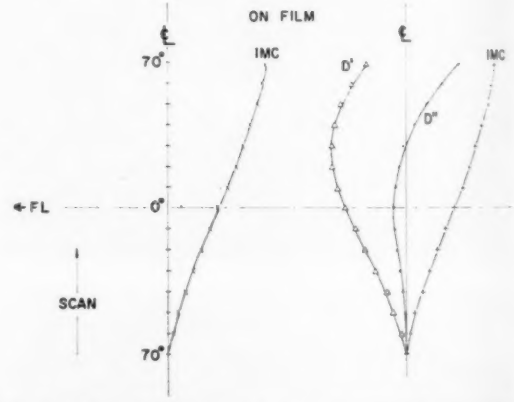

Fig. 5. A (*left*). Trace of lens axis on film in panoramic camera when film moves forward for compensating image movement. B (*right*). Image of D″ of straight line on ground, produced by panoramic camera with image motion compensation.

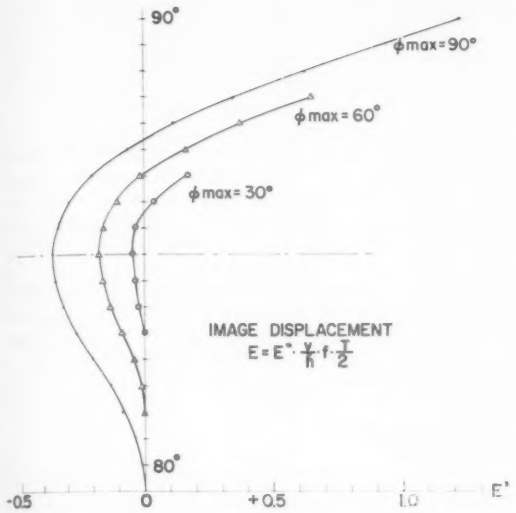

Fig. 6. Component E^* of residual error of y' coordinates in image of straight line on ground, produced by panoramic camera with image motion compensation, plotted vs. scan angle, for different maximum excursion angles.

This result of a graphical method is confirmed and generalized analytically. As shown in Fig. 2, the coordinate of an image point in the direction of flight is

$$y' = \frac{f}{h} \cos \phi \, y \tag{3}$$

The change of the coordinate with scan time is

$$\frac{dy'}{dt} = \frac{f}{h}\left[\frac{dy}{dt} \cos \phi - y \frac{d\phi}{dt} \sin \phi\right] \tag{4}$$

If the forward motion of the airplane is uniform, $y = y_0 - Vt$. Equations (3) and (4) combined yield

$$\frac{dy'}{dt} = \frac{f}{h}\Big[\underset{\text{I}}{-V \cos \phi} \underset{\text{II}}{- y_0 \frac{d\phi}{dt} \sin \phi} + \underset{\text{III}}{Vt \frac{d\phi}{dt} \sin \phi}\Big] \tag{5}$$

The first member (I) of the equation is identical with that for the IMC rate. It represents the effect of the uniform forward motion.

In the second member (II), the quantity V is absent. This means that the effect represented by this member will be felt regardless of the amount of forward motion or even if there is no motion at all. It indicates the growth of y' due to the continuously changing scale of the panoramic camera. If only this second factor were in effect (e.g., for a stationary camera), the image of a grid line through $y_0 = 0$ would be a straight line, and that of any other line parallel to it would be a pure cosine curve.

In the case of a forward-moving panoramic camera with IMC, the displacement of the image from this cosine curve can be derived from the third member (III) of the equation. At the time t after the beginning of the sweep, the error $E(t)$ will be:

$$E(t) = \int_0^t \frac{fVt}{h} \cdot \frac{d\phi}{dt} \sin \phi \, dt \tag{6}$$

Let ϕ_0 be one-half the total sweep angle (or the angular excursion of the lens axis at the beginning of the sweep), and T the total sweep time for the angle $2\phi_0$, and let (as is usually the case) ϕ be proportional to the elapsed sweep time t, then the image displacement at angular position ϕ, denoted $E(\phi)$, will be:

$$E(\phi) = \frac{VfT}{2h}\left[\left(\frac{\phi}{\phi_0} - 1\right)\cos \phi + \frac{\sin \phi_0 - \sin \phi}{\phi_0}\right] \tag{7}$$

In Fig. 6, values E^* of the expression in brackets are plotted vs. angles ϕ for three cases of ϕ_0. These curves verify the result of the graphical method: The displacement has a maximum in the flight direction for $\phi = 0°$, becomes zero again at near one-half the total excursion, and increases with opposite sign towards the end of the sweep.

This analysis provides the values for the image displacement not only for the selected line for which $Y_0 = 0$, but for any point in the coordinate system of flight line (Y-axis) and line through the nadir at the beginning of the scan. On the left side in

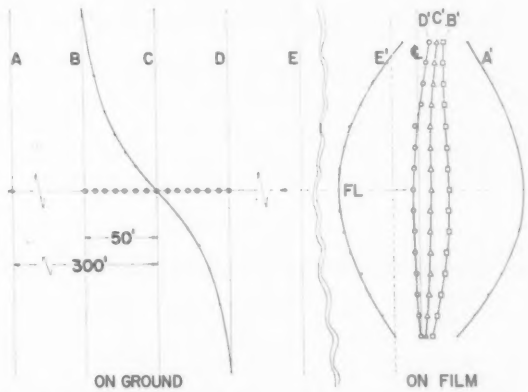

Fig. 7. Set of grid lines on the ground (left), and their images as produced by panoramic camera with image motion compensation.

Fig. 7 are shown grid lines passing through the nadir at $\phi = 0°$ (C), at the beginning and end of the scan when

$$\phi = -\phi_0 \text{ and } +\phi_0$$

(D and B), and two lines far out in front and behind those points on the ground over which the plane travels during one scan (A and E). The latter two intersect the flight line in the middle between the nadir for $\phi = 0°$ shown in this diagram, and the

corresponding nadir points of the previous and following scan, when the scans are spaced to produce 60% overlap. On the right side are the images of these lines, assuming $V/h = 0.25$ radians $\sec^{-1}$, scanning speed 0.25 radians in $^1/_{50}$ sec, $f = 6$ in., and $h = 2000$ ft.

It may be seen that the line images are not symmetrical. A′ and E′, in particular, show clearly that y' for $t = 0$ is different from y' for $t = T$. The curves are displaced with respect to true cosine curves by the same amount that D′ is displaced from the straight line CL′. From $t = 0$ to approximately $t = 3T/4$ the image is on one side of the true cosine curve, then shifts to the other side.

These displacements are important for computing the ground coordinates from unrectified panoramic pictures. They are particularly important for computing elevations from parallax differences. Their magnitude is by no means negligible. In the example of Fig. 7 the displacement at $\phi = 0°$ is slightly over 1 mm.

The analysis assumes that the swing axis of the lens is not tilted with respect to the flight path of the airplane. Tilt as well as roll and yaw of the plane will introduce deformations which are very cumbersome to compute. A high degree of stabilization is, therefore, very important for panoramic photography. The inherent, unavoidable image deformations can be easily computed if the operating conditions are known, in particular V/h, sweep time, and nadir position. If mosaics are to be made from panoramic pictures they must be rectified. Identification of objects becomes easier when the images are rectified, i.e., transformed to uniform scale in the entire picture area. It can easily be seen that a rectifier which eliminates all distortions and deformations introduced by the camera must be a complex precision instrument. It is planned to discuss the design of such an instrument in a later paper.

Acknowledgment

The authors wish to acknowledge the contribution of Sp/4 Robert Degree, Jr., who carefully made the pictures of the terrain model.

Back Issues Available

Photographic Engineering—1950–1956

Volumes 1 through 5 (4 issues each volume)	$5.00 per volume	$1.50 per issue
Volume 6, Nos. 1–3 (supply of No. 4 is exhausted)		1.50 per issue
Volume 7 (two single issues, Nos. 1 and 2; two issues, Nos. 3 and 4, combined under one cover)	5.00 per volume	1.50 per single issue 3.00 for combined issue

Photographic Science and Engineering—since 1957

Volume Number	Price to Members: Per single issue	Price to Members: Per volume	Price to Others: Per single issue	Price to Others: Per volume
1 and 2 (4 issues each volume)	$1.75	$6.00	$2.00	$ 8.00
3 and 4 (6 issues each volume)	1.75	9.00	2.00	12.00
5 (current) (6 issues)	Included in $10.00 annual dues		2.00	12.00

An index appears in the final issue of each volume except Volume 6 of *Photographic Engineering*. This index was published separately and is included with the issues from Volume 6, when ordered.

Order from:

Edward S. Cobb, *Managing Secretary*
Society of Photographic Scientists and Engineers
Box 1609, Main Post Office
Washington, D.C.

PHOTOGRAPHIC SCIENCE AND ENGINEERING
Volume 5, Number 5, September-October 1961

Circuit for Adjusting Automatic Color Printer Response

ROBERT K. RICKARD, *Apparatus and Optical Division, Eastman Kodak Company, Rochester, N.Y.*

Automatic color printers often use photoelectric control of exposure times in order to correct for variations between negatives and produce prints that are uniform in density and color balance. However, the printer response to a series of negatives of increasing density depends on many factors, which can cause the prints to become progressively lighter and exhibit a shift in color balance. This paper describes an electrical circuit that permits adjustment of the printer response to compensate for most of the effects of these factors.

Amateur color negatives exhibit differences in over-all density and color requiring various exposure times and/or printing intensities in each of three colors to obtain pleasing and acceptable color prints.[1,2] Automatic color printers often use photoelectric control of red, green, and blue exposure times to correct for these variations between negatives. For each color, there is a separate control circuit which is designed to produce a constant exposure to the paper regardless of differences in the average transmission of the negative.

It might be expected that all the resulting prints would be uniform in density and color balance. However, there are many factors which can cause a series of prints made from negatives of increasing density to become progressively lighter and exhibit a shift in color balance. One of the factors might be reciprocity failure, which can produce different print densities for equal exposures. Another factor might be mismatch between the spectral sensitivity of the control-circuit-filter–phototube combination and that of the printing-filter–paper combination, causing the exposure "seen" by the control circuit to be different from that given the paper. The purpose of this paper is to describe a simple electrical circuit that will automatically compensate for most of the effects of these factors.

The circuit permits for each color an easy adjustment of the printer response to negatives of varying over-all density. The action of the circuit is termed slope control, since it changes the slope of a response plot of print density vs. negative density.

Presented at the Annual Conference, Binghamton, N.Y., 22 May 1961. Received 3 May 1961.

1. V. R. Pieronek, W. L. Syverud, and W. F. Voglesong, *Phot. Sci. & Tech.*, **3**: 145 (1956).
2. C. J. Bartleson and R. W. Huboi, *Jour. SMPTE*, **65**: 205 (1956).

Principles of Slope Control

The response of a printer may be tested by printing a set of negatives of the same scene, which span the useful exposure range of the negative material. The red, green, and blue print densities can be plotted against the negative density as shown in Fig. 1. Each of the three plots of print density

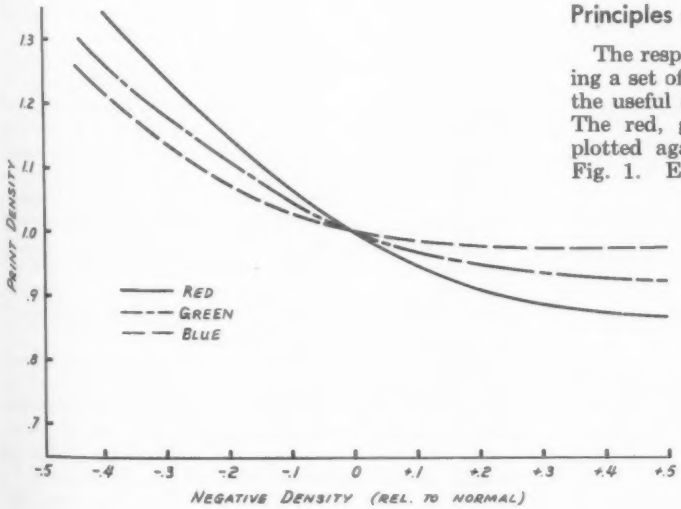

Fig. 1. Uncorrected printer response.

decreases as the negative density increases, resulting in lighter prints. Since the three plots have different slopes, the color balance also shifts.

Assuming that the curve shape is the same for each color, the red and green curves could be made nearly the same as the blue curve by increasing the logarithm of the red and green print exposure linearly with the negative density. This would eliminate the shift in color balance, and further correction to all three curves would counteract the tendency for the prints to become lighter.

Therefore, the circuit should increase, to various degrees, the logarithm of the print exposure linearly with the negative density in order to obtain the desired slope of the printer response. First, a means must be found to automatically measure the negative density. In the usual type of printer control circuit,[3] the printing time is inversely proportional to the average transmission of the negative. It follows that the logarithm of the printing time is a direct measure of the negative large-area transmission density, which, for simplicity, is called the negative density.

In this same type of control circuit, the print exposure is governed directly by the value of an exposure voltage. This exposure voltage may change slowly with time provided it has the proper value at the instant the exposure stops. The exposure voltage can be made a function of time, so that the exposure obtained for a given negative depends on the printing time for this negative. If, after the start of exposure, the voltage is made to vary exponentially with time by charging a capacitor through a resistance, a log-log plot of the voltage vs. time is nearly a straight line over approximately a 10:1 range in time. Therefore, the log of the exposure voltage is a linear function of the log of the printing time over a range sufficient to accommodate most amateur negatives.

Since it was shown previously that the log of the printing time is a measure of the negative density, the desired circuit action is obtained: namely, the log of the print exposure increases linearly with the negative density. However, it should be noted that the print exposure is corrected by changing the printing time, which was the basis for determining the correction needed originally. For small corrections, the printing times for the thinnest and densest negatives will be in about the same ratio as they would for no correction. For very large corrections, the ratio of the printing times will become much greater, and the exponential curve will not be sufficiently linear on a log-log plot over this greater range of time.

Basic Control Circuit

Figure 2 shows a typical circuit used to generate the time variation of the exposure voltage for one color in a printer. The output voltage V_s is proportional to the exposure voltage used to govern

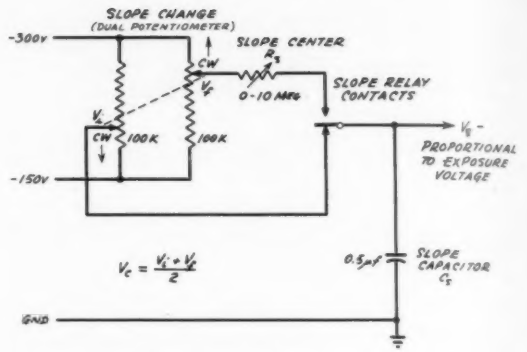

Fig. 2. Slope control circuit.

exposure in the printer integrating circuit (not shown), and it is initially equal to V_i, the voltage tapped off the left side of the slope change dual potentiometer. When the print exposure starts, the slope relay contacts are switched and the output V_s builds up toward V_f, the voltage tapped off the right side of the slope change dual potentiometer. The output builds up at an exponential rate determined by the time constant R_sC_s, formed by the slope center rheostat R_s, and the slope capacitor C_s. The dual potentiometer supplying V_i and V_f is arranged so that the average of these two voltages is always a constant value V_c (-225v in this case).

If the slope change potentiometer is set at the halfway point, $V_i = V_f = V_c$, and the output V_s does not change from V_c (no slope change). If it is now turned fully clockwise, V_s will start at -150v and increase to twice this value (full positive slope change). After a time equal to $0.693\ R_sC_s$, the exponential charging is half completed, and V_s is equal to V_c, momentarily giving no correction. Therefore, thin negatives which have a printing time of less than $0.693\ R_sC_s$ are given less than normal exposure, and dense ones are given more.

If a normal negative used to set the correct exposure level of the printer has a printing time t_n without correction, the slope center rheostat is set so that $t_n = 0.693\ R_sC_s$. Then, regardless of the slope change setting, this negative will have the same exposure, since V_s is always equal to V_c after a time t_n. This is desirable, since the amount of slope change can now be adjusted without readjustment of the exposure level for a normal negative. It also insures that the range of times over which the exponential curve behaves properly is always centered about a normal negative printing time, giving equal correction to both thin and dense negatives.

So for a proper setting of the slope center rheostat, the printer response can be easily adjusted by turning one knob on the slope change potentiometer. The slope of the response curve tilts about the print density for a normal negative. Normally, the slope change is set clockwise from the halfway point to give a positive slope change, which increases the

3. R. K. Rickard, *Phot. Sci. & Eng.*, **4**: 288 (1960).

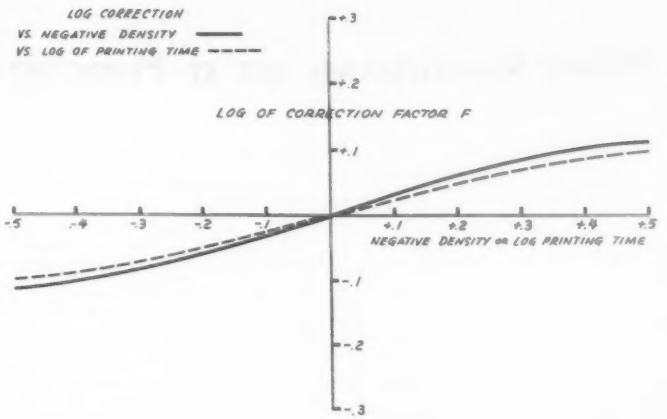

Fig. 3. Log correction to print exposure for full positive slope change.

exposure for dense negatives. However, by turning the slope change knob fully counterclockwise, an opposite or negative slope change can be obtained, which decreases the exposure for dense negatives. This is generally unnecessary, unless the print density is found to increase with the negative density:

Slope Control Equation

An exposure correction factor F can be defined as the ratio of the exposure E_0 for a given negative to the exposure E_n of the normal negative. It can be shown that F is given by Eq. (1):

$$F = E_0/E_n = T_n t_0/T_n t_n = 1 + {}^1/_3 K(1 - 2e^{-0.693 t_0/t_n}) \quad (1)$$

where T_0 = average transmission of a negative
T_n = average transmission of the normal negative
t_0 = printing time of a negative
t_n = printing time of the normal negative
K = slope change setting:
+1 for full positive slope change
0 for zero slope change
−1 for full negative slope change

This equation can be used to make a plot of log F, the log exposure correction, vs. log (t_0/t_n), and is shown on Fig. 3 as the dotted curve for full positive slope change. However, the curve of primary interest is a plot of log F versus $(D_0 - D_n)$, the negative density relative to the normal. This curve can be obtained quite easily from the first curve by subtracting from each abscissa value an amount equal to log F. This follows from Eq. (2):

$$(D_0 - D_n) = \log (T_n/T_0) = \log \left(\frac{t_0/t_n}{F}\right) = \log (t_0/t_n) - \log F \quad (2)$$

The solid curve in Fig. 3 now shows the log E correction added to the print exposure for varying negative densities for full positive change. Other curves between this one and a horizontal line corresponding to zero change may be generated by merely reducing the slope change setting.

Conclusions

This circuit enables the printer response plot of print density vs. negative density to be separately adjusted for each of the three colors. Therefore, color differences between prints from thin and dense negatives may be greatly reduced. Actually, adjustment for only two colors is necessary for this purpose, but the third setting allows compensation for neutral density fall-off as well.

Several automatic color printers for amateur photofinishing have employed this slope control circuit quite successfully to improve the first printing yield.

Acknowledgment

The author wishes to thank H. F. Betz and W. Modney for their assistance and counsel in the preparation of this paper.

PHOTOGRAPHIC SCIENCE AND ENGINEERING
Volume 5, Number 5, September-October 1961

Film Response as a Function of Exposure

FRANK SCOTT AND MILTON D. ROSENAU, JR., *Electro-Optical Division, The Perkin-Elmer Corporation, Norwalk, Conn.*

The fact that the image-forming capability of film varies with exposure is of interest when the film is used as a detector in a photographic system. A technique for determining this capability as a function of exposure is described in this paper. Sine-wave targets of a given modulation and of several spatial frequencies are photographed with a high-resolution camera specifically constructed for this purpose. After processing, the modulation of the light transmission of the images is measured with a microphotometer. The measured transmission modulation for a given spatial frequency is modified to account for the instrumentation and is plotted as a function of exposure. These data make possible the determination of optimum exposure, the loss of image quality accompanying nonoptimum exposure, and the requirements for exposure control mechanisms. The response of the film is determined by comparison of the transmission modulation of the photographic image with the modulation of the optical image incident on the film.

This technique is shown as applied to an aerial film; therefore the image modulation values employed are relatively low to simulate the low contrast of aerial scenes. The use of information obtained by this method of evaluation improves the designer's ability to predict the performance of a photooptical system.

The light transmitted through a processed negative is of fundamental importance since it is necessarily employed in all uses of the negative. The modulation of the transmitted light, or the transmission modulation, is denoted by M_T and is defined by

$$M_T = \frac{T_{max} - T_{min}}{T_{max} + T_{min}},$$

where T is the transmittance.

With given processing conditions, the transmission modulation of an image recorded on film is primarily a function of the exposure, the modulation of the optical image to which the film is exposed, and the size of the image structure. This paper describes a method for determining the transmission modulation as a function of exposure, for given aerial image modulations and spatial frequencies.

The evaluation method proposed here is similar to that proposed by Howlett,[1] except that objective measurements have been substituted for subjective criteria. In the earlier work, resolution targets were exposed and visually evaluated. This procedure resulted in some variation due to differences in visual perception among individuals, and, more important, provided only an evaluation of the limiting resolution. The new method should permit different investigators to obtain identical results because it employs objective measurement. It also accounts for the object contrast variations that Kardas[2] observed, except that modulation, rather than contrast, was chosen to evaluate this effect. Finally, data obtained indicate that variations due to spatial frequency can be handled by this evaluation method, satisfying the requirement, which MacDonald[3] has discussed, to "tune" the photooptical system to match detail size. Even more important is the fact that this instrumental evaluation describes the image at all spatial frequencies and not merely the spatial frequency at the visual limit of resolution.

Procedure

A sample of the film being evaluated is exposed in an instrument called a microcamera (Fig. 1). In the

Presented at the Annual Conference, Binghamton, N.Y., 25 May 1961. Received 4 May 1961; revised 26 June 1961.

1. L. E. Howlett, *Can. J. Research*, **24:** 1 (1946); *ibid.*, **26:** 60 (1948).
2. R. S. Kardas, *Phot Eng.*, **5:** 91 (1954).
3. D. E. MacDonald, *J. Opt. Soc. Am.*, **43:** 290 (1953).

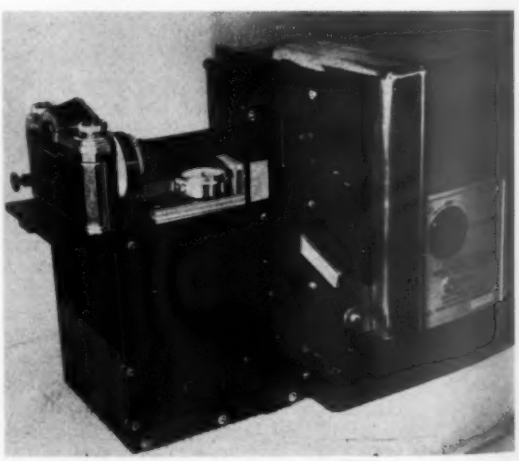

Fig. 1. Microcamera.

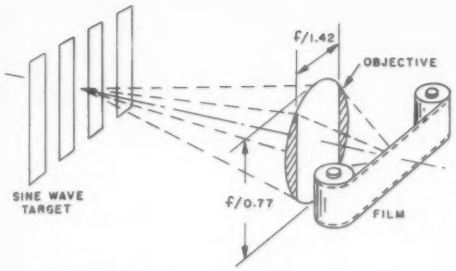

Fig. 2. Schematic of optical arrangement of microcamera.

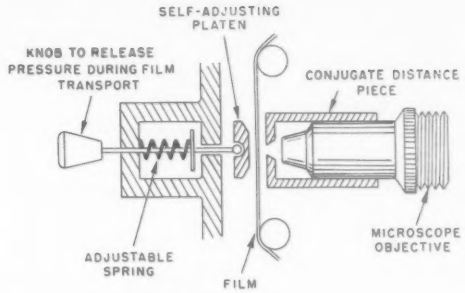

Fig. 3. Microcamera film platen mechanism.

microcamera, the film is exposed to the image of a sine-wave target at a reduction of approximately 25×. A sensitometer is used as a controlled light source.

The exposure time and spectral composition of the light source can be varied and should be identical to conditions of the photooptical system for which the film is being evaluated. Calibrated neutral density filters are used with the microcamera to vary the light intensity in increments of 0.1 log meter-candle-seconds.

Targets for the microcamera were photographically made on Kodak High Resolution Plates and processed to yield spectrally nonselective and practically grainless images. Each target consists of long lines and spaces of one frequency, the transmission of which varies sinusoidally. The effective modulation of the target image is varied by exposing the film sample twice: first to an open field and then to the target. Tests show that this procedure is equivalent to one exposure if the second exposure is made within a few minutes of the first, and if the time between exposure and processing exceeds 1 hr. Thus any sine-wave target of a given modulation can effectively expose on the film sample an image of any modulation lower than that of the target.

An apochromatic microscope objective, designed for use without a microscope slide cover glass, images the target onto the film. The objective is of 8-mm focal length and the aperture is essentially rectangular (Fig. 2). The original aperture was circular, $f/0.77$. Since the film was evaluated for use in an $f/1.42$ photooptical system, to simulate the angle of incidence of light on the film, the short dimension of the aperture was set equivalent to $f/1.42$ and is perpendicular to the lines of the target.[4] The long dimension of the aperture, being parallel to the lines of the target, does not affect the focus or resolution of the lines, and is thus made as large as possible, equivalent to $f/0.77$, in order to transmit as much light as possible.

The emulsion of the film sample is held in the focal plane of the microcamera, repeatable to within 0.5 μ, by a film platen mechanism (Fig. 3). Because the film is pressed onto the conjugate distance piece, which is mounted onto the objective cell, variations of base thickness do not affect the focus position of the emulsion. The pressure the platen exerts is adjustable and is such that it is sufficient to hold the film against the distance piece[5] but is not excessive, which would cause the emulsion to bulge into the 1-mm-diameter aperture of the distance piece. Care is exercised to maintain the film transport mechanism free from dust particles and to operate the camera in a reasonably constant temperature environment to attain correct placement of the emulsion in the focal plane.

All exposures in a single test are made on a small area of the film to avoid variations of results which might otherwise arise due to processing variations. The exposed film is accompanied during processing by a sensitometrically exposed film sample.

After processing, the resulting images are scanned with a microphotometer. A slit is imaged onto the traveling film with a microscope objective and aperture identical with the objective of the microcamera. The slit image is 2.5 μ wide and 125 μ long, which is one-eighth the length of the film image. The output of the microphotometer is graphically recorded and represents the photomultiplier output voltage which in turn represents transmission of the image. The modulation (M_A) of brightness (B_A) of the aerial image incident on the film in the microcamera is equal to the modulation of the target (M_0) as modified by the objective lens L_1 (Fig. 4). As mentioned previously, lens L_1 contains a rectangular aperture, the transfer function for which is:

$$\tau_{L_1} = 1 - N\lambda\nu \text{ for } \nu \leqslant 1/N\lambda$$

where N = f-number of objective
λ = peak wavelength of light in millimeters
ν = frequency in cycles per millimeter

Similarly, the image of the microphotometer slit is modified by lens L_2, which is identical to lens L_1. Account is made also for the finite width of the slit by its transfer function:

$$\tau_S = \frac{\sin \pi\delta w}{\pi\delta w}$$

4. J. M. Gregory, *Proc. Phys. Soc. (London)*, **6**: 769 (1958).

5. G. W. W. Stevens, *Microphotography*, John Wiley and Son, Inc., New York, 1957, pp. 116–127.

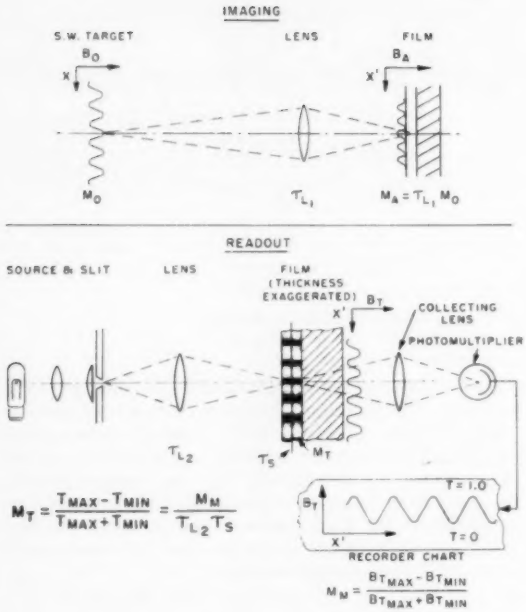

Fig. 4. Schematics of instrumentation and functional relations.

where δ = width of slit image in millimeters
w = frequency of target image on film in cycles per millimeter

The average measured transmission modulation (M_M) of ten cycles on the microphotometer recorder chart is determined, ten cycles being chosen to reduce fluctuations due to granularity. The measured modulation (M_M) represents the transmission modulation (M_T) of the film image as modified by the finite width of the slit image and the slit imaging lens L_2:

$$M_T = \frac{M_M}{\tau_{L_2} \tau_S}$$

Since the photorecording process is generally nonlinear, the spatial variation of transmitted light is sinusoidal in only a small range of exposures, and this correction for readout instrumentation is merely a first order correction which ignores the effect of harmonic distortion caused by any nonlinearity. This procedure is followed for several exposures, for each spatial frequency of the target images, and for each modulation of interest.

It should be noted that residual primary experimental errors will yield values of M_T lower than actual M_T values. Such experimental errors include:

1. Nonoptimum focus of the microcamera image
2. Nonoptimum focus of the microphotometer objectives
3. Misalignment of parallelism of slit and image lines
4. Modulation reduction caused by the thickness of the emulsion which may significantly exceed the depth of focus of the slit image[6]

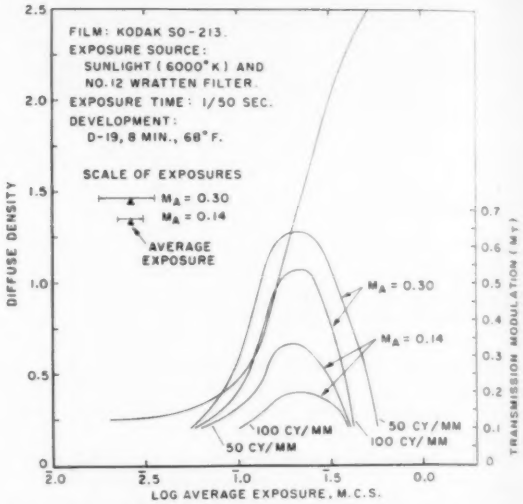

Fig. 5. Transmission modulation and diffuse density as a function of log average exposure for Kodak SO-213 Film. Transmission modulation is parametric in spatial frequency and modulation of image (M_A) incident on the emulsion.

The transmission modulation (M_T) for a given spatial frequency is then plotted as a function of log average exposure (Fig. 5). These curves are parametric in modulation of the aerial image incident on the film (M_A), and the values chosen should be matched to those modulations anticipated; in this case, low modulations were chosen to simulate scenes photographed by airborne cameras. The characteristic curve is also plotted on the same abscissa, so correlation can be made between transmission modulation and density.

Applications

The determination of transmission modulation as a function of exposure, spatial frequency, and modulation of the aerial image incident on the film allows the photooptical system designer to optimize system performance by judicious manipulation of these parameters. (It must be recognized that since the transmission modulation is determined from peak transmission values without regard to wave form, two equal values of M_T may not necessarily represent images with completely similar visual interpretability.) For instance, two different transmission modulation results might be obtainable, as shown in Fig. 6, and the choice of the best system in this case depends on the exposure range anticipated. A photooptical system and film–processing combination producing Curve B probably is better for the narrow exposure

6. N. K. Southwold and W. G. Watters, *J. Phot. Sci.*, **7**: 174 (1959).

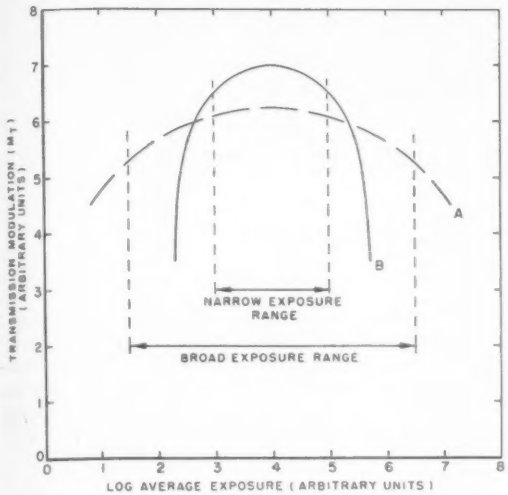
TRANSMISSION MODULATION (M_T) (ARBITRARY UNITS)
LOG AVERAGE EXPOSURE (ARBITRARY UNITS)
A
B
NARROW EXPOSURE RANGE
BROAD EXPOSURE RANGE

Fig. 6. Hypothetical results and exposure ranges for applications discussed in text.

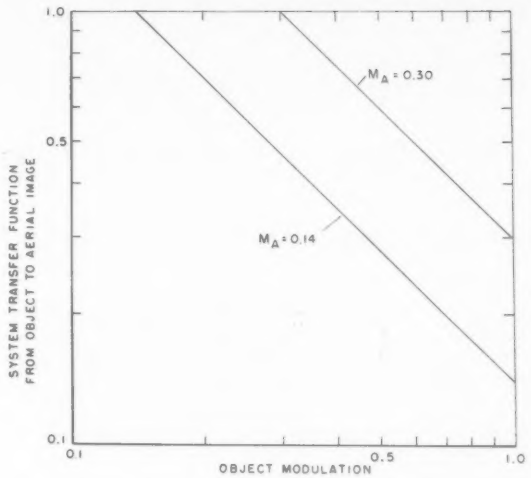

Fig. 7. Combinations of system transfer function and object modulation which will produce aerial image modulations (M_A) equal to those of Fig. 5.

range, but the combination producing Curve A probably is better for the broad exposure range.

The combination producing Curve A might also be better if a small object brightness range with considerable uncertainty in minimum object brightness is anticipated; usually this is the case in aerial photography. Conversely, if transmission modulation of 0.65 is required, then the combination producing Curve B should be employed, and precise exposure control should be added to the photooptical system.

Curves of the nature of those in Figs. 5 and 6 can also be used to set a tolerance on exposure time and/or object illumination, provided the minimum acceptable transmission modulation is known. In the case of aerial photography, the tolerance on object illumination can be used to derive an operational envelope for type of terrain (object modulations), weather (haze), and solar or lunar altitude (season, latitude, and local time). With any system in which image motion is a problem, performance can be accurately evaluated to determine whether less motion obtained by reducing exposure time is advantageous.

The fact that one curve applies to only one spatial frequency and aerial image modulation is not as restrictive as it might first appear. Figure 7 illustrates the range of system transfer functions and object modulations to which the results illustrated in Fig. 5 can be applied directly.

A new property of the photographic recording process is defined as its gain, G, where:

$$G \equiv M_T/M_A$$

Graphical plots of G as a function of M_A (and parametric in spatial frequency) are found usually to be smoother than plots of M_T as a function of M_A for low values of M_A, and this permits more accurate interpolation between transmission modulation curves, as needed, to provide information for design estimates. It should be noted that, for the sample of Fig. 5, the gain is greater than unity at the peak of the transmission modulation curve; specifically, there is a modulation increase.

Conclusions

In conformity with other recent studies, this evaluation method is basically a form of sine-wave modulation analysis, and is thus compatible with the powerful analytic tools developed in those studies. However, this evaluation applies to the modulation of light transmitted through a processed negative and does not yet fully account for harmonic distortion resulting from any nonlinearity in the photorecording process. Nevertheless, the transmission modulation of the processed negative seems to be fundamental, since it is necessarily employed in all uses of the negative. Transmission modulation should be distinguished from the sine-wave response of a film as customarily reported by film manufacturers.[7] Furthermore, this method of evaluation shows transmission modulation as a function of exposure, modulation of the aerial image causing the exposure, and spatial frequency. The added complexity of several curves provides the photographic system designer with more precise information.

Acknowledgment

The authors gratefully acknowledge the assistance of many colleagues and especially numerous discussions with R. V. Sback.

7. R. L. Lamberts, *J. Opt. Soc. Am.*, **49**: 425 (1959).

PHOTOGRAPHIC SCIENCE AND ENGINEERING
Volume 5, Number 5, September–October 1961

A Quantitative Study of the Influence of Tone-Reproduction Factors on Picture Quality

J. L. SIMONDS, *Research Laboratories, Eastman Kodak Company, Rochester, N.Y.*

The subjective qualities of a large number of varied photographic reproductions of several scenes are successfully predicted by an empirically determined function of characteristic vector descriptions of their associated objective tone-reproduction characteristics. A digital technique for predicting the subjective picture quality associated with given tone-reproduction characteristics offers a simple means of determining the effects on subjective quality of varying each of the factors which influence the shape of the objective tone-reproduction curve.

The ultimate test of the quality of a photographic reproduction is the satisfaction it brings to the viewer. Aside from artistic considerations, the viewer will be influenced in his appraisal of the reproduction by many technical factors, which can be grouped into several broad categories, the most important being: (1) tone-reproduction characteristics; (2) image-structure characteristics; and (3) viewing conditions.

The effects of these factors on reproduction quality are interrelated, but it is desirable to determine the main effects of each of the factors, independent of interactions. By maintaining invariance of all factors but one, the main effects of the remaining variant factor can be studied and qualitative and quantitative relationships derived between subjective quality and the levels of the variant factors.

The practical evaluation of the relative subjective qualities associated with black-and-white reproduction systems is laborious, time-consuming, and expensive. It has been recognized that print quality is related to tone-reproduction characteristics, but even though the tone-reproduction characteristics may be known for a given reproduction system, picture tests have been relied upon to evaluate subjective quality. The difficulty of conducting picture tests has precluded extensive studies of the effects on subjective quality of the many factors which affect tone-reproduction characteristics.

The study reported here has been concerned with the determination of an empirical relationship between the subjective qualities of black-and-white prints and a purely numerical characterization of the associated objective tone-reproduction characteristics. The relationship, derived from psychophysical studies of varied reproductions of several scene types, permits the evaluation of the relative qualities of any number of practical or hypothetical reproduction systems by considerations of simply derived digital data representing the tone-reproduction properties of the systems. Subjective quality can be evaluated by purely digital operations well suited to high-speed computing equipment. Once the relationship has been properly established, no further print making is required — only a knowledge of such factors as the D-log E curves of the negative and print materials, the exposures of these materials, and the flare characteristics of the cameras and printing systems.

Experimental Design

The most familiar representation of the sensitometric characteristics of a reproduction system is the *objective* tone-reproduction curve, in which the densities of the reproduction are plotted as a function of the logarithms of the luminances of corresponding areas in the original scene. The *subjective* tone-reproduction curve is a plot of subjective brightnesses of the viewed reproduction as a function of the subjective brightnesses of corresponding areas in the original scene. The objective curve is more simply determined, and, for given illumination and viewing conditions, can be assumed to provide essentially as good correlation with psychometric measures of quality as does the subjective tone-reproduction curve.

In Fig. 1 are two objective tone-reproduction curves representing prints of the same scene, the minimum log luminance of the scene being at point A, the maximum at point B. Since, at point A, curve x has a higher gradient than curve y, luminance differences in the shadow regions of the scene result in greater density differences in print x than in print y. Hence, shadow detail would be more easily discerned in print x than in print y. Most observers would agree that the reproduction of shadow detail in print x is better than that in print y. The curve for print y, however, has a higher gradient in the highlight region (log luminances in the region of point B) than curve x. For scenes in

Communication No. 2188 from the Kodak Research Laboratories. Received 9 June 1961.

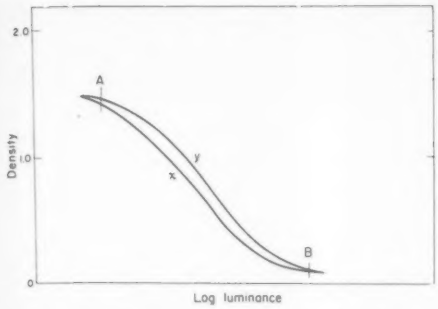

Fig. 1. Two objective tone-reproduction curves.

which highlight detail is of greater importance, the tone reproduction represented by curve y might be preferred, while for scenes in which shadow detail is of greater interest, curve x might be preferred.

Thus it can be seen that print quality is related to the shape of the tone-reproduction curve and to the type of scene being reproduced. These relationships have been known only qualitatively in the past, however. Previous studies of tone reproduction and pictorial quality have developed important qualitative relationships, but little success has been achieved in obtaining a general empirical quantitative relationship between subjective print quality and the shape of the objective tone-reproduction curve, all other factors which influence quality being held invariant. A primary difficulty has been that of adequately characterizing the shapes of tone-reproduction curves by a reasonable number of parameters, in order to permit regression on subjective quality.

The key to deriving an empirical quantitative relationship lies in the ability to describe any practical tone-reproduction curve by a few numbers which are uniquely and completely descriptive of the shape and position of the curve. Such a quantitative representation is provided by the method of principal components, to be described in the section, *Principal Component Specification of Tone-Reproduction Curves*, below.

The ability to describe the shape of a tone-reproduction curve with a few numbers (provided by principal component analysis) permits the design of an experiment in which, for a given scene, a reasonable number of prints representing a comprehensive variety of tone-reproduction curves are judged for relative subjective quality. It is then possible to derive a regression function of the principal component description of the tone-reproduction curves which will predict the relative subjective qualities of reproductions of that scene.

The prediction function permits assessment of the relative quality of any reproduction of that scene, provided only that (1) the tone-reproduction function be within the domain of curve shapes studied (i.e., no radically new type of variation has been introduced), and (2) all other factors affecting the assignment of pictorial quality be at the levels at which the calibration experiment was performed. In this way, it is possible to predict the effects on pictorial quality of changes in the D-log E curve shape of a film or print material, other factors remaining fixed. In general, it is possible to examine systematically the relative subjective qualities which would result from all possible combinations at various levels of all the factors influencing the shape of the objective tone-reproduction curve.

The experimental steps necessary to derive the regression equation are:

A. Specify a set of tone-reproduction curves which systematically sample the domain of tone-reproduction curve shapes obtainable with films and papers generally like those currently manufactured.

B. Obtain prints of a given scene which represent the specified set of varied tone reproductions.

C. Compute the principal component representations of the tone-reproduction characteristics associated with each print.

D. By psychophysical methods, obtain subjective quality assignments for each print.

E. Regress the subjective quality indexes on the principal component descriptions of the tone-reproduction curves associated with the prints.

Since there is a strong interaction effect on quality between the shape of the tone-reproduction curve and the type of scene reproduced, Steps B-E were performed for each of four scene types.

Preparation of Reflection Prints

A tone-reproduction curve for a reproduction system can be determined by measuring the print densities and relating them to log scene luminances, obtained either by visual or photographic photometry. The curve can also be graphically derived, as shown in Fig. 2.

In Quadrant I is a curve of density vs. log scene luminance for a negative film. If no camera flare

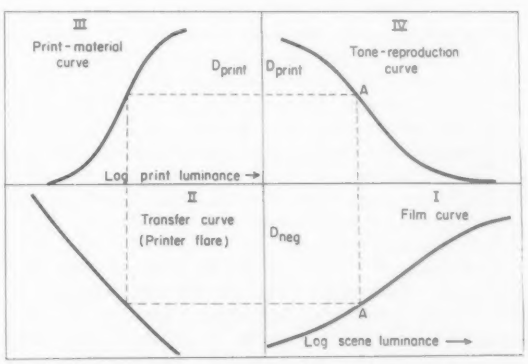

Fig. 2. Graphical derivation of objective tone-reproduction curve.

A. Indoor scene: log luminance range = 2.58; B. Portrait scene: log luminance range = 2.20; C. Portrait scene: log luminance range = 2.20;

D. Outdoor scene: log luminance range = 2.70.

Fig. 3. Four scenes used in the psychophysical study.

exists, log camera exposure is directly proportional to log scene luminance. If camera flare is present, the curve in Quadrant I must be derived from the *D*-log *E* curve of the negative material by taking into consideration the flare characteristics of the camera which was used.

In Quadrant II is a curve relating diffuse densities of the negative to log luminance for the print material. For contact printing, the transfer function in Quadrant II is a 45° straight line. For diffuse enlarging systems, the presence of flare light in the enlarger causes the log luminance scale for the print material to be less than the diffuse density scale of the negative. The transfer curve in Quadrant II has been drawn to take into account an average amount of enlarger flare. It is assumed that a diffuse enlarger is used.

In Quadrant III is a *D*-log *E* curve for the print material. To obtain point *A* on the reproduction curve, the density of the negative at *A* is traced through the printer-transfer function to the luminance scale of the print material. The resulting print density is then located in Quadrant IV at the log luminance of point *A* on the negative curve. The entire tone-reproduction curve can be derived in this manner.

Previous studies[1] have indicated that the number of basically different ways in which the *D*-log *E* curves of films and paper vary is small. Since tone-reproduction curves can be derived, either graphically or digitally, by simple manipulations of the *D*-log *E* curves, the number of basically different ways in which tone-reproduction curves can vary is limited to a small number.

Several thousand graphical derivations of a wide variety of tone-reproduction curves were made, representing reproduction systems possible from combinations of systematic and comprehensive samplings of *D*-log *E* curves of practical negative films and reflection print materials. By principal component analysis, the variations in curve shape were found to be limited in number and type. It was possible to derive a family of tone-reproduction curves which represent a comprehensive sampling of the types of tone reproductions likely to be encountered in practical pictorial photography; the family of curves was used as an aim in preparing the various prints of each scene studied.

The experiment outlined above calls for psychophysical study of a number of reproductions of each of several scene types. The four scenes chosen for study are shown in Fig. 3. Scene A is representative of the type of scene commonly encountered in commercial photography; the difference between the maximum and minimum log luminances of the scene is 2.58. Scenes B and C are typical indoor portrait scenes; the log luminance range of each is 2.20. Scene D is an outdoor scene with a log luminance range of 2.70.

1. J. L. Simonds, *Phot. Sci. and Eng.*, **2**: 205 (1958).

Close approximations to the aim specifications were achieved by photographing each scene with a variety of negative materials, at a variety of camera exposures, varying the *D*-log *E* characteristics and exposures of the print material, and introducing varying amounts of flare light into the printing system.

The negative materials were chosen so as to minimize graininess differences among the prints. All negatives of a given scene were made with a fixed camera-lens aperture and all prints were made with a fixed enlarger-lens aperture. Camera exposures were varied by using neutral filters over the camera lens. The negatives were 5 by 7 in. and were enlarged to 8- by 10-in. prints.

D-log *E* characteristics of the print material were varied by using Kodak Polycontrast Rapid Paper, introducing contrast variability by exposure through different optical filters. The use of the single print material ensured uniform color, texture, and image-structure characteristics throughout each series of prints.

The prints of Scenes A, B, and C were made on Polycontrast Paper with a semimatte (G) surface. The prints of Scene D were made on Polycontrast Paper with a glossy (F) surface.

Sixty prints each of Scenes A and B and 25 prints each of Scenes C and D were used in the psychophysical study. (The reduction in the number of prints of Scenes C and D was considered advisable as a result of the complexity of psychophysical study of the 60 prints of Scenes A and B.)

Principal Component Specification of Tone-Reproduction Curves

Reflection density data were measured by a reflection densitometer employing 45° illumination and 90° collection. The objective tone-reproduction curves for each of the prints were constructed by measuring densities at many areas in the prints and relating these data to the associated log scene luminances determined by photographic photometry. From each of the curves, density data were found by interpolation corresponding to 12 equally spaced values of log scene luminance. The first density value corresponds to the area of lowest luminance and the twelfth corresponds to the area of highest luminance. The 12 pieces of density data are considered definitive of the tone-reproduction characteristics associated with each print.

The 12 densities are reduced to a fewer number of parameters by the method of principal component analysis. To simplify the discussion, the results of the analysis will be reported with a minimum of mathematical details. A more rigorous description of the technique of analysis is given in a paper by H. Hotelling.[2]

For each print of each scene, 12 densities are available. From all prints of all scenes (a total of 170 prints), a 170-row, 12-column matrix of densities can be formed, each row of which contains the 12 densities for one of the 170 prints. Each row is called a "density vector." The mean density vector can be computed by finding the average density at each of the 12 steps. The mean vector is, therefore, the average tone-reproduction curve of the 170 curves.

It is possible to find a unique set of p vectors, called "characteristic vectors," which, when added in the proper amounts, step by step, to the mean density vector, will adequately approximate any density vector in the original family of 170 density vectors. The characteristic vectors, like the density vectors themselves, are sets of 12 numbers. Mathematically stated, the densities of each step of any tone-reproduction curve are given by Eq. (1):

$$\begin{aligned} d_{\text{step 1}} &= \bar{d}_{\text{step 1}} + Y_1 V_{1,\text{ step 1}} \\ &\quad + Y_2 V_{2,\text{ step 1}} + \cdots Y_p V_{p,\text{ step 1}}. \\ d_{\text{step 2}} &= \bar{d}_{\text{step 2}} + Y_1 V_{1,\text{ step 2}} \\ &\quad + Y_2 V_{2,\text{ step 2}} + \cdots Y_p V_{p,\text{ step 2}}. \\ d_{\text{step 12}} &= \bar{d}_{\text{step 12}} + Y_1 V_{1,\text{ step 12}} \\ &\quad + Y_2 V_{2,\text{ step 12}} + \cdots Y_p V_{p,\text{ step 12}}. \end{aligned} \quad (1)$$

The Y's are the amounts of the characteristic vectors which must be added to the mean density vector in order to produce the sample density vector. The characteristic vectors, V_i, are uniquely determined for a given family of curves — in this case, a family of 170 tone-reproduction curves. The values of $Y_1, Y_2, Y_3, \ldots Y_p$ vary from one tone-reproduction curve to another. The Y's, therefore, are a complete specification of the density vector to which they apply. Together with the uniquely determined characteristic vectors and the mean density vector, the Y's are sufficient information with which to reconstruct the density vector from which they were derived.

The number, p, of characteristic vectors required to explain all the differences among a family of curves, each represented by 12 densities, will be equal to or less than 12. For a perfect fit to all density vectors, 12 characteristic vectors may be required. The probability is strong, however, that

TABLE I. Mean Curve and Three Characteristic Vectors of 170 Tone-Reproduction Curves

Step	Mean curve	V_1	V_2	V_3
1	1.57	0.103	0.080	0.030
2	1.52	0.115	0.068	0.016
3	1.44	0.132	0.051	0.000
4	1.32	0.152	0.019	−0.020
5	1.14	0.160	−0.015	−0.034
6	0.89	0.149	−0.046	−0.031
7	0.64	0.118	−0.056	−0.000
8	0.43	0.092	−0.054	0.023
9	0.27	0.066	−0.043	0.039
10	0.16	0.043	−0.028	0.044
11	0.09	0.027	−0.018	0.038
12	0.06	0.016	−0.009	0.032

2. H. Hotelling, *J. Educational Psychology*, **24**: 417 (1933).

a large percentage of the variability among the original family of density vectors may be explained by using less than 12 vectors. For the family of 170 curves studied, only three characteristic vectors were required to produce a satisfactory reconstitution of each of the 170 curves. The data for the mean tone-reproduction curve and the three vectors are listed in Table I.

The Y's, called "scalar multiples," can be determined for each curve of the 170 curves as linear combinations of the densities of the 12 steps of the sample curve and the densities of the 12 steps of the mean curve. Hence,

$$\begin{aligned} &= W_{1,\text{step 1}}\,(d_{\text{step 1}} - \bar{d}_{\text{step 1}}) \\ &\quad + W_{1,\text{step 2}}\,(d_{\text{step 2}} - \bar{d}_{\text{step 2}}) \\ &\quad + \ldots\ldots\, W_{1,\text{step 12}}\,(d_{\text{step 12}} - \bar{d}_{\text{step 12}}). \\ Y_2 &= W_{2,\text{step 1}}\,(d_{\text{step 1}} - d_{\text{step 1}}) \\ &\quad + W_{2,\text{step 2}}\,(d_{\text{step 2}} - \bar{d}_{\text{step 2}}) \\ &\quad + \ldots\ldots\, W_{2,\text{step 12}}\,(d_{\text{step 12}} - \bar{d}_{\text{step 12}}). \\ Y_3 &= W_{3,\text{step 1}}\,(d_{\text{step 1}} - \bar{d}_{\text{step 1}}) \\ &\quad + W_{3,\text{step 2}}\,(d_{\text{step 2}} - \bar{d}_{\text{step 2}}) \\ &\quad + \ldots\ldots\, W_{3,\text{step 12}}\,(d_{\text{step 12}} - \bar{d}_{\text{step 12}}). \quad (2) \end{aligned}$$

The values of the coefficients, $W_{i,j}$, are listed in Table II. The $W_{i,j}$ values are uniquely determined for a given set of characteristic vectors. It can be shown that the $W_{i,j}$ values are simple multiples of the corresponding elements of the characteristic vectors.

TABLE II. Weighting Factors for Computation of Scalar Multiples

Step	W_1	W_2	W_3
1	0.727	3.146	2.948
2	0.812	2.680	1.635
3	0.928	1.987	−0.028
4	1.072	0.756	−1.980
5	1.130	−0.625	−3.312
6	1.051	−1.826	−3.055
7	0.834	−2.188	−0.029
8	0.652	−2.118	2.305
9	0.463	−1.688	3.838
10	0.301	−1.094	4.299
11	0.194	−0.704	3.760
12	0.111	−0.347	3.173

Figure 4 is a plot of the mean tone-reproduction curve, $\bar{d}$, and of the following combinations:

(a) $\bar{d} + 2V_1$. (b) $\bar{d} + 2V_2$. (c) $\bar{d} + 2V_3$.

The three characteristic vectors represent the basically different ways in which the 170 tone-reproduction curves vary. Since only three vectors, together with the mean vector, are necessary for reconstitution of the original density data, a complete description of the shape of each of the 170 curves is given by the values of the scalar multiples, Y_1, Y_2, and Y_3.

Psychophysical Assignment of Quality Indexes

The assignment of quality indexes to the prints was performed independently for each scene. The various prints of each scene were submitted to each of 30 observers who were experienced in recognizing and evaluating tone-reproduction differences. Each observer was asked to rank the prints in order of subjective quality, and the print ranked as highest in quality was given a score of 1, the second-best print was given a score of 2, and so forth. The quality number finally assigned was the mean rank after a large number of observers had ordered the prints. A low mean rank was synonomous with high quality.

The prints were illuminated by a bank of fluorescent lights, the viewing illuminance being maintained at 80 ft-c.

The mean rank numbers were linearly transformed to a scale from 0 to 100 in which $Q = 100$ represented optimum quality and lower values of Q represented poorer quality. The transformation resulted from an additional experiment in which a number of experienced observers were asked to rate each of a series of prints of each scene on a scale from 0 to 100, 100 representing optimum quality reproduction for that scene. The linear transformation from mean-rank numbers to the Q values was the least-squares regression line relating the Q values to the mean ranks assigned to the prints by the panel of observers. It was found that approximately 10 units on the Q scale represent a quality change which would be discerned and similarly ranked by at least 85% of the observers.

Empirical Prediction of Subjective Qualities from the Scalar-Multiple Descriptions of the Tone-Reproduction Curves

Each of the prints can be characterized by two types of data: (1) the subjective quality index, Q, resulting from the judgment data, and (2) the scalar-multiple description of its objective tone-

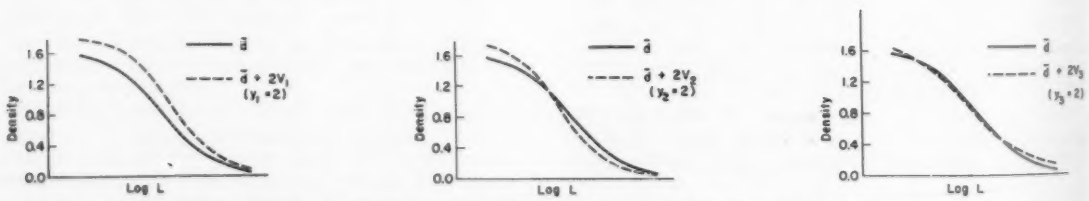

Fig. 4. Plot of the mean tone-reproduction curve and of combinations of the mean curve with each of the three characteristic vectors.

reproduction curve. The purpose of the experiment was to derive an empirical quantitative relationship between Q and the scalar multiples, Y_1, Y_2, and Y_3.

The form of regression equation chosen was:

$$Q = a_0 + a_1Y_1 + a_2Y_2 + a_3Y_3 + a_4Y_1^2 + a_5Y_2^2 + a_6Y_3^2 + a_7Y_1Y_2 + a_8Y_1Y_3 + a_9Y_2Y_3. \quad (3)$$

The coefficients, a_i, were derived by least-squares regression analysis for each scene; the coefficients were different from scene to scene. For each scene, the values of Y_1, Y_2, and Y_3 which make Q a maximum were found by partial differentiation of Eq. (3) with respect to each of the scalar multiples. Setting the partial derivatives equal to zero resulted in three simultaneous linear equations in Y_1, Y_2, and Y_3. The solution resulted in the values, $Y_{1.opt.}$, $Y_{2.opt.}$, and $Y_{3.opt.}$ which maximized Q in Eq. (3). Introducing the change of variable,

$$y_1 = Y_1 - Y_{1.opt.}$$
$$y_2 = Y_2 - Y_{2.opt.}$$
$$y_3 = Y_3 - Y_{3.opt.}$$

Equation (3) becomes

$$Q = b_0 + b_1Y_1^2 + b_2y_2^2 + b_3y_3^2 + b_4y_1y_2 + b_5y_1y_3 + b_6y_2y_3 \ldots \quad (4)$$

The variables, y_1, y_2, and y_3, describe the difference between the sample tone-reproduction curve and the optimum tone-reproduction curve for the scene type recorded.

Although the a_i in Eq. (3) varied from scene to scene, a single set of b_i values in Eq. (4) were found which provide excellent agreement between the psychophysically determined subjective qualities of all prints of all scenes and their associated tone-reproduction curve shapes, as specified by the y_i values. The equation, valid for any of the scene types studied, is:

$$Q = 100.0 - 3.54y_1^2 - 1.95y_2^2 - 5.10y_3^2 + 0.15y_1y_2 - 1.29y_1y_3 - 0.12y_2y_3 \ldots \quad (5)$$

Equation (5) permits the prediction of the subjective quality of any reproduction of a scene from y_1, y_2, and y_3, the differences between the scalar multiples of the sample tone-reproduction curve and the scalar multiples of the tone-reproduction curve which is optimum for the recorded scene type; no direct psychophysical test is required.

The ability to derive a single prediction function, valid for all scene types, means that departures of any given type from optimum tone reproduction for a given scene degrade the reproduction quality by the same amount as similar departures from optimum tone reproduction for any other scene.

Equation (5) is useful for predicting subjective quality for hypothetical or practical tone reproductions which differ in a known manner from optimum tone reproduction for the chosen scene type. Optimum tone-reproduction characteristics may differ from one scene type to another; at present, there is no known functional relationship between optimum tone-reproduction characteristics and objective descriptions of scene type. For the four scenes studied, the scalar multiples of the empirically determined optimum tone-reproduction curves are:

	Scene A	Scene B	Scene C	Scene D
$Y_{1,opt.}$ . . .	−0.52	0.88	0.49	1.05
$Y_{2,opt.}$ . . .	1.62	−0.62	−0.32	0.36
$Y_{3,opt.}$ . . .	−0.41	−0.44	−0.60	0.48

However, the optimum characteristics for the four scenes cannot be assumed to be valid for basically different scenes, and further psychophysical experiments of the type reported here will be necessary to provide optimum specifications for a comprehensive sampling of scene types. On the other hand, Eq. (5) has been shown to be valid for the various scenes thus far studied and an assumption of its validity for predicting subjective quality in other scene types seems justified.

Tests of the Validity of Eq. (5)

The validity of Eq. (5) can be tested by comparing predictions made from it with direct psychophysical tests. To facilitate the computation of tone-reproduction characteristics and predicted quality index pertinent to a given reproduction system, a computational program has been prepared for the IBM-705 digital computer in use at the Eastman Kodak Company. The program requires as input information:

(a) log camera luminances corresponding to equally spaced log scene luminances;
(b) density data at equally spaced log luminance values for the negative material;
(c) log printing luminance values at equally spaced values of negative density;
(d) print density data at equally spaced values of log printing luminance; and
(e) the optimum tone-reproduction characteristics for the assumed scene type.

The computer obtains the resulting tone-reproduction data at the 12 values of log scene luminance specified in the requirements for computing scalar multiples. The scalar multiples are computed and inserted into Eq. (5) to compute the quality index. In one operation, the program provides for computation of tone-reproduction data and predicted quality indexes for all possible combinations of as many as 999 values of each of the four input variables. The computations of tone-reproduction characteristics and subsequent quality predictions are made at the rate of 100 reproduction systems per minute.

The validity of the digital prediction method was tested as follows:

Negatives of Scene A were available from a camera exposure series made with a typical panchromatic negative sheet film. Prints of each negative were made on Kodak Polycontrast Paper at a number of closely spaced printing exposures for each of several

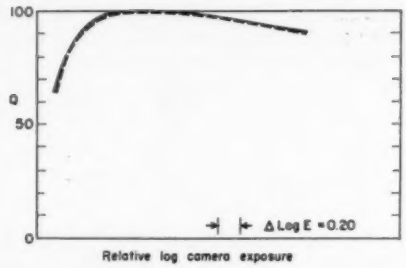

Fig. 5. Optimum print quality vs log camera exposure for a negative–positive system:
—— results of direct picture tests;
----- results of digital prediction technique.

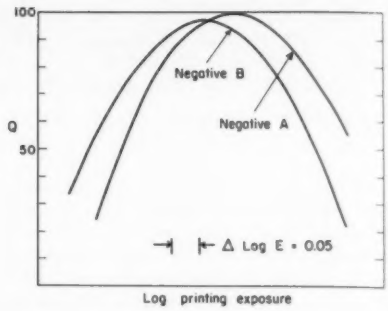

Fig. 6. Print quality as a function of log printing exposure for two negatives having different *D*-log-*E* characteristics.

contrast grades obtained by changing the spectral quality of the enlarging light source.

The prints were then examined by a group of observers, who selected the best print from each negative. The prints (representing the optimum prints which could be made from the negatives) were assigned a quality index on a scale from 0 to 100 by a group of 30 observers. The solid line in Fig. 5 is the resulting curve of quality as a function of log camera exposure.

The same reproductions were simulated digitally on the computer, and digital quality indexes were derived from Eq. (5). The computer result is shown as the dashed curve in Fig. 5. The agreement indicated is typical of the agreement between direct picture tests and predicted results from purely digital considerations based on several other direct tests of the validity of the digital technique.

Applications of the Digital Method

Assessment of the relative qualities of a large number of reproductions by purely digital operations on high-speed computing equipment provides opportunities for more extensive investigation into the characteristics of black-and-white reproduction systems than have been feasible by earlier psychometric methods. Such studies have been made, but the detailed results cannot be given here.

A partial list of the data obtained by the digital method involves print quality as a function of

1. camera flare characteristics;
2. negative exposure;
3. sensitometric characteristics of the negative material;
4. flare characteristics of the printing system;
5. printing exposure; and
6. sensitometric characteristics of the print material.

The studies serve to emphasize one important point: Small, but subjectively significant, quality differences can be realized by changing the *D*-log *E* characteristics of the negative and print materials, although these differences can be appreciated only when the levels of *all* the other variables of the reproduction system are carefully controlled.

The importance of optimizing the printing conditions cannot be emphasized too strongly when comparisons are being made of different negative materials. Even a slight error in printing exposure can obscure a potential quality improvement offered by a negative material with an improved *D*-log *E* curve shape.

In Fig. 6 are digitally derived curves of print quality vs. log printing exposure for prints made from two negatives on films with different *D*-log *E* characteristics. The print materials in both cases had previously been determined as optimum for the negatives. The subjective quality index was computed for each of several printing exposures used for both negatives; the curves of quality vs. log printing exposure demonstrate that, although the negative from Film A is capable of producing higher print quality at optimum printing exposure, even a slight departure from optimum printing exposure for Negative A can result in a print of lower quality than a print from Negative B made at the optimum printing exposure for B. Unless printing conditions are optimized, it is difficult to recognize potential quality improvements offered by a negative material with an improved curve shape.

The choice of negative exposure is a further critical factor in achieving optimum-quality reproduction. Data from extensive digital studies point up the fact that a valid comparison of the relative merits of two films requires extreme care and accuracy on the part of the technician preparing the demonstration prints.

Discussion

The results obtained from digital predictions of the relative subjective qualities associated with particular tone reproductions are in excellent agreement with accumulated experimental evidence. The new data are unique in that they provide quantitative relationships in place of the qualitative relationships that have been deduced from past studies. The use of the high-speed computer makes possible

studies that would be impossible to undertake in the laboratory. A recent digital study of 17,640 practical reproduction systems, represented by digital data, involved approximately 3 hr. of computing time on the IBM-705; a similar study in the laboratory would not be feasible.

The ability to specify quantitatively the effects of tone-reproduction variations on subjective quality encourages a further study of the interactions of tone-reproduction characteristics, image-structure characteristics, and viewing conditions with respect to their effects on the subjective quality of pictorial reproductions. Studies are now in progress to examine the effects of various viewing conditions on tone-reproduction requirements for optimum subjective quality.

Acknowledgments

Most of the laboratory work involved in preparing and measuring the prints used in this study was performed by J. R. Kelch and C. P. Bray, of the Kodak Research Laboratories. The author also wishes to acknowledge the valuable counsel given by C. N. Nelson and J. L. Tupper, of the Kodak Research Laboratories, and by F. C. Williams, of the Management Systems Development Department of the Eastman Kodak Company.

• SPSE Journal Award

Hellmut Frieser

Eberhard Klein

Helmutt Frieser and Eberhard Klein of the Agfa Scientific Photographic Laboratory have received the 1961 SPSE Journal Award "for the best technical paper published in *Photographic Science and Engineering*" during 1960. Their paper, "Contribution to the Theory of the Characteristic Curve," appeared in the September-October 1960 issue (*P S & E*, 4: 264). It dealt with a mathematical representation of the effects of grain size distribution, statistical quantum fluctuations, and sensitivity distribution on the location and shape of the characteristic curve.

Dr. Frieser, who received his doctorate in engineering from the Technical University of Dresden in 1928, has long concentrated on the science of photography. He was associated with the Scientific Photographic Institute of the Technical University, Dresden, until 1930, then went to Berlin, where he was first engaged in research on sound film and color cinematography at Siemens & Halske AG, and next joined the research staff of Zeiss-Ikon AG. In 1936, he returned to Dresden, where he was appointed Professor at the Technical University. He directed its Scientific Photographic Institute from that time until 1946, when he was taken to Russia. Following his release in 1952, he was appointed a Director of the Scientific Photographic Laboratories of Agfa, Bayerwerk, Leverkusen. In 1958, he returned to academic life as Professor and Director of the Institute for Scientific Photography at the Technical University, Munich.

Dr. Frieser's most important work includes photomicrographic investigations of the photographic process, studies of the graininess and resolving power of photographic layers, the application of transfer theory to photography, the theory of color photography, the effect of electrons on photographic layers, and the theory of the characteristic curve.

Dr. Klein studied chemistry in Bonn and Aachen, and was assistant from 1949 to 1952 at the Institute for Physical Chemistry at Aachen, from which he was graduated in 1951.

In 1952, he joined the Scientific Photographic Laboratories of Agfa under Dr. Frieser, and was appointed Dr. Frieser's successor as a director of the Agfa Scientific Photographic Laboratories in 1958. He is also a lecturer on the science of photography at the Technical University of Aachen.

Dr. Klein's principal work has dealt with the complex formation and the growth of silver halide crystals, the theory of development, the theory of the primary process in latent image formation, the sensitivity of photographic layers to electrons, and the theory of the characteristic curve.

PHOTOGRAPHIC SCIENCE AND ENGINEERING
Volume 5, Number 5, September-October 1961

On the Spatial Stability of Photographic Plates

J. H. ALTMAN AND R. C. BALL, *Research Laboratories, Eastman Kodak Company, Rochester, N.Y.*

Position data were obtained for 48 points in a transparent master grid, which was then printed by contact on samples of several current Kodak plates whose dimensional stability is of special interest. Comparable position data were obtained for the plates after development, the two sets of data were compared by an electronic computer, and the root-mean-square values of the position errors were computed for several assumed laws of variation. The best set was found to be that based on the assumption of a second-order over-all distortion, i.e., a distortion larger at the edges of the plate than in the center. The rms value of the residual random error between the actual positions of the plates and the most probable positions in the distorted grid image was of the order of 1.5 μ for Kodak Spectroscopic Plates, Type 103-F. This value includes not only the plate errors but also the comparator and operator errors, which are estimated to be about 1 μ. A few measurements were made on acetate-base film. The effects of some variations in processing and exposure on the magnitude of the random spatial errors were also studied. It was shown that improper handling during processing may have a perceptible effect on dimensional stability.

The fact that photographic materials having flexible bases may undergo dimensional changes during processing has been widely known for many years, and it has long been customary to use glass plates when a high order of dimensional accuracy is required. Even glass plates, however, have not been above suspicion, and several studies of the spatial stability of photographic plates have been reported, especially in the literature of astronomy. A survey of the literature shows that typical values reported for the spatial distortion of plates are generally of the order of 2 to 5 μ, depending upon the details of the experimental technique and the treatment of the data.[1]

Interest in this problem has increased in recent years because of the use of the photographic plate in many applications requiring the utmost in dimensional accuracy, such as the tracking of ballistic missiles.[2] At the same time, advances in the technology of plate manufacture, and especially in adhesion technology, have made it appear that the spatial-stability characteristics of the photographic plate may have been improved. Finally, the availability of electronic computers has made it convenient to analyze the data obtained from spatial-stability measurements more extensively than in the past. A new study of the dimensional characteristics of Kodak photographic plates has therefore been undertaken. The purpose of this paper is to describe the techniques employed in this study and the results obtained.

Communication No. 2198 from the Kodak Research Laboratories. Presented at the Annual Conference, Binghamton, N.Y., 23 May 1961. Received 19 June 1961.

1. H. Gollnow and G. Hagemann, *Astron. J.*, **61:** 399 (1956).
2. D. C. Brown, *Photogrammetric Eng.*, **25:** 372 (1959).

Experimental Procedure

The usual procedure for checking the spatial stability of a photographic material is to print some sort of known grid pattern onto the sample under test and, after processing, to compare the dimensions of the print with those of the original. Techniques have been devised for reducing the labor involved in such comparisons.[3] It was apparent that the accuracy of measurement required for the present project would be 1 μ or less, and it was finally decided that, of the methods available to us, the best would be direct measurement by a suitable comparator. Furthermore, such measurements would provide data in convenient form for subsequent analysis on an electronic computer.

A suitable master grid, consisting of fine clear lines on a very dense background, was therefore prepared. The spacing between adjacent lines was $\frac{1}{2}$ in. in both directions. The positions of 48 line intersections in a 4- by 6-in. area of this master plate were then carefully determined on a high-quality double-screw comparator. There were no requirements for accuracy in the preparation of the master plate, since it was calibrated on the comparator before use.

Having been calibrated, this master plate was then contact-printed onto the samples under test. All the prints were made with a vacuum-contact frame and a point source of ultraviolet radiation. The purpose of this printing procedure was to obtain the sharpest possible lines for subsequent measurement. This precaution proved useful in reducing measurement errors, as will be described later.

In most cases, the plates were processed in a tray, being agitated by rocking, and were allowed to dry slowly while lying flat. The image on the processed test samples consisted of fine dark lines on a clear background. The line width was of the order of 12 μ. Each of the processed prints was then measured on the comparator, and posi-

3. J. M. Calhoun, L. E. Keller, and R. F. Newell, Jr., *Photogrammetric Eng.*, **26:** 661 (1960).

TABLE I. Materials and Processing Conditions

Material	Kodak developer	Devel. time, min
Kodak High Resolution Plate	D-8 (2:1)	2
Kodak Aerial Plotting Plate (Medium)	Dektol (1:2)	1½
Kodak Aerial Plotting Plate (Contrast)	Dektol (1:2)	1½
Kodak Spectroscopic Plate, Type 103-F	D-19	4
Kodak Plus-X Aerecon Film (Nontopographic triacetate support)	D-19	8

tion data for the 48 reference points were obtained. The operator attempted to center the hairline on the image; this was facilitated by the fact that the hairlines of the instrument are discontinuous. Finally, the position data obtained from the prints were compared with those obtained from the original master grid. This was done on an IBM 705 Computer.

Several Kodak materials whose dimensional characteristics are of current interest were analyzed in this manner. Table I lists the materials which were studied and the conditions of the processing.* The High Resolution Plate is a very slow fine-grained material much used for the preparation of reticles, scales, etc. The Aerial Plotting Plates are positive types of materials used to prepare prints for map-making.

Since the Type 103-F Plate is used for missile-tracking, the properties of this material are of great interest. It was studied over a period of time, and samples from a number of coatings were evaluated. The effects on this emulsion of some variations in processing conditions were also noted. Finally, some measurements were made on Aerographic emulsions coated on a flexible support.

Analysis of Data

The final data obtained from the comparator consist of a set of x,y-coordinates describing the position of each of the 48 intersections in the master grid, and a similar set of coordinates giving the measured positions of the 48 intersections in each print. The variations of the coordinates of each point in the print from those of the corresponding points in the master furnish, of course, the desired information. In general, some unknown amount of rotation and translation exists between the two sets of data, since it is unlikely that the master and the sample would be placed on the comparator in exactly the same position. The translation term is readily removed. The rotation term is usually very small, since the operator aligned all the plates on the comparator before measuring them, and it was found to be of the order of 5×10^{-5} radian or less.

For analyzing the spatial distortions of photographic materials, the net error may usefully be treated as consisting of two separate parts. The first is an over-all distortion affecting the entire emulsion surface in some manner which can be determined and described: for example, a uniform shrinkage of the sample, such as is common with acetate supports. If the amount of shrinkage can be determined, mensurational data obtained from the film can be corrected and the systematic error much reduced. Superposed upon this type of error, however, there may remain additional random errors arising from numerous small causes; correction cannot be made for these errors, even if the causes are known, because of their erratic variations. Essentially, these errors determine the limit of accuracy of the photographic system.

The fitting operation is commonly carried out in many applications of photography requiring extreme accuracy, such as in missile-tracking and photogrammetry. Accordingly, the error data of the present experiment have been analyzed not only for the simple case of no over-all corrections, but also with compensation for various types of over-all distortion. Analyses were made for distortions following linear, quadratic, and cubic laws. The linear case corresponds to a uniform shrinkage or swelling of the sample. The quadratic case corresponds to a distortion which increases from the center to the edges of the plate, and the cubic case corresponds to a distortion which first increases outward from the center of the plate, then decreases slightly, and finally increases again.

The data supplied to the computer were the net position-difference values, with translations removed. However, the rotation differences, which were small, were left in the raw data for reasons of convenience. From these data, the root-mean-square (rms) value of the position error was calculated, without compensation for the over-all distortions or the residual rotation. First-order, second-order, and third-order least-square fits were then made to the data, and, for each fit, the rms value of the position error still remaining was determined. Any rotation error in the data was also removed in the calculation of the least-square fits. Errors were calculated for both the x- and the y-coordinates separately, and they were then combined into a "radial-error" figure to give a single value for the error of the sample.

The calculations were carried out as follows: Let Δx and Δy, the departures of the measured positions from the master grid, be functions of x and y which are expanded in a polynomial:

$$\begin{aligned} \Delta x = f(x,y) &= a_0 + a_1 x + a_2 y \\ &\quad + a_3 x^2 + a_4 xy + a_5 y^2 \ldots \\ \Delta y = f(x,y) &= b_0 + b_1 x + b_2 y \\ &\quad + b_3 x^2 + b_4 xy + b_5 y^2 \ldots \end{aligned} \tag{1}$$

Then

$$\begin{aligned} \Delta x - f(x,y) &= \epsilon_x \\ \Delta y - f(x,y) &= \epsilon_y, \end{aligned} \tag{2}$$

where ϵ_x and ϵ_y are the errors remaining after p terms. The standard deviation of the errors is given by

$$\sigma_x = \left[\frac{\Sigma[\Delta x - f(x,y)]^2}{n - \gamma}\right]^{1/2}, \tag{3}$$

where γ is the number of coefficients $a_0, a_1, a_2 \ldots$ in Eqs. (1), and n is the number of values used in the computation—in this case, 48. The radial error is then computed by combining the two standard deviations in the usual manner:†

$$\sigma_R = (\sigma_x^2 + \sigma_y^2)^{1/2}. \tag{4}$$

* The data presented here are representative of the emulsions manufactured at the time the experiment was made. It must be recognized, however, that the characteristics of products of the same name may vary within manufacturing tolerances at any given time and may change significantly from time to time.

† Generally speaking, the x- and y-errors can be combined into a "radial error" in this manner only when the two errors are of the same magnitude and are not correlated. It was found experimentally that the errors for plates were similar in the coating direction and normal to it. Also, analysis of the data indicated that there was no significant degree of correlation between σx and σy after systematic errors had been removed.

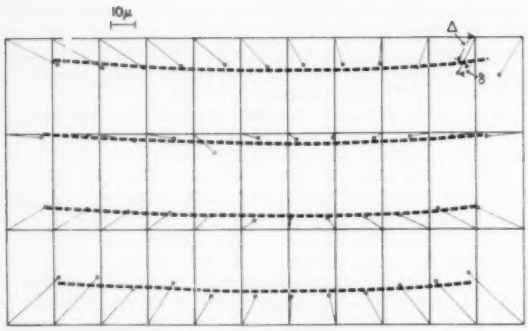

Fig. 1. Spatial distortion of film sample. Small circles represent points in the photographic image corresponding to the intersections of the rectangular grid in the object to which they are respectively connected. Broken lines indicate the computed second-order curves that best represent the image points as a whole. The displacement eliminated by referring the image points to the computed curves instead of to the original grid is Δ; the random displacement still remaining is δ. The measured intersection points in the grid image were $\frac{1}{3}$ in. apart in the horizontal direction and 1 in. apart in the vertical direction.

Thus, for a constant fit,

$$\sigma_C = \left[\frac{\Sigma(\Delta x - a_0)^2 + \Sigma(\Delta y - b_0)^2}{47}\right]^{1/2}. \quad (5)$$

For a linear fit,

$$\sigma_L = \left\{\frac{\Sigma[\Delta x - (a_0 + a_1 x + a_2 y)]^2 + \Sigma[\Delta y - (b_0 + b_1 x + b_2 y)]^2}{45}\right\}^{1/2}, \quad (6)$$

and similarly for higher-order fits.

The fitting process is illustrated in Fig. 1, which shows the analysis of a film sample. For purposes of illustration, the test object has been shown as a perfect grid. The position errors of the intersections, as measured in the sample under test, are shown by the displacements of the small circles from the intersections of the grid. The second-order fit derived by the computer is shown by the broken lines.

Results

The results of our tests on selected materials are summarized in Table II. All are rms radial errors and include the errors of measurement of the experiment. Sixty-three percent of the dimensional errors encountered will be smaller in magnitude than this value, and substantially all the errors will be less than plus or minus three times this value. Eleven batches of the Type 103-F Plate were measured to determine the batch-to-batch consistency of the values.

The experimental error was estimated by comparing two complete sets of readings of the master grid against each other. These data are given by the entry "Master grid" in the table. Since the combined system error for both coordinates is of the order of 1 μ or slightly less, the rms value of the experimental error in either coordinate direction taken singly is of the order of 0.7 μ. This value includes operator error, instrument error, and any long-range changes in the master grid itself, and appears to be reasonable for a comparator calibrated to the nearest micron.

The other entries in Table II give the residual system error, including errors of measurement in all cases. The column heading "No fit" refers to

TABLE II. Results of Evaluations

Material	Date of manufacture	Residual rms error in μ after: No fit	Linear fit	Quadratic fit	Cubic fit	Over-all change
Master grid	——	8.8	1.0	0.9	——	+ 1.5
Kodak High Resolution Plate	——	1.3	1.3	1.2	1.0	+ 0.5
Kodak Aerial Plotting Plate (Medium)	——	1.4	1.0	0.9	0.8	+ 2.0
Kodak Aerial Plotting Plate (Contrast)	——	3.8	1.4	1.1	1.1	+ 2.0
Kodak Spectroscopic Plate, Type 103-F (regular glass)	6/60	——	1.7	1.4	——	——
	6/60	——	1.3	1.2	——	——
	9/60	——	1.2	1.0	——	——
	9/60	——	1.3	1.1	——	——
	10/60	——	1.6	1.4	——	——
	12/60	4.3	1.5	1.4	——	+ 3.5
	1/61	2.7	1.6	1.2	1.1	+ 3.0
	1/61	3.5	1.4	1.2	1.2	+ 3.0
	2/61	2.6	1.3	1.2	——	+ 3.5
	3/61	1.5	1.2	1.1	1.1	——
	3/61	12.9	1.3	1.2	1.0	——
Kodak Spectroscopic Plate, Type 103-F (micro-flat glass)	——	——	1.1	0.9	0.8	——
Kodak Plus-X Aerecon Film Rapidly dried (water spots)	——	54.5	17.2	16.0	15.4	−70.0
Slowly dried (Kodak Photo-Flo)	——	——	3.5	2.6	——	——

the rms error remaining after the removal of translation only; the other types of fit are as discussed. The heading "Over-all change" refers to the differences in the lengths of the grid diagonals between the master and the various prints. It shows the magnitude and sign of the over-all change which occurred in the sample. The nominal length of this diagonal is approximately 183 mm, which may be used as the basis for computing the fractional over-all change.

The magnitude of the reduction in the residual error which may be achieved if it is possible to determine and correct for over-all distortion is indicated by comparing the simple analysis with the more complex ones. Thus, the column labeled "No fit" shows errors which, in many cases, are similar in magnitude to those reported previously in the literature. However, when compensation is made for the first-order distortions of swelling and rotation ("Linear fit"), a significant drop in residual random error is immediately achieved. If the process is then extended to a second-order over-all distortion ("Quadratic fit"), a further reduction in residual error results. However, no consistently significant reduction in residual error appears to be produced by a more complicated formula ("Cubic fit"). It is therefore concluded that, in general, a second-order distortion of the surface is produced by processing, and this conclusion is confirmed by graphic analysis of the data.

When a second-order formula is applied to the data, the residual rms value of random radial distortion of the plates is found to lie between about 1.0 and 1.4 μ. Furthermore, if the variance of measurement adds to the variance of plate positions in the usual fashion (Eq. (4)), then it follows that the net rms value of the plate error must be of the order of 0.5–0.7 μ.

This conclusion is supported by two recent publications. At the National Physical Laboratories, J. M. Burch[4] has measured the spatial stability of a high-resolution plate by means of an elegant technique which employs moiré patterns generated by interference fringes. He concluded that the spatial instability of the material was of the order of micro-inches (1 μ in. = 1/40 μ).

4. J. M. Burch, *Research*, **13**: 2 (1960).

TABLE III. Rapid Process for Kodak Spectroscopic Plate, Type 103-F

	Time, min	Temp, °F
Kodak Developer D-19	2	80
Kodak Stop Bath SB-5c	¼	80
Kodak Rapid Liquid Fixing Bath	2	80
Kodak Hypo Clearing Agent	½	80
Wash	2½	80
Kodak Photo-Flo	¼	80
Dilute ethyl alcohol (3:1)	½	80
Dry in hot air blast	~2	—

Gollnow and Hagemann[1] have also studied the dimensional characteristics of spectroscopic plates. Their results are interesting because they show very large distortions arising at the edges of their samples. The present studies have also shown such errors within a band about 1 cm wide around the edge, although the magnitude of the errors detected in most cases has been considerably less than those of Gollnow and Hagemann. Where extreme dimensional stability is required, a 2-cm-wide band adjacent to the edges of the plate should be avoided. If, however, the points adjacent to the edges of Gollnow and Hagemann's samples are discarded and a line of regression is fitted to the remainder of the data, the residual rms error is found to be less than 1 μ.

The data given in Table II for film coated on acetate support illustrate another aspect of the problem of minimizing random spatial errors. The rms spatial error for a sample of acetate film which was dried in an air blast under conditions permitting the formation of water spots is shown by the table to be about 17 μ for a linear fit. When a similar sample was bathed in Kodak Photo-Flo before being dried and was allowed to dry slowly under minimum tension, the error dropped to 3.5 μ. This is in general agreement with the results of Calhoun, Keller, and Newell[3] and emphasizes the importance of careful handling of the samples, especially those on acetate support. Water-spot distortion can also occur in plates, and in the present experiment all the samples were bathed in Photo-Flo before being dried.

A few data were also obtained from experimental films coated on Estar support. Such films were found to exhibit moderately less shrinkage and random distortion than the acetate samples and to be much more resistant to random errors caused by casual handling. Avoidance of water spots is, of course, desirable in this case also. The dimensional characteristics of Estar films have been discussed by Calhoun, Adelstein, and Parker.[5]

Since rapid readout is very important in some forms of data recording, we have made some measurements with high-speed processes. Of interest is a process for the Type 103-F Plate devised by R. W. Henn, of these Laboratories, in which processing, including drying, is completed in 10 min. Table III summarizes the process, and Table IV shows the re-

5. J. M. Calhoun, P. Z. Adelstein, and J. T. Parker, presented at the March 1961 meeting, Society of Photogrammetry, Washington, D.C.

TABLE IV. Effect of Processing on Residual Error

Error is expressed as rms error in microns for type of fit given. Kodak Spectroscopic Plate, Type 103-F

Process	Linear fit	Quadratic fit	Cubic fit	Over-all change
Regular	1.3	1.2	——	+3.5
Rapid (Table III)	1.5	1.4	1.3	−2
Regular (nonhardening fixer)	3.6	3.3	——	−8

TABLE V. Effect of Line Width on Residual Error

Error is expressed as rms error in microns for a quadratic fit. Kodak Spectroscopic Plate, Type 103-F

Line width	Error
11 μ	1.2
14 μ	1.2
23 μ	1.6

sults compared with the results for the regular type of development for the same coating from Table II. It is evident that even the severe treatment of processing at 80°F and drying in a blast of hot air has not increased the residual error prohibitively. The effect of hardening is shown by measurements on a sample which was processed and handled normally, except that it was fixed in a nonhardening fixing bath. This process produced the largest error encountered in any measurements made on plates and emphasizes the importance of proper hardening of the emulsion.

Finally, we made some measurements to investigate the effect of the image characteristics on the accuracy of measurement. For example, the images upon which the comparator was set have, in all cases, been very fine, sharp lines. Measurements were made on plates bearing grid lines of three different widths, and it was found that the total rms error increased as the line width increased. These data are summarized in Table V, from which it will be seen that the points used for measurement should be made as small and as sharp as possible. This conclusion is hardly surprising, but the data do give some indication of the improvement in accuracy resulting from the use of fine lines.

Acknowledgment

We are indebted to B. E. Bayer and S. A. Tuccio, of these Laboratories, for advice and assistance on the numerical analysis of the data, and to J. M. Burnham, of the Plate Manufacturing Division of the Eastman Kodak Company, for his cooperation.

• Nomenclature for Fourier Transforms of Spread Functions

The International Commission for Optics (ICO) has formed a Subcommittee for Image Assessment Problems. It consists of Prof. A. Arnulf, Paris, Dr. H. H. Hopkins, London, Prof. H. Kubota, Tokyo, Dr. K. Rosenhauer, Braunschweig, and Dr. R. Scott, Norwalk, Conn., with the writer as Chairman. Following a proposal of Dr. G. C. Higgins, Rochester, N.Y., this Committee has made recommendations on nomenclature for what is at present known under a variety of names, e.g. sine-wave response, frequency response, contrast transfer, etc. After extensive correspondence and examination of the matter, the Committee has, at sessions in Paris and London in July 1961, unanimously arrived at the recommendations below. Dr. Kubota could not be present and was represented by Drs. K. Kinosita, K. Murata, and K. Sayanagi; Dr. D. L. MacAdam, Rochester, N.Y., also took part in the discussions and decisions. In making recommendation No. 1, the Committee had in mind first that *response* ordinarily means that the output is of a different nature from the input and should on this account be avoided, and secondly that the word *contrast* is not uniquely defined and is moreover a concept much used in photography in another sense. The recommendations are given here in English, together with the proposed equivalent terms in French and German.

Recommendations

(1) The functions indicated in the heading, the curve representing it, and its value for a given spatial frequency shall be called the:

Optical transfer function/curve/factor; Fonction/courbe/facteur de transfert optique; Optische(r) Übertragungsfunktion/kurve/faktor.

The function as denoted is the complex function. When the modulus is referred to, it shall be denoted by the terms:

Modulation transfer function/curve/factor; Fonction/courbe/facteur de transfert de modulation; Modulationsübertragungsfunktion/kurve/faktor.

The argument of this shall be referred to by the terms:

Phase transfer function/curve/value; Fonction/courbe/valeur de transfert de phase; Phasenübertragungsfunktion/kurve/wert.

It is to be understood that the prefix *transfer* may be omitted when confusion cannot arise.

(2) The variables of these functions shall be termed:

Spatial frequency;
Fréquence spatiale;
Ortsfrequenz.

(3) The unit of spatial frequency shall be described by either:

Cycles per mm or *lines per mm.*

The latter shall be used when no confusion can occur with television lines, since 2 television lines = 1 cycle. The corresponding terms are:

Cycles par mm; lignes par mm;
Perioden pro mm; Linien pro mm.

ERIK INGELSTAM, *Institute of Optical Research, Stockholm 70, Sweden*

PHOTOGRAPHIC SCIENCE AND ENGINEERING
Volume 5, Number 5, September-October 1961

The Adsorption of Development-Restrainers to Silver and Their Effects on Physical Development

R. J. NEWMILLER AND R. B. PONTIUS, *Research Laboratories, Eastman Kodak Company, Rochester, N.Y.*

The adsorption to a clean, metallic silver surface of 1-phenyl-5-mercaptotetrazole, benzotriazole, and potassium iodide was measured. The phenylmercaptotetrazole was found to cover the silver surface completely with an apparent monolayer. The maximum coverage of the benzotriazole was only 10 to 15% of the surface. Potassium iodide was found to cover only about 5% of the surface in an air-free system, but when air was present, rapid adsorption occurred to at least monolayer coverage calculated as silver iodide.

The data obtained from the adsorption measurements were utilized in designing pure physical development experiments. The compounds were added directly to the developers in concentrations adequate for maximum adsorption to the nuclei surface but not great enough to affect the pAg. Phenylmercaptotetrazole completely stopped the development, whereas benzotriazole showed little effect. Potassium iodide, when placed in the developer, gave evidence consistent with the view that prior adsorption of silver ion is required for iodide to inhibit development. The dye cation, 1,1′-diethyl-2,2′-cyanine, was found to adsorb to metallic silver, regardless of whether or not air was present. When added to a physical developer containing iodide, this dye forms an insulating layer on the nucleus, and, like silver iodide, suppresses development.

The mechanism of physical development is generally believed to involve the adsorption of developing agent[1,2] or silver ion,[3] or both,[4] to a suitable substrate. The substrate, usually a metallic or electronic conductor,[5-7] serves as a medium of transfer for the electron to pass from the developing agent to the silver ion. The substrate acts as a catalyst for the reaction, as it permits the reduction to occur at a lower activation energy than would be required in the solution phase. This lowering of the activation energy is a direct result of the adsorption of either, or both, of the reacting species to the substrate.[3] It is felt that direct measurements of the adsorption of materials which enhance or retard the catalytic action of the substrate would greatly benefit our understanding of the mechanism.

Some better known development restrainers are 1-phenyl-5-mercaptotetrazole and benzotriazole. Iodide ions, under proper conditions, can also inhibit physical development. Certain cyanine dyes are restrainers if they are adsorbed in the presence of iodide ion. The adsorption of each of these species to clean metallic silver was measured. The effects of these compounds on nuclei for physical development were determined in pure physical developers, and the results related to the adsorption measurements.

Communication No. 2179 from the Kodak Research Laboratories. Presented at the Annual Conference, Binghamton, N.Y., 26 May 1961. Received 15 June 1961.

1. R. J. Newmiller and R. B. Pontius, *J. Phys. Chem.*, 64: 584 (1960).
2. T. H. James, *J. Chem. Ed.*, 23: 597 (1946).
3. ———, "Catalytic Phenomena Related to Photographic Development," in *Advances in Catalysis*, Vol. 2, p. 105, Academic Press, Inc., New York (1950).
4. T. H. James and G. Kornfeld, *Chem. Revs.*, 30: 1 (1942).
5. G. P. Faerman and E. D. Voeikova, *Uspekhi Nauch. Fot.*, 3: 174 (1955).
6. J. Eggert, *Phot. Sci. and Eng.*, 1: 94 (1958).
7. H. Eggenschwiller and W. Jaenicke, *Z. Elektrochemie*, 64: 391 (1960).

Adsorption Measurements

The procedure previously used to measure the adsorption of photographic developers to clean metallic silver[1] was used to measure the adsorption of phenylmercaptotetrazole and benzotriazole, except that the fine silver wire used in the previous experiments was replaced by an 80 × 80 woven silver mesh. The mesh had a wire diameter of 0.0045 in. and a specific geometric surface of 26.7 sq cm/gram. About 100 grams of mesh were used in each determination. The mesh was wound in a coil and placed in a Pyrex-glass tube. The tube was inserted in a furnace, hydrogen was slowly passed in, and the temperature raised to 600°C for 1 hr. The tube was then cooled and inserted in the system for measuring the adsorption, air being excluded at all times. The system was flushed with pure dry nitrogen, and a known amount (normally 50 ml) of a carbonate-buffered solution (pH = 11.1) containing the restrainer was added. A circulating pump was started and the concentration of restrainer was followed as a function of the optical density at a suitable ultraviolet wavelength on a Beckman DU Spectrophotometer.

Results of Adsorption Measurements

Adsorption isotherms at 25°C have been measured for benzotriazole and phenylmercaptotetrazole and are presented in Fig. 1. The isotherms show that the phenylmercaptotetrazole covers the silver far better than does the benzotriazole. If the phenylmercaptotetrazole is assumed to cover 30A² of silver surface adsorbed end-on, then the amount adsorbed is about 60% greater than that which would be calculated on the basis

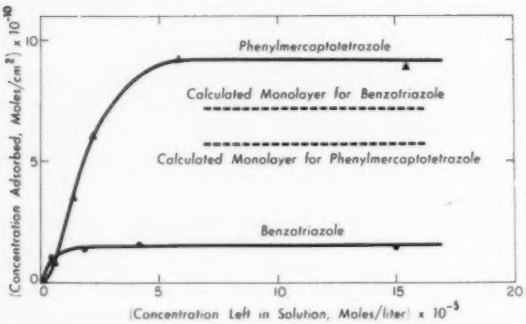

Fig. 1. Adsorption isotherms for restrainers at 25°C on clean metallic silver, pH 11.1. ▲ — phenylmercaptotetrazole; ● — benzotriazole.

of monolayer coverage of a smooth geometric surface. The actual surface of the wire is not perfectly smooth, and a roughness factor of 1.6 would account for the additional material adsorbed. It is probable that the phenylmercaptotetrazole covers the silver surface completely with a close-packed monolayer.

In contrast, benzotriazole does not appear to adsorb very strongly and the equilibrium coverage is considerably less than a monolayer. The benzotriazole should present an end-on area of about 23A²/molecule, and from this the surface covered is calculated and found to be only about 10 to 15% of that covered by phenylmercaptotetrazole. The reason for the failure of benzotriazole to complete a monolayer on the surface may be that the adsorptive forces are only strong enough to hold the molecules at active sites, such as surface defects.

The adsorption, particularly in the case of the phenylmercaptotetrazole, is very sensitive to small traces of air. If air is allowed to enter the system, adsorption occurs much more rapidly and the equilibrium concentration attained usually is slightly greater. This effect is probably caused by the oxidation of the silver surface, forming silver ions which then react with the restrainer to form a silver salt. The isotherms presented represent the adsorption in a system which is as free from air as possible without resorting to high-vacuum techniques.

Adsorption of Cyanine Dyes

The adsorption of 1,1′-diethyl-2,2′-cyanine chloride and 1,1′-diethyl-2,2′-cyanine iodide to metallic silver has also been measured by a technique similar to that used with the restrainers. The dye solutions were buffered with carbonate at pH 11.1 and the residual dye was analyzed at a suitable wavelength of visible radiation. Figure 2 shows that there is little difference between the adsorption isotherms for the chloride or iodide salts of the dye. The presence or absence of air

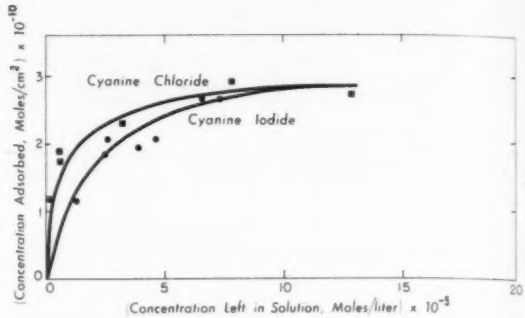
Cyanine Chloride
Cyanine Iodide
(Concentration Adsorbed, Moles/cm²) x 10⁻¹⁰
(Concentration Left in Solution, Moles/liter) x 10⁻⁵

Fig. 2. Adsorption isotherms for two cyanine dyes at 25°C on clean metallic silver, pH 11.1. ■ — 1,1′-diethyl-2,2′-cyanine chloride; ● — 1,1′-diethyl-2,2′-cyanine iodide.

had no significant effect on the amount of dye adsorbed.

The saturation level of both dyes corresponds to monolayer coverage of the silver mesh if each dye molecule is assumed to cover 79A² of surface.

The Adsorption of Iodide

Iodide adsorption was measured by a technique similar to that used with the restrainers and dyes, except that the method of analysis was different. Larger volumes of solution (about 200 ml) were used and small aliquots were removed periodically. The residual iodide was then analyzed by a spectrophotometric determination of a palladium-iodide complex, as described by Chapman and Sherwood.[8]

The iodide ion, in the absence of air, will adsorb only to a maximum coverage of about 5% of the surface. However, when air is not excluded from the system, larger quantities of iodide are adsorbed. Equilibrium is established at a level approximately corresponding to monolayer coverage, if the monolayer coverage is calculated as silver iodide. Veselovsky[9] has found that the presence of air will oxidize a clean silver electrode in solution to the extent that the silver-ion concentration may be as high as 10^{-5} M or greater. Iodide would then be expected to adsorb readily to a silver surface already covered with silver ion.

Effects of Adsorption on Physical Development

In view of the fact that the extent of the adsorption of these various materials to clean silver is now known, it is desirable to see how this information can be applied to actual physical development. All of the compounds studied have some effect on chemical development. It is necessary, therefore, to use a system in which only physical development can take place. The pure physical developers described by Cole and Pontius[10] were found to be quite suitable for the purpose. In these developers, the silver ion is buffered at a very high pAg by a thiosulfate–silver-ion complex. Two developers were used in this work:

8. F. W. Chapman and R. M. Sherwood, *Anal. Chem.*, **29**: 172 (1967).
9. V. T. Veselovsky, *Acta Physiochimica, URSS*, **11**: 815 (1939).
10. R. M. Cole and R. B. Pontius, *Phot. Sci. and Eng.*, **5**: 154 (1961).

CD-3 Developer

Silver-ion concentration 4×10^{-13} *M*; pH 12.0; temp. 25°C.

Solution A

Deaerated distilled water	800	ml
* CD-3 Developing Agent	2.25	grams
Tribasic potassium phosphate	50.0	grams

Solution B

Potassium chloride	0.61 grams dissolved in 50 ml distd. water
Silver nitrate	0.61 grams dissolved in 50 ml distd. water

The AgCl was precipitated and allowed to stand in a dark bottle. The supernatant liquid was decanted and the precipitate dissolved in a solution of 6.20 grams of sodium thiosulfate pentahydrate dissolved in 100 ml of distilled water.

Solutions A and B were mixed and diluted to a final volume of 1000 ml. 6*N* sulfuric acid was used to adjust the pH to 12.00.

MQ Developer

Silver-ion concentration 1×10^{-13} *M*; pH 11.0; temp. 25°C.

Solution A

Deaerated distilled water	800	ml
Metol Developing Agent	0.444	grams
Hydroquinone	0.284	grams
Dibasic potassium phosphate	50.0	grams

Solution B

Same as for Solution B of CD-3 Developer, except that a solution of 10.50 grams of sodium thiosulfate pentahydrate in 100 ml of distilled water was used to dissolve the AgCl.

Solutions A and B were mixed and diluted to 1000 ml. The pH was adjusted to 11.00 with 25% potassium hydroxide solution.

The majority of the development experiments were carried out on coatings of 15 mg/sq ft of Carey-Lea-type colloidal silver dispersed in gelatin. Nitrogen-burst agitation was used in all experiments.

The mean size and specific surface of these colloidal silver particles have been determined from electron micrographs and found to be 140A and 3.8×10^5 sq cm/gram, respectively. It should be stated here that the true status of the surface of this colloidal silver has not been determined. It is assumed, however, that it is at least representative of the surface presented by developing silver filaments. It is also realized that, in addition to the restrainer, the complexing ion, the buffer, water, gelatin, and any other ions which may be present in the system may compete with the developer for the adsorption sites. The effects of these species will have to be assessed in future work.

The low silver-ion concentration of the physical developers makes it possible to add separately each of the restrainers in a concentration corresponding to saturation levels of adsorption without exceeding the solubility product. The two materials which have the most insoluble silver salts are the iodide ion (silver iodide, $K_{sp} = 1.5 \times 10^{-16}$) and phenylmercaptotetrazole (silver salt, $K_{sp} = 9.3 \times 10^{-15}$).[11] Concentrations of 5×10^{-5} *M* of either of these materials can be added to a developer containing the thiosulfate–silver-ion complex with a silver-ion concentration of 1 to 4×10^{-13} *M* without precipitating any of the restrainer.

The effect of 5×10^{-5} *M* benzotriazole and phenylmercaptotetrazole on pure physical development by CD-3 Developer is shown in Fig. 3 by Curves B and C. The data are presented as analyzed silver in milligrams per square foot plotted against time of development, with the initial level of colloidal silver subtracted out. The weakly adsorbing benzotriazole causes only a slight restraint of the development while the stronger adsorbing phenylmercaptotetrazole completely halts the catalytic reduction of silver ion. Since the concentration of both restrainers was at a saturation level, there is strong evidence that the retardation is a direct function of the amount of colloidal silver surface covered. To test this hypothesis, a concentration of phenylmercaptotetrazole was chosen (see Fig. 1) which should yield a surface coverage similar to that of benzotriazole at the saturation level. The concentration chosen, 2×10^{-7} *M*, was added to CD-3 Developer. Curve D on Fig. 3 shows that the amount of suppression is very close to that obtained with saturation coverage of benzotriazole (Curve B). Concentrations of 5×10^{-6}, 1×10^{-5} and 5×10^{-5} *M* of phenylmercaptotetrazole were also tested in the MQ Developer. As the concentration of the restrainer is reduced from the saturation level, the amount of development suppression also decreases, as is seen in Fig. 4.

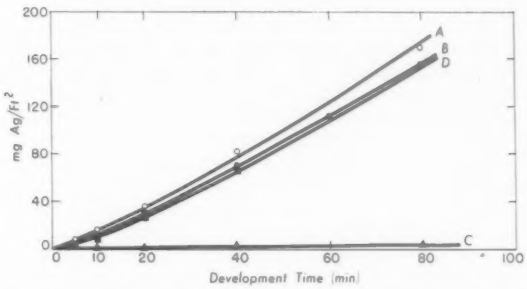

Fig. 3. Effect of restrainers on CD-3 (pure physical) Developer at pH 12. CD-3 concentration, 0.00516 M. Silver-ion concentration, 4×10^{-13} M. Curve A. ○ — control; Curve B. ● — 5×10^{-5} M benzotriazole; Curve C. ▲ — 5×10^{-5} M phenylmercaptotetrazole; Curve D. ■ — 2×10^{-7} M phenylmercaptotetrazole.

* CD-3 is the commercial designation of Kodak Developing Agent, 4-amino-3-methyl-N-ethyl-N-(β-methylsulfonamidoethyl)aniline sesquisulfate monohydrate.

11. G. P. Faerman and A. P. Pletner, *Uspekhi Nauch. Fot.*, 5: 114 (1957).

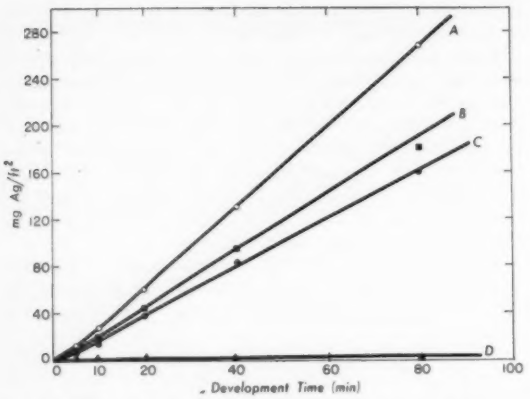

Fig. 4. Effect of various concentrations of phenylmercaptotetrazole on a Metol-hydroquinone pure physical developer at pH 11.0. Developer concentrations, 0.00516 M (total of MQ in equimolar concentrations). Silver-ion concentration, 1×10^{-13} M. Curve A. ○ — control; Curve B. ■ — 5×10^{-6} M phenylmercaptotetrazole; Curve C. ● — 1×10^{-5} M phenylmercaptotetrazole; Curve D. ▲ — 5×10^{-5} M phenylmercaptotetrazole.

Effect of Iodide Ion

The mechanism of the iodide adsorption and its inhibition of physical development is somewhat different from that of the organic restrainers. In the absence of air, 5×10^{-5} *M* of potassium iodide adsorbs very little to silver. If this concentration of iodide is added to CD-3 Developer, the analyzed-silver results are found to be only slightly less than the control, as can be seen in Fig. 5. The iodide, however,

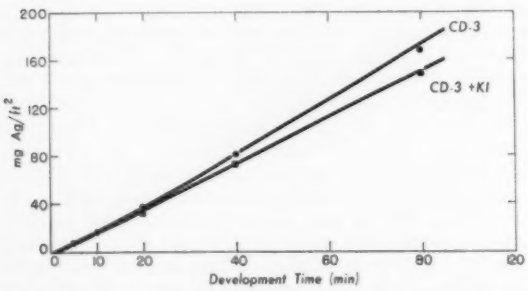

Fig. 5. Effect of iodide on CD-3 Developer at pH 12.0. CD-3 concentration, 0.00516 M. Silver-ion concentration, 4×10^{-13} M. ● — control; ■ — 5×10^{-6} M KI in developer.

has a very pronounced effect on the covering power, as seen in Fig. 6. Covering power is defined as net diffuse density to a broad-band red filter times 100, divided by the net amount of developed silver in milligrams per square foot. This effect can be explained by recalling that iodide in the presence of air (and therefore silver ion) can adsorb to silver, apparently forming silver iodide. In the 15-mg/sq ft coating of

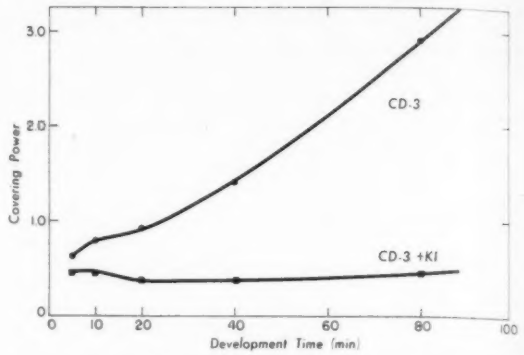

Fig. 6. Effect of iodide on covering power. CD-3 concentration, 0.00516 M. Silver-ion concentration, 4×10^{-13} M; pH 12.0. Covering power is (net density divided by silver in mg /sq ft) $\times 10^2$. ● — control; ■ — 5×10^{-5} M KI in developer.

colloidal silver, silver nuclei are present in excess of the amount necessary for maximum development. As soon as a given nucleus becomes covered with adsorbed silver ion, iodide present in solution competes with the developer. In a short time, the iodide has formed an insulating layer of silver iodide on the nuclei and development stops at this site. The over-all reduction, however, is not significantly slowed down because there are always more nuclei available for development. Without iodide, most of the development occurs very near the surface of the coating. When iodide is added, the development occurs quite uniformly throughout the layer. If this excess of nuclei were not present, iodide would stop development in a very short time. This behavior was verified by lowering the level of the colloidal silver in the coating from 15 to 0.04 mg/sq ft. With the lower level of silver, 5×10^{-5} *M* of iodide almost completely stops the development, as shown in Fig. 7. In this case all of the nuclei are known to be utilized for reaction. Since the

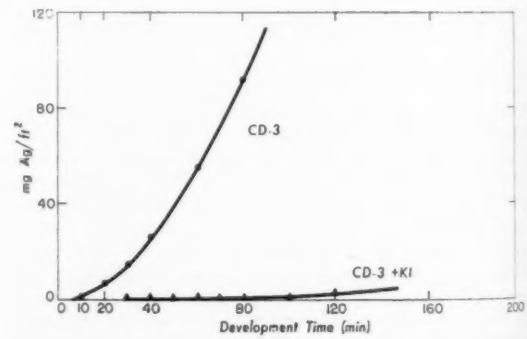

Fig. 7. Effect of iodide on silver developed from a 0.04-mg/sq ft coating of colloidal silver at pH 12.0. CD-3 concentration, 0.00516 M. Silver-ion concentration, 4×10^{-13} M. ● — control; ▲ — 5×10^{-6} M KI in developer.

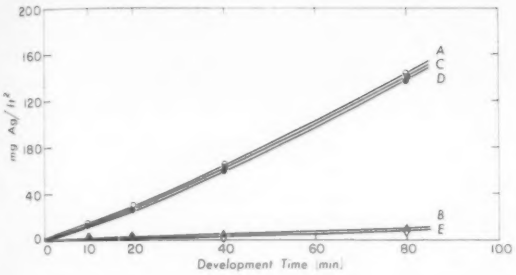

Fig. 8. Effect of dyes on a CD-3 pure physical development at pH 12.0. CD-3 concentration, 0.00516 M. Silver-ion concentration, 4×10^{-13} M. Curve A. O — control; Curve B. ▲ — 5×10^{-5} M 1,1′-diethyl-2,2′-cyanine iodide in developer; Curve C. ■ — 5×10^{-5} M 1,1′-diethyl-2,2′-cyanine chloride in developer; Curve D. ● — 2.5×10^{-5} M 1,1′-diethyl-2,2′-cyanine sulfate; Curve E. ▽ — 5×10^{-5} M (each) 1,1′-diethyl-2,2′-cyanine chloride + potassium iodide.

iodide appears to inhibit only the developing surface, the reaction is strongly retarded.

The dye 1,1′-diethyl-2,2′-cyanine iodide, in concentrations of 5×10^{-5} *M*, was found to inhibit physical development greatly. Curve B in Fig. 8 shows this effect in a plot of analyzed silver vs. time of development. Since it had been shown that both the chloride and the iodide salt of this dye adsorb to silver, it was thought that the chloride salt would also suppress development. However, Curve C shows that the chloride gave only a very slight deviation from the control. The sulfate salt (at equimolar concentration of cation) also gave only a very slight effect (Curve D). Evidently it is not the cationic portion of the dye which is causing the inhibition in the iodide salt, but the combination of both the dye cation and the iodide. This was verified when 5×10^{-5} *M* each of the chloride salt and potassium iodide were placed in CD-3 Developer. Curve E coincides exactly with Curve B. Apparently, the combination of dye cation and iodide can form an insulating layer on all of the nuclei very rapidly, and this layer cannot be easily displaced by the developer reactants.

Discussion

The data which have been obtained strongly support the theory that the mechanism of physical development involves an electron transfer through a solid substrate. Faerman and Voeikova[5] have found that such materials as silver bromide and silver iodide do not form as good a substrate for physical development as do some metals. When a conducting catalytic surface, such as colloidal silver, is covered with an insulating layer of a material like silver iodide or phenylmercaptotetrazole, the transfer of electrons from developer to silver ions is impeded. Both paraphenylenediamine and Metol-hydroquinone developers are affected similarly by the retarders. Since the *p*-phenylenediamines are known to adsorb to silver[1] and the Metol-hydroquinones adsorb weakly, if at all, the prevention of adsorption of developing agent is not a critical factor. On the other hand, the adsorption of silver ion to the conducting substrate is a common factor with both types of developing agents. The prevention of silver-ion adsorption to silver may possibly account for the effects observed. Further work is being done to try to resolve some of these questions.

PHOTOGRAPHIC SCIENCE AND ENGINEERING
Volume 5, Number 5, September-October 1961

Test Methods for Rating Abrasion Resistance of Photographic Film

J. F. CARROLL AND J. O. PAUL, *Manufacturing Experiments Division, Eastman Kodak Company, Rochester, N.Y.*

The abrasion resistance of photographic films is becoming increasingly important in several fields of reproduction. There exist many test methods for rating abrasion resistance of different materials by various mechanisms of abrasion. Although many of these are applicable to photographic film, different tests do not always produce results which agree. This paper describes some of the test methods used for photographic film and compares the results obtained with typical photographic film materials, including the response of the various test methods to such variables as film lubrication and changes in relative humidity. Various test results and the results from a simulated practical handling test are compared. It is concluded that the type of test should be determined by the practical abrasion problem in question. A stylus scratch test, in one form or another, is a likely candidate for correlation with most photographic film applications.

In trade usage, photographic film is subjected to many abrading operations, such as cinching and contact with dirt particles. The greater specularity of motion picture and still picture printers, as well as the desire to achieve greater size reduction in copy films and data handling systems, has led to more emphasis on abrasion resistance. This is evidenced by the increasing number of commercially available film lubricants and treatments and by the relatively recent innovation of liquid printing.[1] Protective lacquer coatings have also been used for some time.

Abrasion resistance in general, and scratch resistance in particular, have always been rather ill-defined with respect to both the testing methods and the influential variables. (In this paper, "abrasion" is used as a general term to encompass all kinds of surface marring, including scratch with a sharp point or particle.) Many tests have been developed to rate abrasion resistance by different mechanisms of abrading, but these tests frequently give differing results. No single test method has been found to be entirely satisfactory for comparison with all possible trade conditions that cause abrasion.

The purpose of this paper is to cite some of the well-established test methods, to describe some of them in detail, and to compare results obtained with them on typical photographic film materials under various conditions.

A rather complete listing of both the hardness and the abrasion tests that are used on plastic materials can be found in the literature.[2,3] It is desirable to select a test method or methods that approach the mechanism of the relevant practical situation, but it is not always easy to duplicate or even to know the mechanism of practical abrasion of photographic film in the trade. The next best approach is to know which of the tests correlate regularly with trade experience in each field of film usage.

While the abrasion mechanism is important, it is only one aspect of the test procedure. The degree of abrasion of the specimen has to be rated, preferably in such a way as to yield a numerical value. This is commonly done by one of several means, such as weight loss (which is hardly suitable for photographic film testing), by optical haze measurement, or by subjective estimate of the load or degree of abrasion treatment that is required to produce the first visible damage.

Description of Test Methods

Four general abrasion test methods, involving distinctly different abrasion mechanisms, will be described and compared in detail here, with the greatest emphasis given to those tests which appear to be most applicable to photographic film testing. The tests utilize the film types listed below, and throughout this paper the films will be referred to by the letter-code shown:

A. Black-and-white motion picture negative film.

B. Black-and-white motion picture release positive film.

C. Color motion picture negative film.

Presented at the Annual Conference, Binghamton, N.Y., 23 May 1961. Received 7 June 1961.

1. J. G. Stott, G. E. Cummins, and H. E. Breton, *Jour. SMPTE*, **66**: 607 (1957); J. R. Turner, D. E. Grant, and H. E. Breton, *ibid.* p. 612. Also, Donald A. Delwiche, James D. Clifford, and William R. Weller, *ibid.*, **67**: 678 (1958).

2. L. Boor, *ASTM Bull.*, **244**: 49 (Feb. 1960).

3. L. Boor, J. Ryan, M. Marks, W. Bartoe, *ibid*, **145**: 68 (March 1947).

D. Color motion picture positive film.

E. Black-and-white recording microfilm.

All these films utilize cellulose triacetate support and were developed, without exposure, in continuous processing machines prior to abrasion testing.

ASTM Test D673-44, Mar Resistance of Plastics

In this test, described in great detail in the American Society for Testing Materials Standard D673-44,[4] a weighed quantity of standard 80-mesh carborundum grit slowly drops through a 1-in. diameter vertical pipe and impinges upon a specimen mounted on a holder pitched at 45° to the horizontal, producing an elliptical pattern of haze approximately 1 in. across. By using a series of weights of carborundum, each on a separate specimen, a series of haze levels is produced. Better uniformity was achieved by rotating the sample during the test. This produced a circular pattern on which the abrasion damage could be measured in terms of the percentage haze level. The haze level is defined as the percentage of the transmitted light that is scattered at angles exceeding 2.5° when specular light is normally incident on the specimen, as described in ASTM Method D1003-59T, *Haze and Luminous Transmittance of Transparent Plastics*. While this is not part of the D673 procedure, it is more practical for photographic film than the reflected gloss rating incorporated in the latter.

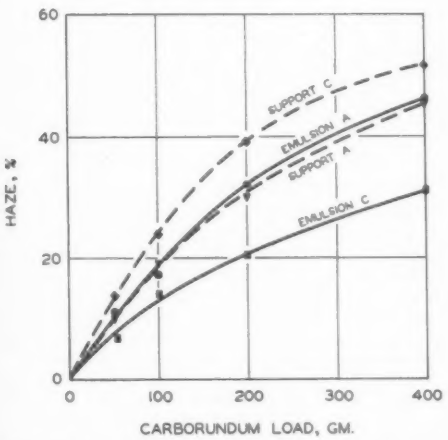

Fig. 1. Mar Resistance Test (ASTM D673–44). Typical relationships of haze to carborundum load for emulsion and support surfaces at 70°F, 50% R.H.

Some typical relationships of *corrected haze* to carborundum weight are shown in Fig. 1 for both sides of two motion picture films. (*Corrected haze* is defined as the haze after abrasion, corrected for the haze present prior to abrasion.) Films A and C represent very nearly the gamut of abrasion resistance for the support side of processed photographic films that do not have a gelatin backing. They also illustrate the differences observed between black-and-white and many color emulsions. As the weight of carborundum increases, the corrected haze rises rapidly at first and then levels off. For photographic film, the abbreviated form of the test recommended by ASTM, i.e., measurements at 200 and 400 grams of carborundum, is usually satisfactory. Despite the weight of carborundum used, this test has a very slight depth of penetration.

This test method has some advantages as well as several disadvantages. It has been in use with photographic film for over twelve years in this Laboratory, and, therefore, its reliability is well established. Advantages are: it has a large range, i.e., it can measure the hardest plastics as well as the most abrasion-susceptible plastics without any change in procedure or scale of values; it is a fairly reproducible test in which small differences in haze percentage are quite significant; when used with a dependable travelling control material, the results of this test can be corrected to a meaningful absolute level. Disadvantages are: because photographic films cover only a small part of the large abrasion range of this test, differences in films may approach the same magnitude as the experimental error; softer, more resilient materials such as some color emulsions, which are known to be lower in abrasion resistance, are often rated as superior by this test (see Fig. 1, Color Emulsion C); this test is cumbersome and sensitive to inadvertent variation, e.g., in the quality and uniformity of the carborundum.

ASTM Test D1044-56, Resistance of Transparent Plastics to Surface Abrasion

The requirements of this method, described in great detail in the ASTM Standard D1044-56,[4] are met by the Taber Abraser. Briefly, it consists of a driven turntable on which the specimen is mounted horizontally. A pair of bonded abrasive wheels is lowered onto the specimen by means of a hinged arm. The wheels turn by virtue of being in contact with the rotating specimen. The points of contact of the parallel aligned wheels are on a large chord of the circular turntable instead of on a diameter, so that scuffing occurs during rotation of the wheels. This produces a circular track of abrasion on the specimen. The severity of the test may be varied by changing the coarseness of the wheels, the load on the arm, or the number of revolutions of the turntable.

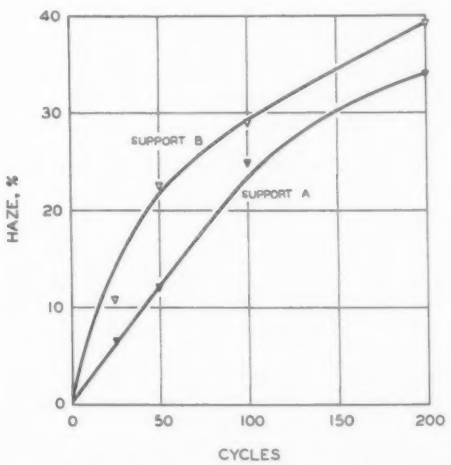

Fig. 2. Taber Abraser Test (ASTM D1044–56). Variation of haze with number of cycles for support surfaces at 70°F, 50% RH, using 500-gram load and CS 10F wheels.

4. "ASTM Standards on Plastics," 11th ed. (1960), Am. Soc. for Testing Materials, 1916 Race St., Philadelphia 3, Pa.

Unlike the Mar Resistance Test, this test has a very severe depth of penetration even under mild conditions. For use with photographic film, the same haze rating method is employed as described in the Mar Resistance Test.

The Taber Abraser test method has the advantage over the Mar Resistance Test that it more nearly approximates one kind of abrasion that film might possibly receive. Disadvantages are: its depth of penetration is, perhaps, unrealistically severe; the haze pattern is not wide enough to fill the aperture of most haze rating instruments and the specimen (a quadrant of the circular haze pattern) must be positioned in the light beam with precision; the Taber turntable requires a 4-in. square specimen and cannot accommodate 35mm specimens.

The haze of the support surface as it varies with the number of cycles of the Taber turntable is shown in Fig. 2. Support A is again rated superior. Emulsion tests were not run with this test because all the 35mm films used were machine processed, and tray processing of wider films for the purpose of this test might change their abrasion characteristics.

This test has been of value largely for experimental films and for sheet films that are not slit to narrow dimensions. Rubbery resilient emulsions give more realistic results with this test than with the Mar Resistance Test.

Wheel Brush Tests

Wheel brushes with fibers radiating from the hub have been used to abrade photographic film and film support. The depth of penetration is largely a function of the fiber material and the contact pressure. The extent of abrasion is determined by the number of revolutions of the brush. Since haze is also used as a measure of abrasion in this test, it is desirable to use a brush made of a fiber material that will not penetrate too deeply. Steel is too hard. Good results have been achieved with the soft body-hair of a horse. This produces abrasion which is of low penetrating power and of much lower haze level than the Mar Resistance Test.

The Soft Hair Wheel Brush Test uses an 8-in. diameter brush that is 1 in. thick at the periphery. The specimen is mounted on a hinged holder that swings up against the brush with a mild spring tension that varies negligibly with any eccentricities in the brush. The long narrow holder surface is flat in the narrow direction parallel to the brush axis, but is circular in the plane perpendicular to this, so that it curves away from the brush at the ends of the holder. This imposes a lengthwise curvature upon the 35mm specimen, which eliminates any widthwise film curl that might affect the abrading operation. The brush turns at 1 rotation/sec, and either 5 or 10 rotations are usually sufficient.

The variation of haze with the number of rotations of the brush for the support side of several films is shown in Fig. 3. These results agree rather well with Figs. 1 and 2. This test regularly gives quite logical results for film supports. Similar curves for the emulsion side of two films are also shown in Fig. 3. Again the color film is ranked, contrary to trade experience, as more abrasion resistant than the black-and-white film. The relative ranking of some emulsions depends on the number of rotations of the brush, although this is not the case in Fig. 3.

The Soft Hair Wheel Brush Test has several advantages. It is a very rapid and easily run test. It scratches the film surface in a manner that appears very similar to film scratched in actual trade usage. The hair fibers are brittle, and the ends powder off continuously, yielding a fresh surface. This is of special advantage in testing lubricated films. It has the disadvantage that the abrasion is not perfectly uniform and, therefore, extra care is required in positioning the specimen for rating the abraded haze.

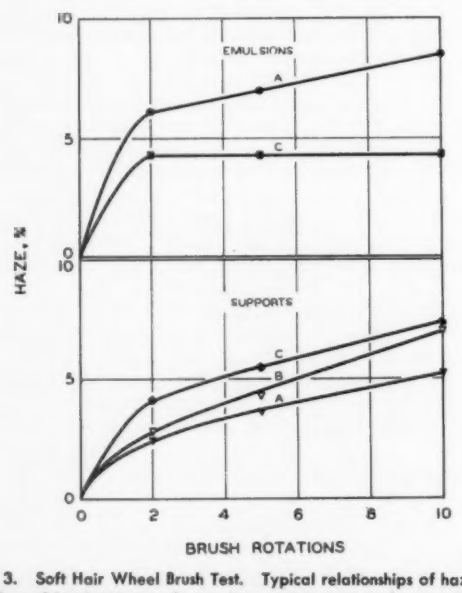

Fig. 3. Soft Hair Wheel Brush Test. Typical relationships of haze to number of brush rotations for emulsion and support surfaces at 70°F, 50% RH.

Spherical Stylus Scratch Tests

The spherical stylus for abrading film has been used in many modifications, of which a number are reported in an historical study.[5] The stylus is incorporated in certain commercially available testers.[6] Variations are possible in the radius of the spherical point, the material from which the stylus is made, the number of styli used at a time, the manner of loading the stylus with weights, and the means of rating the resulting scratches.

I. B. Current[7] described a test in which nine sapphire styli, each loaded by a different weight and displaced laterally from each other, were used to scribe lines simultaneously on an emulsion. This mechanism was found, in the work described below, to produce results that correlate rather well with emulsion abrasion resistance known in the trade. Three variations of the spherical stylus method are discussed here. In each of these variations, sapphire styli obtained from the Moser Jewel Company were found to be very satisfactory.

Single Arm Scratch Test. The simplest application of the spherical stylus scratch mechanism, the "Single Arm Scratch Test," consists of determining the load in grams required to produce by means of a spherical sapphire stylus of 3-mil radius (Fig. 4) a visible scratch on a piece of film. The instrument used has a pivoted and balanced arm, at one end of which is mounted the stylus and a

5. E. C. Bernhardt, *ASTM Bull.*, **157**: 123 (March 1949).
6. Bulletin 58203: *Shear/Scratch Tester*, Taber Instrument Corporation.
7. I. B. Current, *Phot. Eng.*, **5**: 227 (1954).

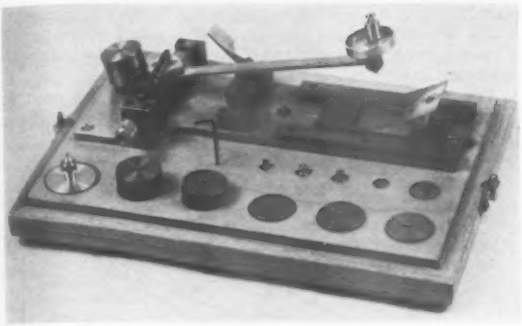

Fig. 4. Single Arm Scratch Tester.

small pan for weights. The specimen holder for 35mm film contains a glass plate which serves as a hard smooth backing for the film specimen and a spring brass strip which holds the specimen flat. The holder is rigidly constrained in the lateral direction but can easily slide back and forth. In operation, the arm is lowered so that the loaded stylus contacts the specimen, and the holder is drawn forward. The speed of scribing is unimportant within reasonable limits. As shown in Fig. 4, the stylus arm is pivoted on a threaded hinge which permits precise lateral positioning of the scratch by turning the knurled knob.

The instrument is used to scribe a pair of lines (approximately 0.01-in. apart) at each of several loads. A pair of lines is scribed at 1-gram intervals up to 10 grams, and at 5-gram intervals thereafter up to 100 grams. As a rule, it is possible to eliminate more than half of this range by having some knowledge of the sample.

Once scribed, the specimens may be rated subjectively by transmitted light in any of several ways. Obviously only processed-clear films can be rated in this manner. The viewing may be done microscopically, directly, or by projection of the scratch image onto a screen. The endpoint, or choice of value, is defined as the minimum load in grams that produces some visible effect, e.g., the "first visible line," "first continuous line," "first visible plowing," or "first continuous plowing." For general purposes, the first and third from this list are often chosen.

The single arm scratch ratings for the support side of the same films tested previously are shown in Table I. In this test a higher value indicates better abrasion resistance. As usual, the data on the support side of these films correspond well with the ranking of these films in the Mar Resistance Test (Fig. 1) and the Wheel Brush Test (Fig. 3). On the other hand, the black-and-white film ranks superior to the color film, in agreement with trade experience. This differs from the Mar Resistance Test and Wheel Brush Test (Fig. 3).

TABLE I. Single Arm Scratch Test
Typical Stylus Load Values for Various Films at 70°F, 50% RH

Film	First visible scratch, grams	First visible plow, grams
Emulsion A	2	40
Emulsion B	2	60
Emulsion C	2	30
Emulsion D	6	30
Support A	20	70
Support B	15	40
Support C	6	50

Advantages of the Single Arm Scratch Test are: it correlates well with trade experience; it is simple and quick; the instrument is small and inexpensive; the test is not as critical with respect to initial haze and density of the sample as those tests that are rated by haze.

Disadvantages are: the rating procedure is subjective; the rating environment is difficult to standardize. The direct viewing method of rating has proved to be the most consistent, but also the most difficult to standardize between laboratories, and the endpoint cannot be defined specifically.

A single load value cannot completely describe the scratch resistance of a material. For example, two materials may form a visible scratch at the same minimum load, but one may form very objectionable scratches at slightly higher loads, while the other still forms only mild, innocuous scratches. Both, however, would be rated the same in this scratch test. In order to partially overcome this disadvantage it is possible to obtain two projection scratch ratings. For one, the observer is near the screen, say 4 ft. distant. For the second rating, the observer should be away from the screen, say 15 to 30 ft distant. In this way, two load levels for endpoints will be established. If the two load ratings are very similar, the scratch becomes appreciably worse with increasing load.

Electronic Scratch Test. In order to overcome the subjectivity in rating of the Single Arm Scratch Test, several variations have been tried. One of these, the Electronic

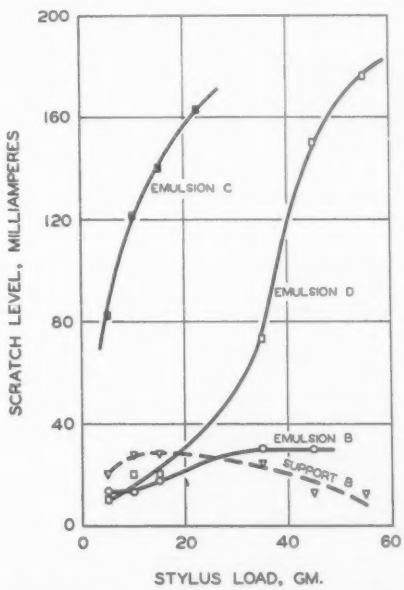

Fig. 5. Electronic Scratch Test. Typical curves of electrical measurement of scratch level against stylus load for emulsion and support surfaces at 70°F, 50% RH, after 10 rotations, using 3-mil sapphire stylus. Measurements made in 1957.

Scratch Test, consisted simply of graphing the noise output (against time) from a phonograph cartridge attached to a 3-mil-radius sapphire stylus that was permitted to ride repeatedly, under various loads, in the same path on a rotating disk or cylinder of film. Figure 5 shows some results. The superiority of the black-and-white emulsion over the color emulsions is shown.

The reproducibility of this test method and its sensitivity to small differences are excellent. Note, for example, the difference between the two color emulsions, C and D. The method has one big disadvantage, namely, the measurement is very indirect.

Haze-Rated Scratch Test. The Haze-Rated Scratch Test is basically a means of objectively rating stylus scratch lines according to the measurable haze which they produce. Since a single scratch produces very little haze, several scratches at the same load are required. This could conceivably be accomplished by scribing ten lines at each load increment and rating each set of ten lines for haze. A faster procedure is to scribe ten long lines on a specimen with the load on the stylus increasing continuously from one end of each line to the other. The haze is then rated at progressive points along the lines.

The instrument used to make the scratches, the Continuous Loading Scratch Tester (Fig. 6), is similar in principle to the Single Arm Scratch Tester except that a weight is mounted on a ball bushing which rolls along the cylindrical stylus arm. As the specimen holder is

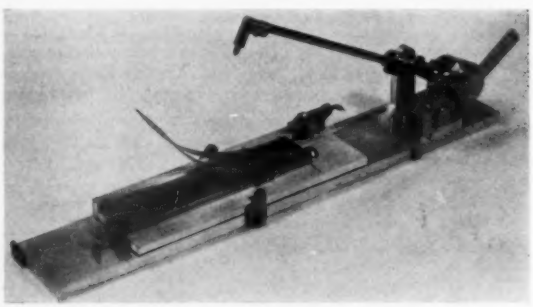

Fig. 6. Continuous Loading Scratch Tester.

pulled forward to scribe the specimen, it engages the sliding weight which increases the load on the stylus progressively from zero to 60 grams. This is repeated to make ten parallel lines, $\frac{1}{8}$ in. apart, on a specimen. Weights can be added directly above the stylus in order to cover an equivalent range at a higher load level.

The specimen holder accommodates a test specimen 5 in. by 35 mm and has a removable brass plate which serves as a support backing for the test specimen during the scratching operation. By removing the plate from below, the holder can be used to hold the test specimen while measuring its haze. The initial haze measurement is made prior to scratching, at five successive positions along the 5-in. sample. After abrasion, the final haze measurements are made at exactly the same five positions as the initial measurements. The corrected haze at any point is taken as the difference between the initial haze and the final haze measurements.

This test method has several advantages: it uses the spherical stylus mechanism of scratching, which corresponds well with trade experience with photographic film; it is completely objective; it is rated optically; it gives a complete description of the scratch resistance with changing load level.

The advantage of this last feature can be seen in Fig. 7. The support sides of all three films rise above

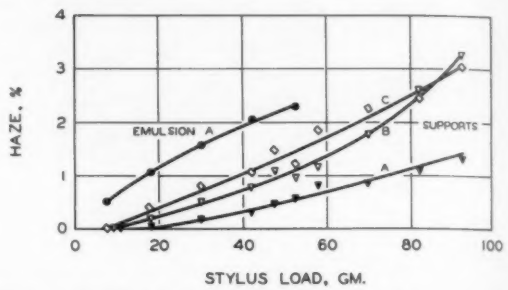

Fig. 7. Haze-Rated Scratch Test. Typical curves of haze vs. stylus load for emulsions and support surfaces at 70°F, 50% RH, using 3-mil sapphire stylus.

the zero (first visible) haze line at approximately the same load, but at higher loads there are significant differences between these film supports. The ranking is similar to that of the previous tests and to trade experience. A curve for the emulsion side of Film A, also shown in Fig. 7, is typical of black-and-white film emulsions.

No color emulsion is shown in Fig. 7 because of a failing of this test. The oily quality of many color emulsions tends to momentarily lubricate the stylus upon penetration. This results in random skips in the scratch lines and ruins the haze rating. Other disadvantages are: the test is not quick; it is very critical with respect to initial haze and optical density; the sensitivity is reduced by the clear (unscratched) areas of the specimen; and it is not as sensitive to small changes as the Electronic Scratch Test.

Measurement of Haze

Many commercially available instruments can be used to measure haze. The dependability and precision of the measurements differ considerably among these various instruments. Because of their high haze levels, the Mar Resistance and Taber Abraser Tests do not require extreme sensitivity, but do require precision. The Soft Hair Wheel Brush Test and especially the Haze-Rated Scratch Test require great sensitivity and precision at low levels of haze. An instrument such as the Lumetron Colorimeter (Model 402E), manufactured by Photovolt Corporation, is adequate for the first two tests. The Standard Gardner Integrating-Sphere Hazemeter (Model AUX 10a), which conforms to ASTM Method D1003-59T, gives satisfactory results for the latter two tests. In no case, should results from two different instruments be compared. The slightest difference in the angle of rejection of near-specular light can, in some cases, result in two-fold differences in haze value.

Most photographic films have a measurable inherent haze, frequently of the order of 2% and sometimes as high as 8%. The measured (final) haze must be corrected for the initial haze of the specimen prior to abrasion.

The most direct method of correction is simply to subtract the initial haze from the final haze. It is assumed that the abrading operation does not alter the structure that produced the initial haze. However, this mode of correction is legitimate only when the area of the scratches is very small compared to the total area covered by the initial haze, e.g., in the Haze-Rated Scratch Test. In tests such as the Mar Resistance Test and the Wheel Brush Test, the initial haze interacts with that due to abrasion over the whole specimen area to produce a measured final haze that is somewhat less than the algebraic sum of these two components, and a theoretical correction must be made, as follows:

$$\% \text{ corrected haze} = \left(\frac{\% \text{ final haze} - \% \text{ initial haze}}{100 - \% \text{ initial haze}} \right) (100)$$

The derivation of this correction involves several assumptions, but M. R. Goff of this Laboratory has demonstrated empirically that the correction is quite valid except when the initial haze is extreme or is largely on the surface to be abraded.

Interpretation of Abrasion Effects

In order to demonstrate the degree of usefulness of data obtained from the various test methods, some of the factors known to affect abrasion resistance were studied, and the test data were compared with the results of simulated practical handling abrasion.

Effect of Lubrication on Abrasion

For some years, lubricants and various film treatments have been used to increase the abrasion resistance of film.[8] In the present investigation, tests were made with a solution of Kodak Movie Film Cleaner (with Lubricant) diluted with methyl chloroform (1,1,1-trichloroethane) to several different levels of wax concentration below the normal level, and several films were lubricated with this series of wax concentrations.

Friction tests were run on each of the films, using the "Point Contact Friction Tester." In this test, the film is contacted only by three spherical sapphire points of 3-mil radius. (Previous work in this Laboratory has shown that scratch data correlate better with this friction method than with the usual sled method.) The results are shown in Fig. 8. It is apparent that there is a threshold concentration of wax below which the lubricant is relatively ineffective. There is also a point of diminishing return above which any increase in wax concentration is useless in this test. All of the films used in this investigation reach equivalently low values of friction coefficient at the normal full concentration of lubricant.

No consistent difference was found by the Mar Resistance Test between the fully lubricated and the unlubricated films. The Taber Abrasion Test was not run because of the difficulty of waxing a sheet of film in a manner dependably comparable to the 35mm waxing operation.

Results obtained by the Soft Hair Wheel Brush Test are shown in Fig. 9. The most dilute wax application had a profound effect on the emulsion, but higher concentrations were of no further benefit. The support side of the film was affected in the same way but to a much less significant degree.

As shown in Fig. 10, the Single Arm Scratch Test is profoundly affected by lubrication of the film. Furthermore, the difference between the films is more apparent at high levels of lubrication where the frictional characteristics are equalized.

8. F. J. Kolb, Jr., and E. M. Weigel, "Protective Treatments for Microfilm," presented at meeting of the National Microfilm Assn., Chicago, April 6, 1961.

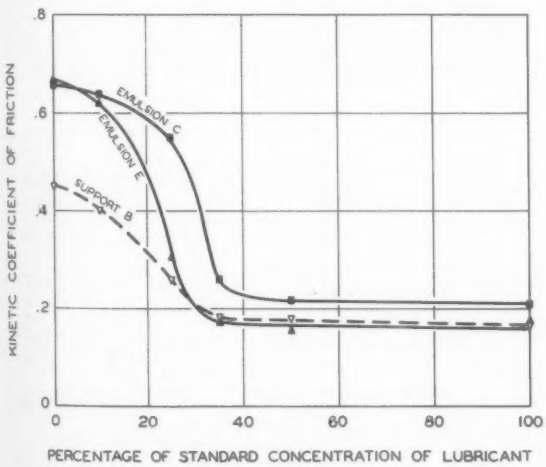

Fig. 8. Point Contact Friction Test. The effect of various concentrations of Kodak Movie Film Cleaner (with Lubricant) on the coefficient of friction of emulsion and support surfaces at 70°F, 50% RH.

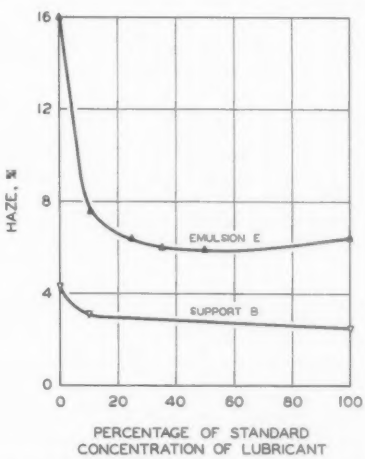

Fig. 9. Soft Hair Wheel Brush Test. Effect of various concentrations of Kodak Movie Film Cleaner (with Lubricant) on the abrasion resistance of emulsion and support surfaces at 70°F, 50% RH, after 5 rotations.

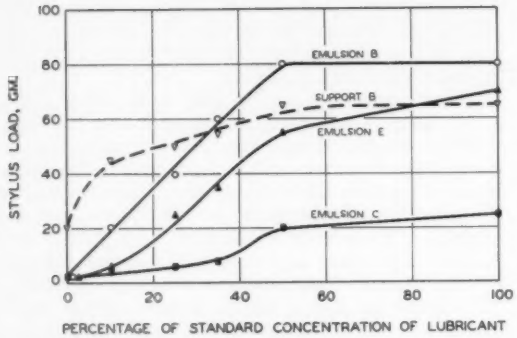

Fig. 10. Single Arm Scratch Test. Effect of various concentrations of Kodak Movie Film Cleaner (with Lubricant) on the first visible scratch rating on emulsion and support surfaces at 70°F, 50% RH, using 3-mil sapphire stylus.

The results of the Haze-Rated Scratch Test at several levels of lubrication are shown in Fig. 11. These curves are typical of those obtained on all films, except, of course, for the absolute level of the curves. A comparison of several films by this test at the 100% lubricant level is shown in Fig. 12. When lubricated, the color films can also be tested by this method. Although lubrication greatly reduces the level of abrasion in this test, the inherently greater abrasion resistance of the black-and-white film emulsions, which is observed in the trade, is still evident.

Effect of Humidity on Abrasion

The moisture content of film supports and especially of film emulsions changes with varying relative humidity. This can cause a change in physical properties, including abrasion resistance.

Several films were conditioned to 5%, 20%, 50%

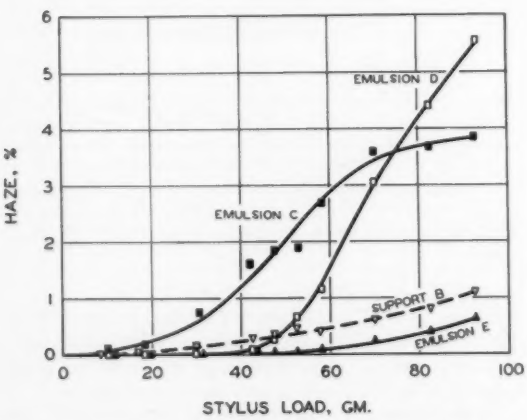

Fig. 12. Haze-Rated Scratch Test. Typical haze-rated scratch curves for emulsion and support surfaces treated with the standard concentration of Kodak Movie Film Cleaner (with Lubricant). Abrasion performed at 70°F, 50% RH, using 3-mil sapphire stylus.

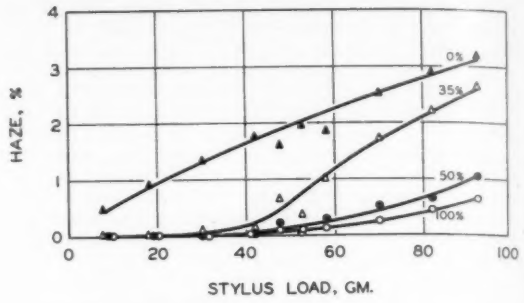

Fig. 11. Haze-Rated Scratch Test. Effect of various concentrations of Kodak Movie Film Cleaner (with Lubricant) on the haze produced on Emulsion E at 70°F, 50% RH, using 3-mil sapphire stylus.

and 80% RH for abrasion tests. The increase in haze produced in the Mar Resistance Test with increasing relative humidity is shown in Fig. 13. Although the color emulsion is distinctly lower in haze than the black-and-white emulsions, the effect of relative humidity is similar. Results for film supports are not shown, since no significant change was found with varying relative humidity.

Figure 14 shows the effect of relative humidity on the results of the Taber Abraser for two film emulsions (tray processed). The Taber Abraser Test is obviously a very sensitive one. Again, abrasion resistance improves with decreasing relative humidity.

The Soft Hair Wheel Brush Test gives somewhat peculiar results. At low levels of humidity, the haze of the support side of several films drops rapidly as relative humidity increases (Fig. 15). Since it is unlikely that a significant change occurs in the support, it is probable that the bristles of the brush change in abrading power as the humidity rises. Further evidence of this is found in the same figure, where the abrasion resistance of film emulsions also shows a general, though less consistent, improvement with rising humidity, contrary to the results of all the other tests. Therefore, it is concluded that the Soft Hair Wheel Brush Test must be run at

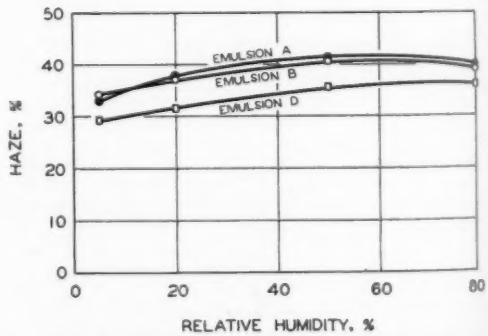

Fig. 13. Mar Resistance Test. Effect of relative humidity on the abrasion resistance of several emulsion surfaces at 70°F, using 400 grams of carborundum.

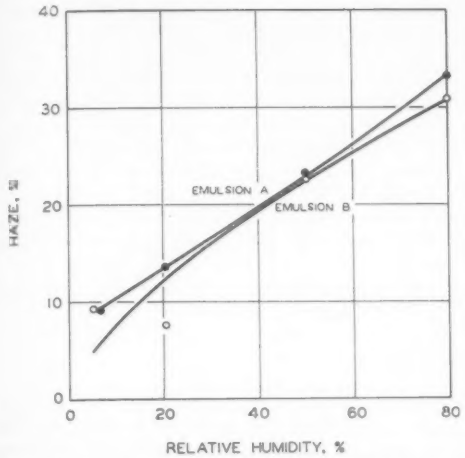

Fig. 14. Taber Abraser Test. Effect of relative humidity on abrasion resistance of emulsion surfaces at 70°F after 50 cycles, using 500-gram load and CS 10F wheels.

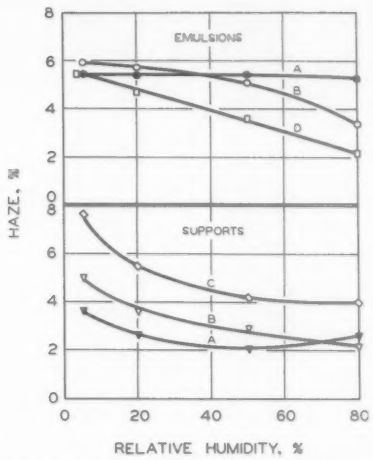

Fig. 15. Soft Hair Wheel Brush Test. Effect of relative humidity on abrasion resistance of emulsion and support surfaces at 70°F after 5 rotations.

controlled humidity conditions, and the results at different humidities cannot be compared.

With decreasing humidity, the Single Arm Scratch Test shows a significant increase in the scratch resistance of the emulsion side of the films (Fig. 16), particularly for the color film. The support side of these films, however, showed no change in this test throughout the 5-to-80% RH range.

In the Haze-Rated Scratch Test (Fig. 17), many emulsions show a rather continuous improvement with decreasing relative humidity throughout the entire load range. However, the particular film shown in Fig. 17 appears to change its mechanism of scratching at low humidities and high loads. The scratch actually is more innocuous at the highest loads at 5% RH than at intermediate loads. This, again illustrates how the Haze-Rated Scratch Test yields more complete information than a simpler scratch test such as the Single Arm Scratch Test.

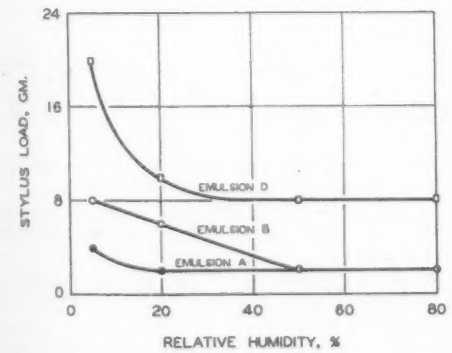

Fig. 16. Single Arm Scratch Test. Effect of relative humidity on the first visible scratch rating for several emulsion surfaces at 70°F, using 3-mil sapphire stylus.

In addition, the scratches can also be examined for their visual characteristics.

Correlation with Practical Test

It has been shown that the results obtained from different kinds of abrasion tests may not agree with each other. Sometimes this is the fault of the test, as in the case of the humidity effect on the Soft Hair Wheel Brush Test. More often it is due to the differences in the abrasion mechanisms utilized. The results of all these tests, when properly run, are quite valid, but some tests simply are not relevant to certain practical applications. No single test can simultaneously simulate all the modes of abrasion encountered in the trade.

One common mode of abrasion is that sometimes encountered by motion picture film when it is passed between the folds of a wiper cloth that is not perfectly clean. An attempt was made to simulate this action by rubbing some granules of corundum into the surface of a soft cloth pad. The film was passed

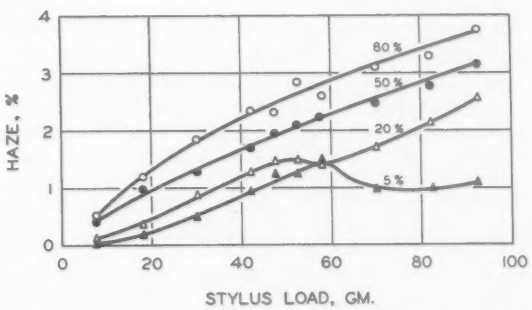

Fig. 17. Haze-Rated Scratch Test. Effect of relative humidity on the haze produced on Emulsion B at 70°F, using 3-mil sapphire stylus.

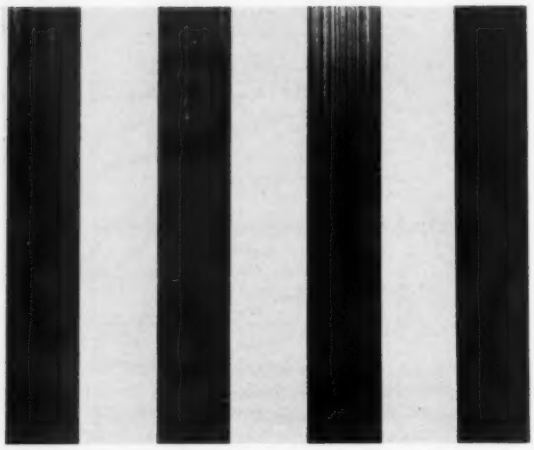

Fig. 18. Effect of Kodak Movie Film Cleaner (with Lubricant) on the scratch susceptibility of a black-and-white motion picture negative film in a simulated practical handling situation. Film is drawn over a pad containing 0.015 to 0.025-in. corundum abrasive particles under approximately a 1000-gram load. This test simulates the abrasion occurring during the cleaning of film as the result of accumulation of abrasive on the cleaning pad.

through the folded pad which in turn was compressed under constant load. Six unlubricated and six fully lubricated films were tested in this manner. All showed the same results, as illustrated for one film in Fig. 18. The two strips of film on the right illustrate the difference between lubrication and no lubrication.

A thinner wiping pad was used on the pair of strips on the left in Fig. 18. This allowed less room for the film to force the particles out of its way and into the matrix of the cloth. While this change of pad thickness had little effect on the degree of scratching of the unlubricated film, it seriously lowered the ability of the fully lubricated specimen to resist scratching. A test such as the Haze-Rated Scratch Test would predict the behavior of the pair on the right. However, a test similar to the Taber Abraser Test might as closely predict the behavior of the pair on the left. A stylus test would also do so if the degree of penetration, rather than the load on the stylus, were fixed.

Conclusion

A minor change in the variables surrounding a trade operation which inadvertently abrades photographic film can significantly change the mechanism of abrasion. Therefore, the type of abrasion test which will produce relevant results may also require a change. Consequently, in testing the abrasion resistance of a photographic film product, it is important not to adhere unwaveringly to a single abrasion test mechanism. Rather, with each problem, it is essential to select a test which approaches the parameters of actual trade usage.

Acknowledgment

Acknowledgment is made to P. Z. Adelstein and J. M. Calhoun for their advice and many valuable suggestions in the writing of this paper.

• Coming Technical and Scientific Meetings

Optical Society of America, October 18–20, Biltmore Hotel, Los Angeles, Calif.

International Symposium on Photoelasticity, October 29–31, Chicago, Ill.

Photo-Cinema-Optique, Third Biennale Internationale, November 9–20, Paris, France

Air Force Office of Scientific Research, Second International Conference on the Exploding Wire Phenomenon, November 14–16, Boston, Mass.

Society of Reproduction Engineers, Visual Communications Congress, December 1–4, Hotel Biltmore, Los Angeles, Calif.

American Association for the Advancement of Science, Annual National Meeting, December 26–31, Denver Hilton, Brown Palace, Cosmopolitan, Shirley Savoy Hotels, Denver, Colo.

American Society of Photogrammetry, Annual Convention, March 11–17, 1962, Shoreham Hotel, Washington, D.C.

Society of Motion Picture and Television Engineers, 91st Semiannual Convention, April 29–May 4, 1962, Ambassador Hotel, Los Angeles, Calif. Program Chairman, Edward P. Ancona, Jr., 3170 Lake Hollywood Drive, Hollywood 28, Calif.

1962 Annual Conference, SPSE, May 7–11, Somerset Hotel, Boston, Mass.

6th International Congress on High-Speed Photography, September 17–22, 1962, Hotel Kurhaus, Scheveningen, Netherlands

Society of Motion Picture and Television Engineers, 92nd Semiannual Convention, October 21–26, 1962, Drake Hotel, Chicago, Ill.

PHOTOGRAPHIC SCIENCE AND ENGINEERING
Volume 5, Number 5, September-October 1961

Dependence of Covering Power and Spectral Absorption of Developed Silver on Temperature and Composition of the Developer

T. H. JAMES AND L. J. FORTMILLER, *Research Laboratories, Eastman Kodak Company, Rochester, N.Y.*

The spectral absorption and the mass of silver per unit area were determined for images developed in solutions of various compositions over a temperature range of 4° to 50°C. Emulsion coatings with a moderate level of hardening showed a marked increase in covering power and in the ratio of densities measured at 400 mμ to those measured at 700 mμ when a surface developer was used and the development temperature was increased from 20° to 40°C. The relative changes in the temperature region below 20° and above 40° were much smaller. The changes in covering power and spectral absorption correlate with the softening and swelling of the gelatin. The changes diminished or vanished when the level of hardening was increased. The activation energy of development was not affected by the hardening. The relative amount of solution physical development occurring in the action of some sulfite-containing developers depends upon temperature, and some changes in spectral absorption and covering power with change in temperature of development can be explained on this basis. A linear relation was obtained between diffuse density and the total surface area of the developed grains, calculated on the assumption that the area was substantially the same as that of the original grains when a "distortionless" developer was used.

The relation between the density and the mass of developed silver can depend markedly upon the photographic material and how it is processed and dried.[1–6]* Under some conditions, information on the mechanism of the processes occurring during development can be obtained by making use of measurements of both density and mass of silver, and measurements of density at several wavelengths of light may give further information.

The absorption spectrum and the covering power (ratio of optical density to mass of silver) of the silver image can vary considerably with the composition of the developer and the conditions of development. The following factors appear to be of importance for development in the absence of added tone modifiers:

(1) *The size of the silver particles for nonfilamentary silver.* For sufficiently small particles, e.g., yellow colloidal silver, the optical density may be proportional to the mass of the particles.[7,8] For larger particles, covering power decreases with increasing size, and for sufficiently larger spherical particles, e.g., 0.1–0.5 μ in diameter, a linear relation holds between the covering power and the reciprocal of the diameter.[9] The absorption spectrum of roughly spherical particles of diameter less than about 0.15 μ is adequately accounted for by the Mie theory on the basis of selective absorption and scatter.[10] The absorption spectrum of larger particles, under some conditions, may depart markedly from neutrality and still be nearly independent of size.[11] This color of larger particles has not been adequately explained, although it evidently depends upon the surface of the particles.

(2) *The size of the developed silver grain and the degree of development when the silver is predominantly in the filamentary form.* Covering power generally decreases with increase in grain size,[9,12,13] although for sufficiently small grains this relation may not hold. When an increase in degree of development produces primarily an increase in the number of developed grains without significant change in size, e.g., when the rate of development is diffusion-controlled or is controlled by the variation in induction periods of the individual grains, such as may be the case in the toe region of the characteristic curve, neither the covering power nor the absorption spectrum changes significantly. When an increase in the degree of development produces an increase in the extent of development of the individual grains, the absorption spectrum shifts towards neutrality, and covering power generally decreases.[11,14]

(3) *The relative compactness of the filamentary silver.*[11,15] The observed shift towards spectral neutrality with increasing degree of development probably is a result of the increased degree of compactness of the filamentary silver. From electron-microscope observations and from crystal-size measurements,[16] the shift does not appear to result from an increase in the size of the filaments. The degree of compactness, however, depends also upon factors other than the degree of development. Some of these other factors are also considered in this paper.

Communication No. 2168 from the Kodak Research Laboratories. Received 12 April 1961.

* Literature references will be found at the end of this paper.

(4) *The relative amount of solution physical development involved in the formation of the silver.*[8] Except for the very early stages of development of the grain, where nonfilamentary silver is formed even in direct interface development, the covering power decreases and the departure from neutrality becomes more marked with increasing relative amount of solution physical development.

(5) *When the silver is not spectrally neutral, covering power depends on the wavelength of the measuring light.* Variations of twofold and more have been observed over the range 400 to 700 mμ, although the variation is usually less than this.[11]

The present paper is concerned primarily with the influences of the temperature of development and the hardness of the emulsion upon the covering power, absorption spectrum, and relative amount of solution physical development. Some data are included on the influence of hardness of the emulsion on the activation energy of development.

Experimental Materials and Procedure

Two types of photographic emulsion grains were used and two aldehyde-type hardeners were employed. Emulsion *A* was a coarse-grain negative-type pure silver bromide material with a wide spread of grain sizes. The coating was hardened to a melting point of over 90°C in distilled water. When further hardening was desired, the coated emulsion was bathed after exposure for 5 min at 20°C in a solution of 10 ml of 40% formaldehyde and 5 grams of sodium carbonate monohydrate in a total volume of 1 liter, then washed 15 min in running water before development. Emulsion *B* was a high-contrast iodobromide positive type with a relatively small spread of grain sizes, and coatings were prepared with three levels of hardening. Some experiments also were made with a commercial fine-grain motion-picture-positive emulsion.

A low-salt-content, surface latent-image-type developer was used in part of the work. It had the composition:

Metol	1.4 grams
Ascorbic acid	3.3 grams
Potassium bromide	1.0 gram
Sodium metaborate	5.0 grams

Water to make 1 liter; pH 8.5 at 20°C.

Several conventional developers and several developers of special composition also were used.

Sensitometric exposures were made on an Eastman IIb Sensitometer (time-scale). Uniform exposures were made to a 6- or 40-w tungsten lamp operated at 115 v at a distance of 140 cm from the film, with a ground-glass diffuser interposed, but without filters. The exposures were for 0.5 or 2 min, and were sufficient to make substantially all grains developable. The film was developed in a jacketed glass apparatus with nitrogen-burst agitation, fixed in Kodak Fixer F-5, washed 30 min in running water at 20°C, and dried in still room-air at approximately 23°C and 40% RH. Total transmission density spectrophotometric curves were obtained on most uniformly exposed samples, and silver analyses were made by the x-ray fluorescence method. Covering powers are expressed as the ratio of the density, measured at a specified wavelength, to the mass of silver per square decimeter. The "color ratio," i.e., the ratio of the densities measured at 400 mμ and at 700 mμ, is used as a measure of the departure from spectral neutrality.

The data on the relation between density and grain size were obtained in 1947 on a series of pure silver bromide emulsions and on a series containing 2.56 mole % of silver iodide, prepared according to the procedure of Trivelli and Smith.[17] Strips of these emulsions were exposed on both sides to produce maximum developability, developed for 15 min in a "distortionless" hydroquinone developer,[18] then given additional development in the same solution after the addition of small amounts of the powerful fogging developer, hydroxyhydroquinone. The latter agent was added to bring about development of any grains which were not made developable by the light exposure, but in most instances this added step proved to be unnecessary.

The "distortionless" developer had the composition:

Hydroquinone	0.025 *M*
Sodium sulfite	0.020 *M*
Sodium carbonate	0.500 *M*
Potassium bromide	0.020 *M*

Electron micrographs of the undeveloped and developed grains indicate that little distortion occurs in the shape of the silver bromide grains during development, although significant distortion of the iodobromide grains does occur. This result is in agreement with Loveland's observations with the optical microscope.

Experimental Results

Effect of Temperature on Absorption Spectrum and Covering Power of Silver Formed by the Surface Developer

The general shape of the spectrophotometric curves of silver formed by the Metol–ascorbic acid surface developer is illustrated in Fig. 1 for Emulsion *A* at a constant exposure level. Similar curves were obtained for Emulsion *B*. The solid curves show the effect of increasing temperature of development on the shape of the curves obtained with the untreated Emulsion *A* and the unmodified developer. The silver developed at 4.4°C is almost neutral, but a marked shift towards warmer tones occurred when the temperature of development was increased from

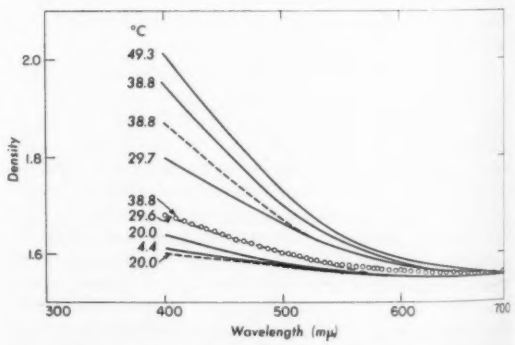

Fig. 1. Spectrophotometric curves of silver developed in Emulsion A by the Metol–ascorbic acid surface latent-image developer. Development temperatures are listed to the left of the curves. Solid curves, low-salt developer; broken curves, developer with 100 grams of Na_2SO_4/liter; circles, formaldehyde-treated emulsion developed at 38.8°C.

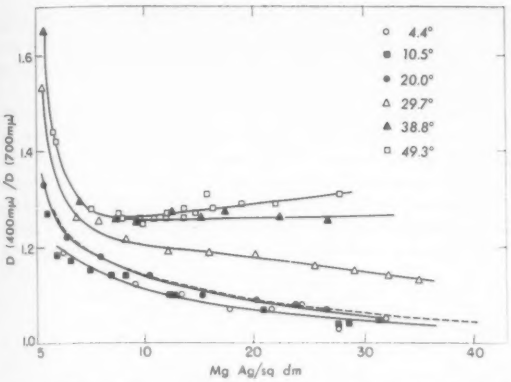

Fig. 2. Effect of temperature of development on the density ratio, $D(400\ m\mu)/D(700\ m\mu)$. Solid curves, untreated Emulsion *A*; broken curve, formaldehyde-treated emulsion.

20° to 38.8°C, and a slight further shift occurred when the temperature was increased by another 10°. The broken curves represent silver formed by development in the Metol–ascorbic acid solution to which 100 grams of sodium sulfate was added per liter. The effect of the sulfate was to shift the image tone towards neutrality for silver formed at a given temperature. Prehardening the film in the formaldehyde solution produced a still greater shift towards neutrality for development in the regular developer (no sulfate) at the higher temperatures (circles, Fig. 1) but formaldehyde treatment caused a slight shift towards warmer tones for development at the low temperatures.

Figure 2 illustrates the dependence of the color ratio on the mass of developed silver for a constant exposure level and varying time of development.

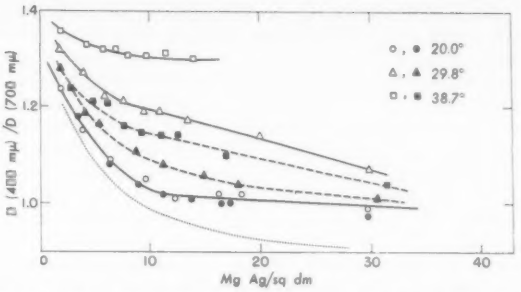

Fig. 3. Effect of temperature of development on the density ratio, $D(400\ m\mu)/D(700\ m\mu)$, for Emulsion *B*. Open points, level 1 hardening; solid points, level 2 hardening; dotted curve, level 3 hardening.

The ratio for the emulsion without pretreatment shows no significant dependence on temperature in the region, 4.4° to 10.5°C, but increases markedly with increasing temperature in the region, 20° to 39°C. On the other hand, the ratio for the emulsion which had been pretreated in the formaldehyde hardener is almost independent of temperature over the range, 6° to 39°C, and is substantially the same as that for the untreated film developed at 20°C. Figure 3 shows similar data for the fine-grain Emulsion *B* for the three levels of hardening. The variation in ratio with the temperature of development is greatest for the lowest level of hardening, and is negligible for the highest level.

Figure 4 shows the dependence of covering power on the temperature of development for Emulsion *A*. The covering power of the untreated emulsion increases with increasing temperature over the range, 20° to 39°C, but the covering power of the emulsion pretreated in formaldehyde hardener is essentially independent of temperature over this range. Results obtained with Emulsion *B* (Fig. 5) were similar.

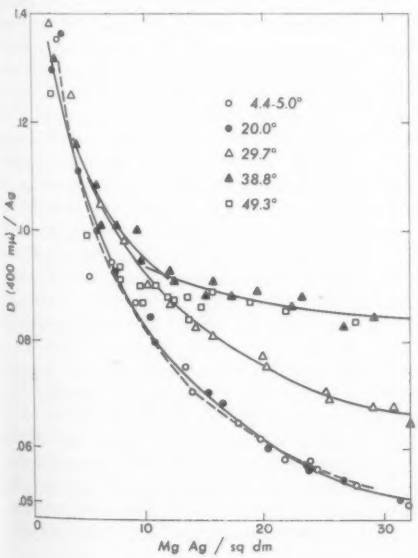

Fig. 4. Effect of temperature of development on covering power of Emulsion *A*. Solid curves, untreated emulsion; broken curve, formaldehyde-treated emulsion.

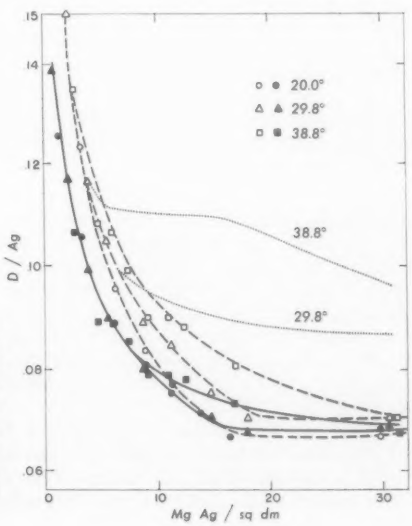

Fig. 5. Effect of temperature of development on covering power of Emulsion *B*. Solid points, covering power for densities measured at 700 mμ; open points, for densities measured at 400 mμ. Dotted curves, level 1 hardening; solid and broken curves, level 2 hardening.

A marked variation in covering power with temperature was obtained for the coating with the lowest level of hardening, whereas the coating with the highest level of hardening showed essentially no variation. The dotted curves in Fig. 5 represent the variation of the covering power at the lowest hardening level for densities measured at 700 mμ on silver developed at 29.8° and 38.8°C. The corresponding curve for silver developed at 20°C is not shown, but follows closely the lower solid curve. The solid curves represent the variation at hardening level 2 for densities measured at 700 mμ. The dependence on the temperature of development is slight. The broken curves represent the variation at hardening level 2 for densities measured at 400 mμ. The covering power for densities measured at 400 mμ shows a greater dependence on temperature than that for densities measured at 700 mμ. This is true also for Emulsion *A*. The covering powers of both emulsions for both wavelengths were essentially independent of the temperature of development, however, when the emulsions were hardened to a high level with formaldehyde. The silver–density relation for Emulsion *A*, hardened by the formaldehyde bath, is shown on a logarithmic basis in Fig. 6 for densities

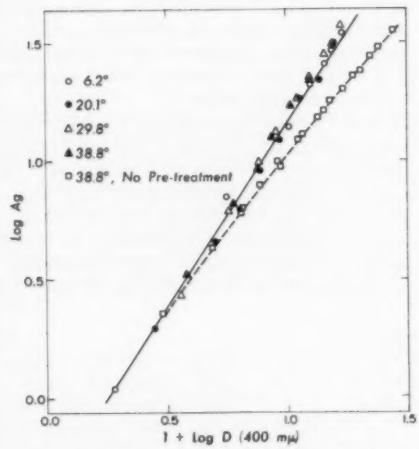

Fig. 6. Variation of density with mass of silver in Emulsion A. Solid curve, formaldehyde-treated emulsion; broken curve, emulsion without formaldehyde treatment.

measured at 400 mμ. The points for the various temperatures of development fall upon the same straight line (solid). The points for low-temperature development of the emulsion which has not had the formaldehyde hardening-treatment also fall on this line (points not shown), but the points for development at higher temperatures fall to the right of the line. The broken line represents development at 38.8°C.

The further hardening of Emulsion *A* by prebathing in the formaldehyde solution had no significant effect upon the rate of development at any temperature tested when the rate was determined in terms of the mass of developed silver. However, the rate in terms of developed density was decreased by the formaldehyde hardening for the higher temperatures of development.

The over-all activation energy of development can be determined from the dependence of the rate of development upon the temperature, provided the proper measure of rate is used. When the rates are determined in terms of the mass of silver, a satisfactory straight line is obtained for all coatings. Figure 7 illustrates the results obtained with Emulsion *A*

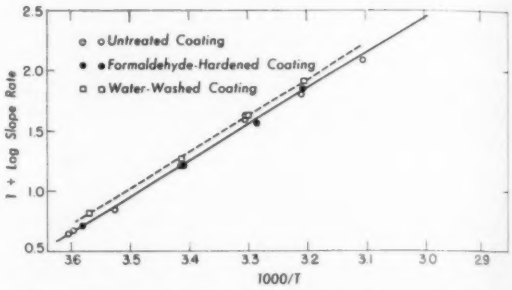

Fig. 7. Temperature-dependence of rate of development of Emulsion A.

under three conditions: untreated, water-washed, and pretreated in the formaldehyde bath. The over-all activation energy is independent of the treatment. A satisfactory straight line also is obtained in a log rate *vs.* $1/T$ plot for the formaldehyde-hardened emulsion when rates based on density measurements are used, but a straight line is not obtained for the untreated coating.

Physical Measurements on Emulsion A

Some measurements made by Marilyn Faust, of these Laboratories, on the temperature-dependence of swelling of the undeveloped Emulsion *A* coating are of interest in connection with the covering-power and color-ratio changes. The swelling was determined on samples which had been immersed for 15 min in distilled water at the various temperatures. The samples were weighed before immersion, after removal from the water (blotted to remove excess), and after drying. Both the percentage swelling of the emulsion layer in the water and the amount of material removed by the water treatment were calculated from these weights. The results are plotted in Fig. 8. The curves for swelling and washout are quite similar in form, and the major change in both quantities takes place in the range, 20° to 40°C.

The average size of the developed silver filaments and the pressure exerted by the gelatin on the filaments were determined by C. R. Berry from x-ray measurements[16] on samples of film developed at the two extreme temperatures used in the present work. For the same amount of developed silver, 27.7 mg/sq dm, the filament crystal sizes were 296 A and 309 A, respectively, for development at 4.4° and 49.3°C.

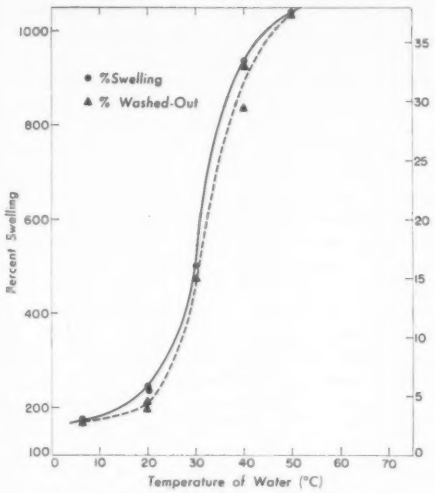

Fig. 8. Effect of temperature of distilled water on the degree of swelling and wash-out of Emulsion A.

The corresponding pressures were 840 and 550 atmospheres. The variation in size of the filaments is not significant, but the difference in pressure exerted by the dry gelatin on the silver is well beyond the limits of experimental error.

Effect of Solution Physical Development

The increase in the color ratio and the decrease in covering power which accompany an increase in the relative amount of solution physical development, when comparisons are made at equal amounts of developed silver, can readily be seen from a plot of the data given in Table III of Ref. 11, for the case where the solution physical development is varied by changes in the composition of the developer. Changes in temperature also can bring about variation in the relative amount of solution physical development, since the temperature coefficient of solution of the silver halide generally is different from that of chemical development. The amount of solution physical development which occurs during development of a normal silver bromide or iodobromide emulsion by the Metol–ascorbic acid developer is too small to exert a significant influence. Experimentally, no effect of temperature upon either the color ratio or the covering power of the commercial motion-picture-positive film was observed when this film was developed in the surface developer over the range, 6.1° to 38.7°C. Significant dependence on temperature was observed, however, when a solution consisting of 1.0 gram of Metol and 50.0 grams of sodium sulfite per liter was used at pH 9.3 (with sodium metaborate added to adjust the pH). The variation in color ratio with temperature is shown in Fig. 9. A similar shift towards warmer tones was observed as the temperature of development by Kodak Developer D-76 increased from 6.5° to 38.9°C.

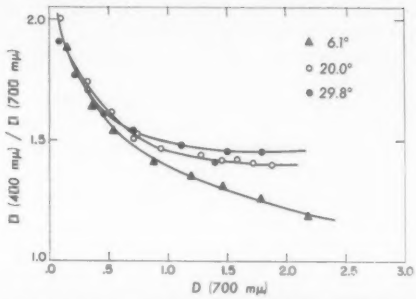

Fig. 9. Effect of temperature on the ratio, $D(400\ m\mu)/D(700\ m\mu)$, for development of motion-picture-positive film in a Metol–sulfite developer.

Solution physical development plays a more important part in the action of Kodak Developer DK-20 than it does in the action of either D-76 or the experimental Metol–sulfite developer.[19] The temperature-dependence of the rate of development by DK-20, however, is substantially the same as that of the rate of solution of the silver halide grains in this developer. Hence, it would not be expected that a change in temperature would change the relative participation of solution physical development in the over-all development process, and no change with temperature should occur in image tone because of solution physical development. Several development tests made with DK-20 at 6.7° and 39.0°C showed no significant difference in the absorption spectrum of the images developed at the two temperatures.

When a developer acts with little or no induction period and the rate of development is largely controlled by the rate of diffusion, the image tone is nearly neutral (apart from possible toning effects of oxidation products) and the tone does not depend significantly upon the duration of development. The increase in density with increasing duration of development is caused largely by an increase in the number of grains which are rather fully developed. An unusual effect was observed, however, with a developer which had the composition: Phenidone, 0.14 gram; chlorohydroquinone, 0.70 gram; sodium sulfite, 14.0 grams; and potassium bromide, 1.0 gram/liter, with sodium carbonate to give a pH of 10.6. Sensitometric strips of motion-picture-positive film developed in this solution at 20°C had an image which appeared to have the same tone when viewed from the emulsion side as when viewed from the base side of the fixed strips. In the very early stages of development, the image was warm in tone and electron micrographs showed that it consisted of tiny nonfilamentary particles. As development proceeded, the image became black and the silver became filamentary. The appearance of strips developed at 47°C, however, was the same when viewed from the emulsion and the base sides only during the early stages of development. The image produced by fuller development in the high-exposure-level areas was black when viewed from the emulsion side, but greenish-gray when viewed from

the base side, and the greenish-gray image was surrounded by a black fringe (halation). In the low-exposure-level areas, the image appeared black when viewed from either side.

Photomicrographs (see Fig. 10) of cross sections of the heavily exposed areas, made at intermediate stages of development at 47°C, suggest an explanation for the difference in appearance of the two sides of the developed strip. In Fig. 10, for example, the

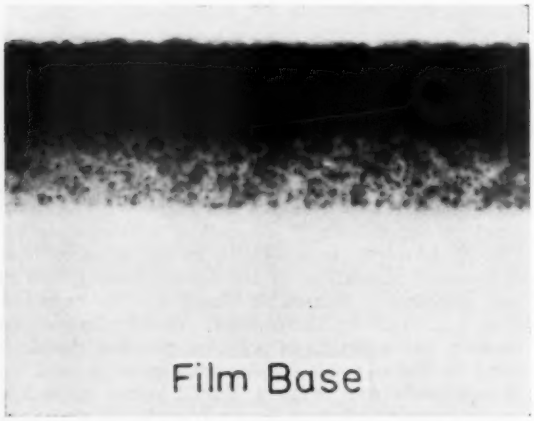

Fig. 10. Cross section of high-exposure-level area of motion-picture-positive film developed for 2 min in the Phenidone–chlorohydroquinone solution at 47°C.

silver near the base side of the emulsion consists of tiny particles which are much smaller than the fully developed grains, whereas the upper layer of silver consists of fully developed grains. The grains in the upper layer resemble closely those observed in cross sections of an emulsion layer which had been partially developed by a solution in which the rate was diffusion-controlled.[20]

The Phenidone–chlorohydroquinone developer at 47°C differs from the diffusion-controlled Amidol developer described in Ref. 20 in that the former shows a significant induction period, whereas the latter does not. In the induction-period region, the rate of diffusion exceeds that of development, and developer penetrates through the gelatin layer. Grains start to develop throughout the emulsion layer. Once the induction-period phase is past and rapid development takes over, diffusion becomes largely rate-controlling at the high temperature (but not at 20°C).

Temperature-coefficient measurements made in the region of 47°C support this suggestion. The calculated activation energy of reaction in the induction-period region is 11.7 kcal/mole, too high for a diffusion-controlled reaction. The calculated activation energy for the reaction beyond the induction period, however, is only 7.1 kcal/mole, which is within the range found in earlier work for diffusion of developer through a gelatin layer.[20] As development progresses, therefore, developer is used up by reaction with the grains near the surface almost as fast as it diffuses into the emulsion, and very little developer penetrates into the lower portions of the layer to continue development of the grains which have already started to develop in that region. For an active developer of this kind, the relative extent to which solution physical and direct chemical development occur in the emulsion layer depends upon the concentration of developing agent. Near the solution–emulsion interface, the rapid supply of developing agent by diffusion favors chemical development, since the specific rate of chemical development is high and increases with concentration of developing agent. For these agents at the particular pH, the rate of solution physical development is determined primarily by the rate of solution and, over a wide range, is independent of the concentration of the developing agent. The development in the lower portion of the emulsion layer, accordingly, may take place largely by the solution physical mechanism, and this would lead to the warmer tone in the developed silver.

In the low-exposure areas, where net diffusion is faster because the number of reacting grains which use up developing agent is much smaller, the solution physical development is relatively less important. Moreover, the contribution of grains in the region near the film base to the total developed silver is relatively smaller in the lower-exposure-level region because of the attenuation of exposure in the depths of the emulsion layer.

The color difference between the two sides of the film was not observed for the diffusion-controlled Amidol development at any level of exposure. This can be explained on the following basis: (1) No developer or insufficient developer is supplied to the lower part of the emulsion layer while development is still in progress in the upper part; and (2) suitable nuclei for physical development are not supplied by an initial "induction-period" reaction by this developer, since this developer shows no induction period.

Relation between Developed Density and the Size of the Silver Halide Grain

When pure silver bromide emulsions of the type used in this investigation are developed at 20°C in the "distortionless" hydroquinone developer, the developed grains are nearly pseudomorphs of the original bromide grains and the effective projection area appears to be approximately that of the original grain. Even though distortion occurs in the development of the iodobromide grains, the area of these developed grains may not differ greatly from that of the original grains. It is of interest, therefore, to see how the optical density of the silver formed by this developer is related to the measured size of the original silver halide grains.

The data in Table I indicate that, in general, the maximum specular densities increase with increasing total projection area, $N\bar{a}$, of the original grains, where N is the total number of grains per unit area

TABLE I. Density and Surface-Area Data for Silver Bromide and Iodobromide Emulsions

Average area $\bar{a}$ and thickness $\bar{t}$ data refer to original silver halide grains. Densities are for emulsions developed in the "distortionless" developer.

AgI, %	$\bar{a}$, sq μ	$\bar{t}$, μ	$\overline{Na}$, sq cm	Total surface, sq cm	$D\perp$	$D\parallel$	mg Ag/ sq dm	D 400/ D 700
0	0.11	0.223	63.7	280	1.02	1.41	10.0	1.18
	0.47	0.217	39.6	120	0.47	0.77	6.1	—
	0.47	0.217	61.7	186	0.75	1.10	9.5	1.10
	1.76	0.243	245.4	650	2.30	—	41.8	1.04
	3.70	0.289	204.5	515	1.80	2.31	41.4	1.04
	8.53	0.395	138.8	344	1.30	1.99	38.5	1.02
2.56	0.07	0.167	97.2	409	1.50	1.70	11.4	1.16
	0.20	0.222	73.7	277	1.08	1.60	11.5	1.06
	0.67	0.367	169.1	615	2.38	—	43.6	1.04
	1.38	0.504	110.4	392	1.55	2.13	39.0	1.03
	3.77	0.800	58.1	202	0.89	1.65	32.7	1.04

(relative) and $\bar{a}$ is the mean projection area. The maximum diffuse densities of the iodobromide emulsions increase linearly with the total projection area, but, as indicated by previous data,[14] the diffuse densities of the pure bromide emulsions show some departures from a linear relation. On the other hand, diffuse-density data for both the pure bromide and the iodobromide series fall on the same straight line when density is plotted against a *total surface area* calculated on the assumption that the grains can be treated as cylinders (Fig. 11).

Both diffuse and specular densities referred to in this section were measured with white light. Spectrophotometric curves, however, showed that little variation of density with wavelength occurred in these fully developed film samples (see Table I, last column).

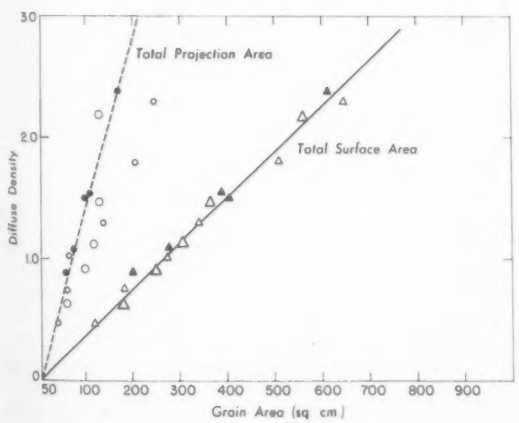

Fig. 11. Relation between diffuse density of developed silver and area of emulsion grains. Triangles: density plotted against total grain surface; circles: density against total projection area. Open triangles and circles: pure bromide emulsions; solid triangles and circles: iodobromide emulsions. Large triangles and circles represent a series of pure bromide emulsions coated at equal weight of silver bromide per unit area.

Discussion

The effects of variation in the temperature of development upon the absorption spectrum and the covering power of the silver produced by the surface developer correlate well with the data on the hardness, the degree of swelling of the gelatin, and the amount of material lost by the emulsion layer during immersion in water at the various temperatures. In the earliest stages of development, where electron micrographs show no filamentary silver, the form of the absorption spectrum curve is about that expected for the finely divided silver.[10] In the later stages of development, where the silver is filamentary, the tone shifts towards neutrality and the covering power decreases as the filamentary structure becomes more compact.[11,15]

During development, filaments may extend beyond the boundaries of the silver halide grain, provided the gelatin layer surrounding the grain can be readily penetrated. Swelling and softening of the gelatin would favor this penetration, whereas hardening would tend to prevent it. Accordingly, for a given degree of development, the filamentary silver formed by development of a given grain is less compact when the degree of swelling and softening of the gelatin is greater. Increased temperature promotes softening and swelling in the emulsions which have not been excessively hardened. Microscopic observations showed that the developed grains formed at the higher temperatures actually are larger, and hence have a less compact filamentary structure, since the mass of silver is the same. The amount of gelatin washed out of the emulsion layer during processing also may be an important factor. An irreversible loss of density upon drying of a processed emulsion occurs with many materials, and this can be attributed to a compression of the filamentary structure by the contracting gelatin.[5,6] The measurements made by Berry on the pressure exerted by the dry gelatin on the silver filaments suggest that the compression forces are weaker in the emulsion layer developed at the high temperature.

The weaker force may be a result of the wash-out of part of the gelatin or may be associated with some other change occurring in the gel structure during the high-temperature development.[6]

The results shown in Figs. 2 and 3 are similar in form to those previously obtained[21] in development by a ferro-EDTA solution in that, for a given amount of developed silver, the ratio $D(400\ m\mu)/D(700\ m\mu)$ increases with increasing temperature. The change in this ratio in the ferro-EDTA development may be explained in terms of changes in the degree of development of the individual grains as temperature increased, but the same explanation is not applicable to the present results with the Metol–ascorbic acid developer. The commercial motion-picture-positive film used with the ferro-EDTA developer does not show the shift in image tone when the Metol–ascorbic acid developer is used. The marked change in apparent activation energy of development which characterized the ferro-EDTA development in the temperature region in which the tone change occurred has no counterpart in the present work with the Metol–ascorbic acid developer. Finally, the form of the curve representing $D(400\ m\mu)/D(700\ m\mu)$ as a function of mass of developed silver is not the same for the two developers used at the elevated temperatures.

When solution physical development occurs to a significant extent, a change in temperature can change the relative extent to which this form of development participates in the total process, provided a significant difference exists between the activation energies of solution and of direct interface development. Some of the observed changes in covering power and image tone which accompany a change in development temperature can be explained on this basis.

The data plotted in Fig. 11 suggest that diffuse density is determined more by the total surface area of the developed grains than by the projection area. The densities for the iodobromide emulsions fit either relation, since the total surface, calculated as described, is nearly proportional to the projection area. In the pure bromide series, however, the thickness of the grains is nearly constant for grains of markedly different projection areas, and total surface is not proportional to projection area. The relation between density and projection area breaks down in this series, whereas the relation between total surface and density holds.

References

1. D. R. White, *Jour. SMPE*, **19:** 340 (1932).
2. J. Roig and J. Thouvenin, *Compt. rend.*, **202:** 1982 (1936).
3. R. Pinoir, *Sci. et inds. phot.*, (2) **14:** 241 (1943).
4. B. Maury, *Photo-Revue*, **58:** 42 (1946).
5. H. Zwicky, *Z. wiss. Phot.*, **50:** 415 (1955).
6. R. K. Blake and B. Meerkamper, *J. Phot. Sci.*, **9:** 14 (1961).
7. T. H. James, *J. Am. Chem. Soc.*, **61:** 648 (1939).
8. T. H. James and W. Vanselow, *Phot. Sci. and Tech.*, **2:** 135 (1955).
9. E. Klein, *Z. Elektrochem.*, **62:** 993 (1958).
10. Cf. E. Klein and H. J. Metz, *Phot. Sci. and Eng.*, **5:** 5 (1961).
11. T. H. James and W. Vanselow, *ibid.*, **1:** 104 (1958).
12. P. G. Nutting, *Phil. Mag.*, **26:** 423 (1913).
13. J. Eggert and A. Küster, *Kinotechnik*, **18:** 381 (1936); B. Koch, Thesis No. 2183, Eidgenöss. Tech. Hochschule, Zurich, 96 pp. (1953); J. Eggert and B. Koch, *Z. wiss. Phot.*, **49:** 104 (1954).
14. T. H. James, *J. Franklin Inst.*, **240:** 83, 229 (1945).
15. W. Koerber, *Wissenschaftliche Photographie* (*Ergebn. Intern. Konfer. wiss. Phot., Köln, 1956*), O. Helwich (ed.), Dr. O. Helwich Verlag, Darmstadt, 1958, p. 535.
16. C. R. Berry, *ibid.*, p. 72.
17. A. P. H. Trivelli and W. F. Smith, *Phot. J.*, **79:** 330 (1939).
18. R. P. Loveland in C. E. K. Mees, *The Theory of the Photographic Process*, rev. ed., Macmillan, New York, 1954, p. 507.
19. T. H. James and W. Vanselow, *Phot. Eng.*, **7:** 90 (1956).
20. T. H. James, *Phot. Sci. and Tech.*, **2:** 81 (1955), Figs. 4B, 4C.
21. ———, *Phot. Sci. and Eng.*, **4:** 271 (1960).

PHOTOGRAPHIC SCIENCE AND ENGINEERING
Volume 5, Number 5, September-October 1961

Effect of Development Temperature on Covering Power of a Developed Silver Image

D. A. NEPELA, *Ansco Research Laboratories, Binghamton, N.Y.*

The influence of development temperature on the covering power of an ammonia-type emulsion of 1.5-μ average grain diameter has been related to several factors. This dependence is shown to be proportional to $\exp(-7600/RT)$, a value which is in good agreement with the temperature dependence of the rigidity modulus of gelatin gels found by Ferry. These data, coupled with the observed correlation of the thermally induced covering power effect with a chemically induced covering power effect, indicate that intermolecular hydrogen bonding of the matrix gelatin, with its attendant effect on mechanical properties, is the dominant factor involved. The dependence of covering power on the development temperature is related to the hardening level of the emulsion and progressively increases with decreased emulsion hardening. Also, this thermal dependence of covering power was found to correlate well with the equilibrium swell ratio of the emulsions used.

The efficiency with which the developed silver of a coated photographic layer is utilized in formation of optical density is to a large extent dependent upon several factors, among which are the conditions of drying after processing. This has been pointed out by several authors,[1-3] the most recent and most comprehensive publication along these lines being that by Blake and Meerkamper.[3] Additionally, Koerber[4] pointed out that the degree of chemical hardening of the coated layer influences the degree of compactness of the filamentary silver formed in a chemical developer. There are, of course, other factors which can influence the covering power (optical efficiency) of the developed silver image, such as the average crystal diameter of the emulsion layer, as shown by Eggert and Kuster.[5] The ratio of chemical to physical development also can play a role in influencing the covering power of a developed silver image.

This paper is concerned primarily with those aspects of the problem which are independent of grain size and of the influence of the developer with respect to the ratio of physical to chemical development. Further, the material discussed in this paper will attempt to separate those contributions to covering power which occur during the drying of the developed layer from those which are produced during the development phase of the normal photographic processing cycle. The evidence presented indicates that profound changes in the covering power of a coated film layer can be effected by variation of the development temperature. This evidence is consistent with the view that a change in development temperature causes a significant change in the mechanical properties of the gelatin matrix surrounding the developing grain. The change is primarily effected through increasing labilization of intermolecular hydrogen bonding of the gelatin matrix with increasing development temperature. The effect is essentially independent of the events occurring during the drying cycle of processed film.

Received 19 August 1961.

1. D. R. White, *Jour. SMPE*, **19**: 340 (1932).
2. R. Pinoir, *Sci. Ind. Phot.*, **14**: 241 (1943).
3. R. K. Blake and B. Meerkamper, *J. Phot. Sci.*, **9**: 14 (1961).
4. W. Koerber, *Photo-Tech. u. Wirtsch.*, **10**: 414 (1959).
5. J. Eggert and A. Kuster, *Kino-Technik*, **18**: 381 (1936).

Experimental

A coarse-grained (1.5-μ average diameter) ammonia-type emulsion was used throughout the experimental work reported below. Development was carried out in both a Metol–ascorbic acid surface developer and a more conventional Metol–hydroquinone commercial x-ray developer. A normal acid stopbath and chrome alum hardening fixer were used. Only the results on covering power obtained with the commercial developer are reported in this paper, since a qualitative similarity between a Metol–ascorbic acid surface developer and this commercial developer was taken as an indication that solution physical development was not playing a major role in the commercial developer. The magnitude of the increase in covering power with the two developers obtained by increasing the development temperature was very similar, both developers showing only a very slight shift to warmer tone with increased development temperature.

The observation that increased development temperature caused a significant increase in covering power was further extended by making studies of development rate effects both in terms of the rate of

formation of silver mass (x-ray fluorescence measurements) and in terms of optical ASA diffuse density measurements. The index of development rate was taken as the reciprocal of the time required to form a particular density or a corresponding mass of developed silver at various development temperatures. Both the mass and the density measurements provided a good fit to the Arrhenius equation. Apparent activation energies from the data are shown in Fig. 1 and in Table I. In all three cases—that

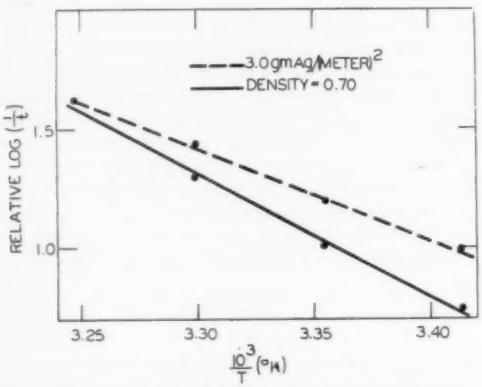

Fig. 1. Activation energy diagram derived from development rate measurements in terms of both silver mass and density for Emulsion B. Rate expressed as the reciprocal of the time required to develop a given density or mass of silver per unit area; temperature in degrees Kelvin.

TABLE I. Activation Energy for the Development Process in a Commercial X-Ray Developer, Derived from Both Optical Density and Silver Mass Measurements

Emulsion	Kcal/mole		
	Q_D	Q_{Ag}	$Q_D - Q_{Ag}$
A	24.2	17.1	7.1
B	25.3	18.1	7.2
C	25.4	16.8	8.6

is, for Emulsions A, B, and C, Emulsion A being moderately hardened, Emulsions B and C being hardened to a lower level—the apparent activation energy Q_D for the development process, measured in terms of optical density, was greater than the activation energy Q_{Ag} for the process when measured in absolute terms of silver mass.

The difference in activation energy $Q_D - Q_{Ag}$ was found to be approximately constant, and for the three materials an average value of 7.6 Kcal was found. Since optical density and mass are related through the equation

$$\text{covering power} = \left(\frac{\text{density}}{\text{silver mass/unit area}}\right)$$

it appears logical to assign the difference in activation energies $Q_D - Q_{Ag}$ to the energy of the reaction responsible for the covering power change with change in development temperature. The mode of measurement of rate is, of course, intended to measure the effects of the chemical reactions during development which produce optical density or silver mass. Each measurement will inherently account for all of the individual chemical energy terms that make up the observed total activation energy term. The measurement of rate in terms of density will include an additional term responsible for the physical state of the developed filamentary silver, in the sense that the optical properties of the developed silver are a function of the physical state of this developed silver, and are dependent upon the chemical reaction causing the change in mechanical properties of the matrix gelatin. The mass measurements, however, will be completely insensitive to the physical state of the developed silver image, and therefore to the chemical reaction occurring in the matrix gelatin causing this change in physical state.

With this reasoning in mind, the covering power dependence on development temperature is interpreted as being caused by a mechanical matrix gelatin effect occurring during the development cycle. To support this conclusion, we cite the following evidence:

1. The value of 7.6 Kcal found for the process responsible for the covering power effect is in the proper energy range to be interpreted as the energy required to cause rupture of intermolecular hydrogen bonds of the matrix gelatin. This would lead to a change in the mechanical properties of the matrix gelatin, which in turn would be expected to lead to a change in the physical state (degree of compactness) of the developed filamentary silver.
2. Independent data by Ferry[6] on the temperature dependence of the rigidity modulus of gelatin gels (a pure mechanical property) lead to a temperature dependence proportional to $\exp(-7300/RT)$ and $\exp(-7900/RT)$ respectively, whereas the data on the temperature dependence of covering power reported here lead to a value proportional to $\exp(-7600/RT)$, which is in good agreement with Ferry's data.

Emulsion D, which is a highly hardened coating of essentially the same grain size as Emulsions A through C, shows only a very slight dependence of covering power on the development temperature. This result, in the light of the previous reasoning, is interpreted to mean that the mechanical properties of the gelatin matrix are controlled to a much greater extent by the high degree of covalent hardening introduced by the aldehyde hardener present. The greater number of covalent bonds which cannot be thermally dissociated tend to override the contribution to the mechanical properties of the intermolecu-

6. J. D. Ferry, *J. Am. Chem. Soc.*, **70**: 2244 (1948); *J. Phys. Colloid Chem.*, **53**: 184 (1949).

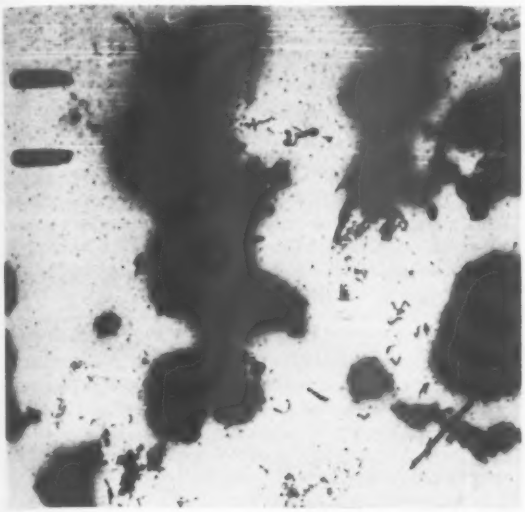

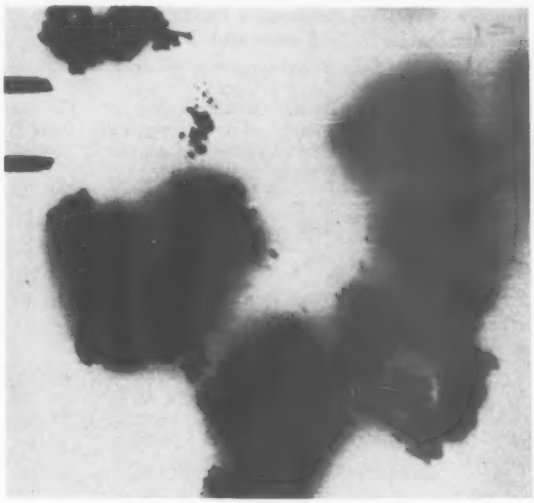

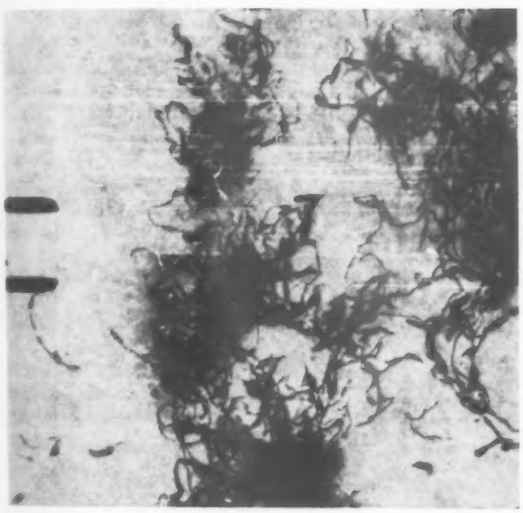

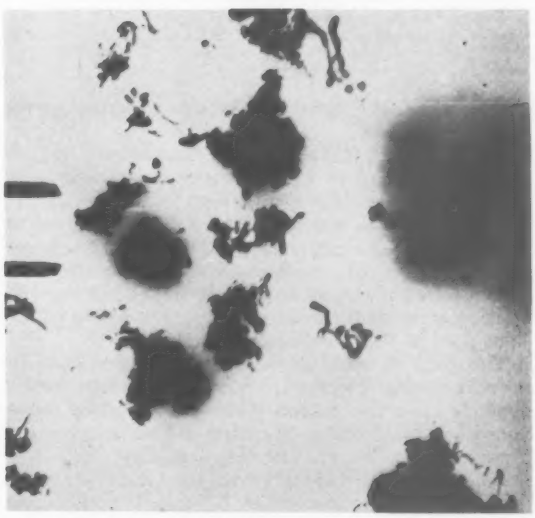

Fig. 2. Electron micrographs of image silver of Emulsion C, developed in the Metol–ascorbic acid surface developer. *Top:* 20°C development temperature. *Bottom:* 30°C development temperature. 1 μ between markers.

Fig. 3. Electron micrographs of image silver of Emulsion D, developed in the Metol–ascorbic acid surface developer. *Top:* 20°C development temperature. *Bottom:* 30°C development temperature. 1 μ between markers.

lar hydrogen bonding, which can be dissociated by heat. This dependence of the covering power on the development temperature is viewed as being a function of the ratio of intermolecular hydrogen to intermolecular covalent bonding. The primary bonding system (covalent) is virtually unaffected by development temperatures in the temperature range used (20–35°C), while the secondary bonding system (hydrogen) is known to be heavily dependent upon temperature in this range. Figures 2 and 3 are reproductions of electron micrographs of Emulsions C and D developed in the Metol–ascorbic acid surface developer at 20° and 30°C. Table II lists the detailed covering-power temperature-dependence data for Emulsions A–D.

Swelling Characteristics

The swelling characteristics of Emulsions A through D were determined in the same commercial developer as was used to obtain the rate data. Summarizing the results: at both a 20°C temperature and at an elevated temperature of 30°C, the swelling rate and the equilibrium swell value paralleled the covering power data. That is, the greater the increase in the degree of swelling with elevation in

TABLE II. Covering Power as a Function of Development Temperature in a Commercial X-Ray Developer

Emulsion	Devlpr. temp., °C	Devel. time, min	Total density above base	Ag in mg/100 sq cm	Covering power
A	20	5	1.875	73.0	25.7
	25	2½	1.895	71.0	26.7
	30	1½	2.19	74.5	29.4
	35	1	2.81	70.0	40.2
B	20	5	1.86	70.0	26.6
	25	2½	2.485	88.0	28.3
	30	1½	2.71	75.0	36.2
	35	½	2.47	38.5	64.2
C	20	5	2.69	93.2	27.8
	25	2½	2.67	89.8	29.8
	30	1½	3.16	85.0	38.4
	35	¾	4.44	81.2	54.6
D	20	5	2.10	100	21.0
	25	3½	2.19	95.0	23.3
	30	1½	2.29	96.0	23.8
	35	1	2.35	95.0	24.8

temperature, the greater was the covering power increase obtained.

Figures 4 and 5 illustrate for Emulsions C and D the swelling curves for developer temperatures of 20°C and 30°C. It is readily seen from these figures that Emulsion C has a greater rate and degree of swelling at both temperatures, and that it increases its swelling percentagewise to a greater degree when processed at elevated temperatures. This type of correlation holds throughout all the processing conditions used in the preceding rate studies.

The swelling effect parallels the emulsion hardening relationship discussed previously and undoubtedly depends upon the degree of covalent bonding introduced by the chemical hardener. The temperature dependence of the equilibrium degree of swelling is probably linked intimately with the temperature dependence of intermolecular hydrogen bonding of the gelatin system.

Experiments Utilizing Gelatin Denaturing Agents

If the dependence of covering power upon development temperature is intimately connected with the intermolecular hydrogen bonding of the matrix gelatin, it should be possible to duplicate essentially these large covering power changes by addition of a specific gelatin denaturing agent to a developer.[7,8] Thus, chemical denaturation, or labilization of intermolecular hydrogen bonding, should be entirely equivalent to the thermal effect, both, of course, taking place during the development phase of the process. That this is essentially true is illustrated in

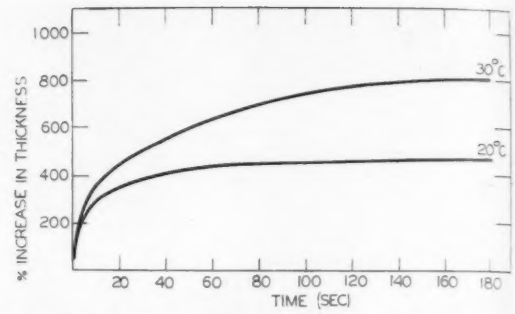

Fig. 4. Swelling curves of Emulsion C in a commercial x-ray developer.

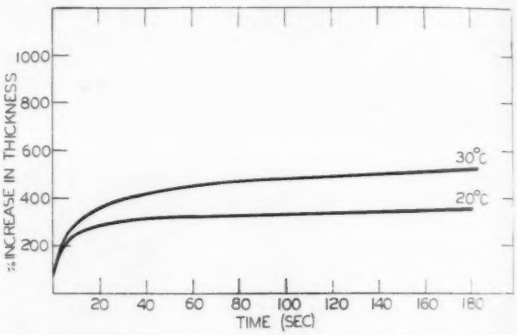

Fig. 5. Swelling curves of Emulsion D in a commercial x-ray developer.

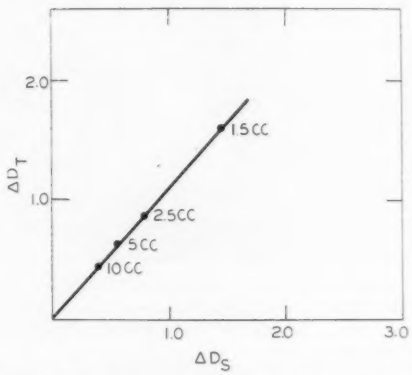

Fig. 6. Relationship between the change ΔD_T in maximum density for a change in developer temperature and the change in maximum density ΔD_S caused by addition of 25 grams salicylic acid per liter developer. Development time for the higher temperature case is adjusted to yield approximately an equal degree of development. Various levels of aldehyde hardening, in terms of cubic centimeters of aldehyde per unit of emulsion, are indicated by the points on the curve.

Fig. 6, where ΔD_T is plotted vs. ΔD_S for four levels of hardening of the emulsion. The value ΔD_T represents the change in maximum density which occurs by virtue of development at two different development temperatures. In this case, the development temperatures were 20°C and 25°C. The

7. F. Dersch, *J. Phot. Soc. Am.*, **11**: 467 (1945).
8. H. Champlin, *Champlin on Fine Grain*, Camera Craft Publishing Co., 1937, p. 53.

degree of development (as measured by the mass of developed silver) is held essentially constant by adjustment of the development time. The value ΔD_s refers to the change in maximum density which was effected by incorporation of 25 grams salicylic acid per liter of developer, with pH adjusted to that of the reference developer. Development was carried out at 20°C in both the reference developer and the developer containing salicylic acid, so that an equal degree of development was obtained. The differences ΔD which occur under these circumstances are proportional to increases in covering power obtained either thermally (development temperature) or chemically (developer containing salicylic acid).

Inspection of this figure reveals that, with decreasing aldehyde content in the emulsion, a progressively greater change in maximum density occurs for either a development temperature increase, or for the isothermal system at 20°C where the change in maximum density relative to the control developer is effected by salicylic acid. For all cases, the degree of development (developed silver per unit area) was essentially constant.

The observation that this maximum density change (due to covering power increase) yields a linear relationship between the thermal effect and the chemical effect is significant. The interpretation offered is that both the thermal system and the chemical system act on the same bonding system of the matrix gelatin (hydrogen bonding) and can produce completely equivalent changes in the mechanical properties of the matrix gelatin surrounding the developing silver halide crystal.

Table III illustrates the equilibrium swell ratios at 20°C of Emulsions C and D in both a normal Ansco A-30 developer and an A-30 developer containing 50 grams of salicylic acid per liter, the pH being readjusted with sodium hydroxide to the pH of the reference developer. The presence of salicylic acid in the developer causes both Emulsions C and D to increase the rate of swelling as well as the equilibrium value attained. Again, Emulsion C responds percentagewise with a greater increase in swelling rate with increasing temperature than does the harder Emulsion D, recalling that this same qualitative observation was obtained for the temperature dependence of swelling of these two emulsions.

TABLE III. Effect on Emulsion Swelling of 50 Grams of Salicylic Acid per Liter in a Commercial X-Ray Developer

$$\left(\frac{\text{Thickness in microns on swollen emulsion}}{\text{Original dry thickness}}\right) 100$$

Emulsion	Reference developer	Devlpr. containing 50 grams salicylic acid per liter
C	400	690
D	350	470

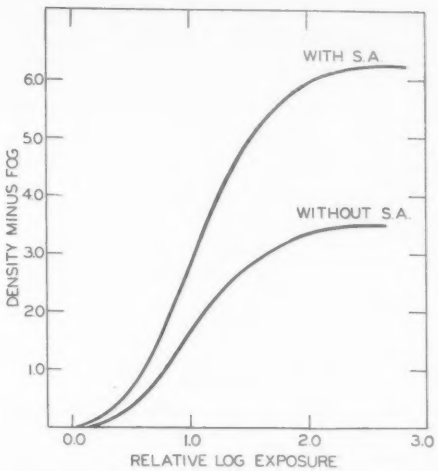

Fig. 7. Sensitometric curves of Emulsion C developed in A-30 developer, with and without 50 grams salicylic acid per liter developer.

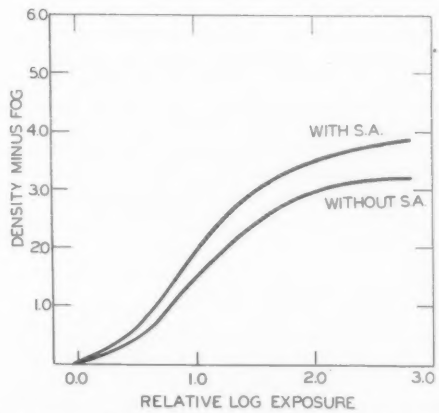

Fig. 8. Sensitometric curves of Emulsion D developed in A-30 developer, with and without 50 grams salicylic acid per liter developer.

Figures 7 and 8 illustrate the sensitometric curves obtained for development at 20°C, at equal times, of Emulsions C and D in the A-30 developer with and without salicylic acid.

Covering Power as a Function of Emulsion Hardening

In an earlier section, the temperature dependence of covering power was discussed with reference only to a qualitative hardening level. Essentially analogous experiments were performed on a set of aldehyde-hardened emulsions. This same set was previously used in the section on chemical denaturing agents.

The commercial x-ray developer was used at temperatures of 20°C and 30°C on a set of emulsions containing 0, 1, 2.5, 5, 10, and 15 cc of aldehyde

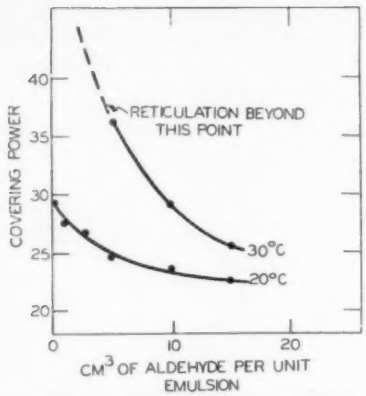

Fig. 9. The effect of various concentrations of aldehyde hardener on the covering power for development in a commercial x-ray developer at 20°C and 30°C.

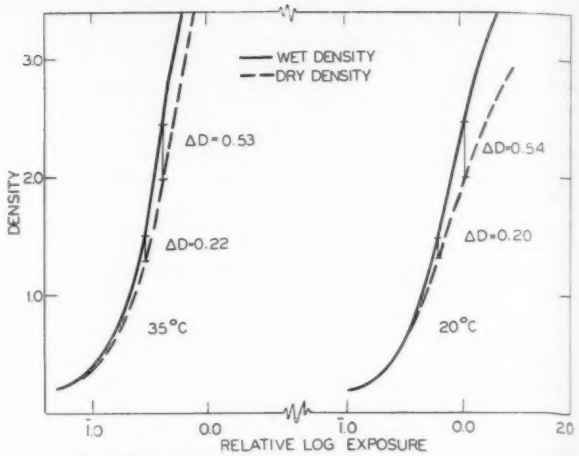

Fig. 10. The effect of drying on the characterstic curve for Emulsion C, for both 30°C and 35°C development temperatures.

hardener per unit weight of emulsion. The results for both processing temperatures are summarized in Fig. 9. At either temperature, decreasing aldehyde hardener content yields progressively increasing covering power. However, with increasing development temperature the degree of chemical hardening becomes progressively more important with respect to its influence upon the "covering power."

With progressively increasing chemical hardening the two temperature curves approach one another, indicating that marked overhardening can completely mask or eliminate the temperature dependence of covering power.

The Effect of Drying

One might suspect from the data included in the recent paper by Blake and Meerkamper[3] that the covering power changes reported here may to a large extent be due to drying effects. Several experiments aimed at establishing the influence of drying were performed. Emulsion C was chosen, since it possessed the least compressed structure in the developed silver of the films investigated, and therefore would be expected to yield the largest changes upon drying.

Figure 10 illustrates the sensitometric curves obtained for Emulsion C under two radically different processing conditions:

(a) Commercial x-ray developer at 20°C for 4 min
(b) Commercial x-ray developer at 35°C for 1 min

These development conditions yield approximately equal degrees of development with respect to silver mass. The processed film strips were dried under identical conditions and read in both the wet state and the final dry state. The magnitude of loss of density upon drydown is seen to be very similar for the two processing conditions. Thus one can state that the large density changes due to the thermal dependence of covering power upon development temperature are only influenced to a relatively minor degree by the events occurring during the drying of the film, compared to the events occurring prior to the drying cycle.

Discussion

The covering power of the silver deposit of a developed silver layer has been shown to depend markedly upon the development temperature. This increase in covering power is not dependent upon the change in the ratio of chemical to solution physical development as evidenced by the data obtained with a solvent free Metol–ascorbic acid surface chemical developer. Further evidence of independence of the effect from a change in the degree of solution physical development is the observation that in all experiments discussed herein only negligible changes occur in the ratio of the density measured at 700 mμ to the density measured at 400 mμ. These changes in the ratio have not exceeded 5%. They tend, however, to go to slightly lower values of the ratio $D700/D400$ with increasing development temperature, thus shifting to slightly warmer tones with increasing temperature.

The temperature dependence of the covering power has been shown to vary markedly with the degree of emulsion hardening, and can be essentially eliminated by considerable overhardening. This temperature dependence has been clearly related to the mechanical properties of the matrix gelatin, in that the temperature dependence of the change in covering power was found to have the same temperature dependence as the rigidity modulus (a pure mechanical property) of gelatin. The variation of covering power with development temperature has been ascribed to the dependence upon temperature of intermolecular hydrogen bonding of the gelatin. Thus the covering power varies according to the mechanical properties of the matrix gelatin, which can be influenced by both temperature and the chemical composition of the developer.

Both the swelling data and the effect of gelatin denaturants correlate well with the covering power changes in emulsions with various hardening levels. Both of these properties depend heavily upon the degree to which intermolecular hydrogen bonding contributes to the total mechanical properties of the gelatin matrix.

The results obtained are only marginally influenced by drying effects and are therefore primarily attributed to events which occur during the development phase of the processing cycle.

Acknowledgment

The author wishes to express his thanks to William Yeager, R. H. Lee, and to R. H. Clark for contributions made to this paper.

• Short Communications

Rapid Processor for the KA-30 Camera

JEROME S. GOLDHAMMER, *Advanced Engineering and Research, Chicago Aerial Industries, Inc., Barrington, Ill.*

One method of achieving rapid availability of photographic intelligence in tactical and combat surveillance air photography is inflight development of the pictures. Various approaches may be taken: examination of the photographs aboard the aircraft, telemetry to surface stations, or physical delivery of the film direct to the surface forces that requested the photographic mission, ready for photographic intelligence viewing.

In order to meet these requirements, a rapid processor has been designed and developed as part of the KA-30 Camera System. The initial design was for the Air Force RF-101 McDonnell Voodoo, the current standard reconnaissance aircraft in the Tactical Air Command. The RF-101 is subject to severe temperature fluctuations in the camera compartment as a result of supersonic speed, with its attendant skin heating, and rapid climb to the stratosphere, with exposure of the plane to subzero conditions. Thus customary processing techniques which are extremely temperature dependent are rendered undesirable. Because the camera bay is not pressurized, the pressure fluctuations caused by the RF-101's rate of climb of up to 20,000 ft/min and ceiling of over 50,000 ft also pose problems, in terms of elevated temperature during processing with possible boiling of processing fluids. Finally, the RF-101, retaining the maneuverability of its strike-fighter ancestry, may send fluids flying in all directions.

Because of these aircraft characteristics, it was necessary to employ a processing technique which had the following characteristics: 1. relative independence from temperature fluctuations; 2. freedom from harmful effects from pressure fluctuations; 3. attitude independence.

A monobath could be designed to meet the first two of these requirements (Fig. 1) and was accordingly selected. The use of a saturated web technique was dictated by the desire to be attitude-independent, and to avoid both the complicated seals required by an immersion system and the pumps and applicators required by a viscous system.

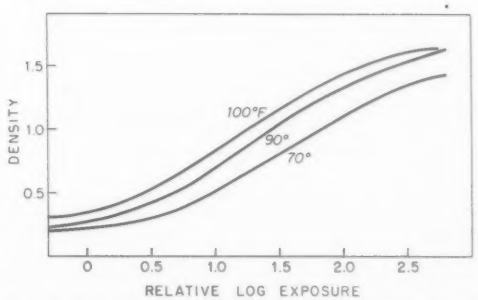

Fig. 1. Characteristic curves obtained with 60-sec monobath at three processing temperatures. Du Pont Type 131 Film.

The high- and low-altitude capability of the RF-101 require that the camera cycling rate vary from 6 cycles/sec at high speed and low altitude, to as little as 1 cycle/min, at low speed and maximum altitude. As a result of this tremendous variation in film-drive rate, (from 30 in./sec down to less than $\frac{1}{4}$ in./sec), a very flexible film take-up system had to be designed. This is shown schematically in Fig. 2. A swinging arm is provided,

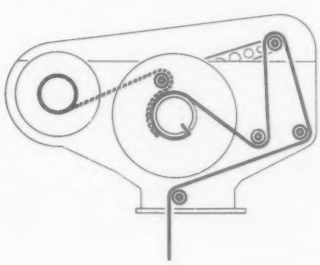

Fig. 2. Schematic diagram of film take-up system.

Presented at the Rapid Processing Symposium, Washington, D.C., 14 October 1960. Received 5 July 1961.

which senses the size of slack loop, and adjusts take-up drive speed to match film output rate from the camera. The take-up drive motor is controlled by a magnetic amplifier. The position of the idler arm controls a potentiometer, which changes the pulse duration of motor power, thus increasing the revolutions per minute as pulses are broadened, and vice versa. Response of the drive train must be immediate, because when the camera is operated on "pulse" mode, film feed is discontinuous, so that the take-up must go to maximum speed and back to zero 3 times/sec.

Monobath processing is actually completed on the take-up, but no harmful effects from continued contact of the film with the saturated web are observed for several hours. Beyond that point, some bleaching out of image and failure of the film-base/emulsion bond may occur. However, these effects do not occur within the 2-hr flight time of the RF-101, so they do not constitute a problem.

The rapid fluctuations in pressure encountered make it essential that entrapped air in the web be avoided, because expansion of the air at high altitudes might cause leakage. This problem has been solved by winding the web rolls dry under constant tension, and then immersing them in monobath solution, standing on one flange, with the other exposed, in a vacuum chamber. Capillary action fills the web, the air bubbles being released through slots in the exposed flange. If the vacuum chamber is held at a higher pressure altitude than will be encountered in flight, leakage can be avoided.

The high temperature encountered made the choice of a prehardened emulsion mandatory. Du Pont 131 gave the highest sensitivity of any type of film capable of surviving the elevated temperatures. Subsequent use of the unit has indicated that in a more normal environment, in the 70° to 80°F range, standard Eastman Plus X-Aerecon and Tri-X are entirely suitable. Under more severe temperature conditions, Ansco Hyscan Pan might be employed, provided some sacrifice of sensitivity can be accepted.

Fog level is about 0.2 above base for Du Pont 131, and image structure is virtually unaffected. ASA Exposure Index is 125 at 90°F, the optimum temperature, falling to 60 at 70°F, and remaining at 125 at 100°F, but with the fog increasing to 0.4 above base. Available density range is about 1.5 at all temperatures, and gamma about 0.7. Results with Plus X-Aerecon are comparable, gamma for the same monobath being about 1.2 at 75°F, with a fog level of about 0.2, ASA Index remaining at the 125 level. No effort has been made to compound a special monobath for Plus X-Aerecon, because of the circumstances dictating the use of Du Pont 131. However, such work is proceeding now, and even higher gamma should be obtainable if required.

The Camera Calibrator, Model III

GOMER T. MCNEIL, *Photogrammetry, Inc., Rockville, Md.*

The Camera Calibrator has been in development for a period of nearly six years, during which three models have been produced. The development started in June 1955, with an award of a contract by the Bureau of Aeronautics for the design and development of a camera calibrator for delivery to the Naval Photographic Interpretation Center.

The Camera Calibrator, Model III (Fig. 1), is a relatively small precision instrument that provides a known angular array of targets located at optical infinity. These targets, each consisting of a center cross and resolution charts, are photographed by the camera under test. The images of the targets are then read and measured to yield the necessary data for the determination of focal length, location of principal point, radial and tangential distortion, and radial and tangential resolution.

The Camera Calibrator two-bank array of collimators is illustrated in Fig. 2. The collimators in each bank lie in a plane perpendicular to the plane of the other bank and are spaced at 7½° intervals. Each bank covers a full field of 90°. The 25 collimator bundles intersect in a common central area. The lens of the camera under test is placed in the center of this area.

The collimator lens was designed by Dr. Robert E. Hopkins, Institute of Optics, University of Rochester. The achromatic objective consists of an air-spaced doublet with a full field of 2°. The coated collimator lens has a focal length of 14 in. and a clear aperture of 2½ in., thus producing an $f/5.6$ optical system. The collimator lenses are manufactured by Goerz American Optical Co.

The target is a reticle consisting of a center cross and 13 resolution patterns, ranging from 1 to 64 lines/mm, with graduated steps proportional to the $\sqrt{2}$. The reticles for each 7½° zone are corrected for the tilt effect so that the images of the targets in the focal plane of the camera under test will be the same size. The tangential tilt correction is equal to the cosine of the zone angle, while the radial tilt correction is equal to the cosine squared of the zone angle. The reticles are photographically produced from Kodak High Resolution Plates.

The off-axis collimators have a folded optical system as shown in Fig. 3. The front-surface mirror is flat within ¼ wavelength and has an aluminized surface with a silicon monoxide overcoating. The reticle is adjustable both radially and tangentially. Neutral density and Kodak Wratten filters 25A, 78AA, and K2 are supplied. The cosine fourth-power illumination loss is approximately balanced by the neutral density filters. Filters of 0.6 density are used in the central and first three zones, filters of 0.3 density are used in the fourth and fifth zones, and no filter is used in the sixth zone. The illumination assembly is comprised of a condenser lens and a General Electric #1482 miniature lamp with a life rating of 100 hr. The collimator housing is a Meehanite casting that

Presented at the Annual Conference, Binghamton, N.Y., 23 May 1961. Received 16 June 1961.

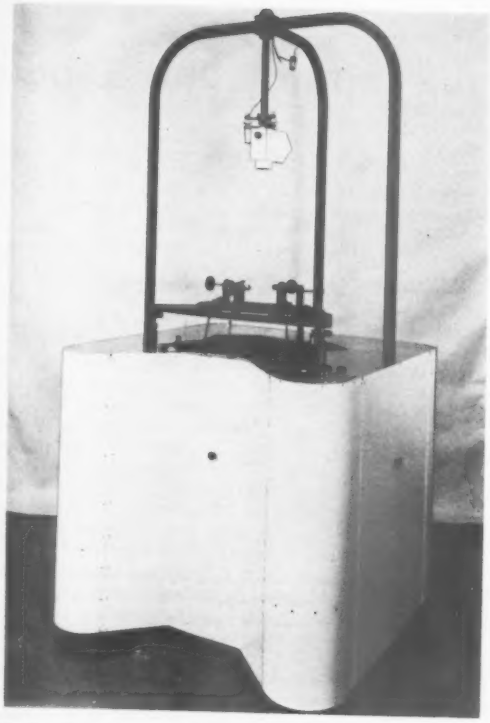

Fig. 1. Over-all view of the Camera Calibrator, Model III.

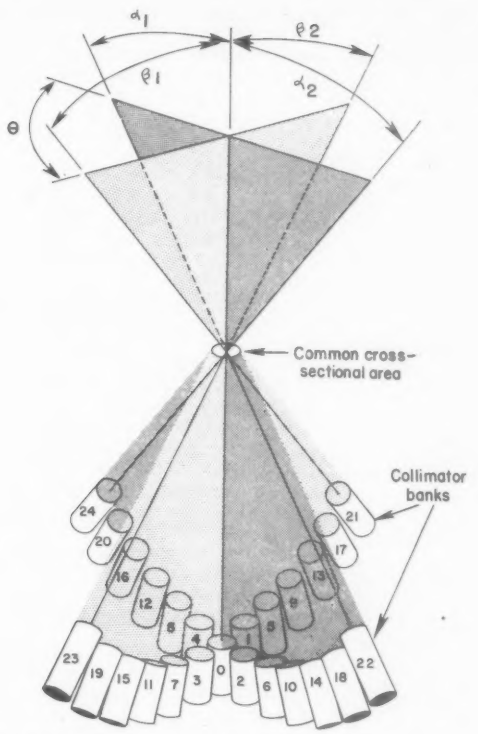

Fig. 2. Relation of collimators (0-24) in two-bank array.

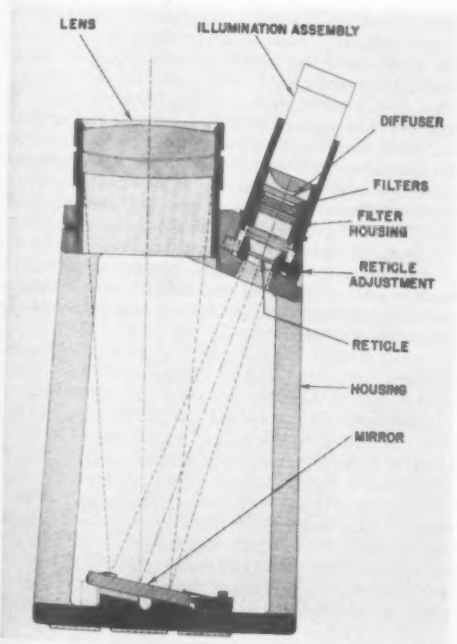

Fig. 3. Schematic diagram of folded optical system of off-axis collimator.

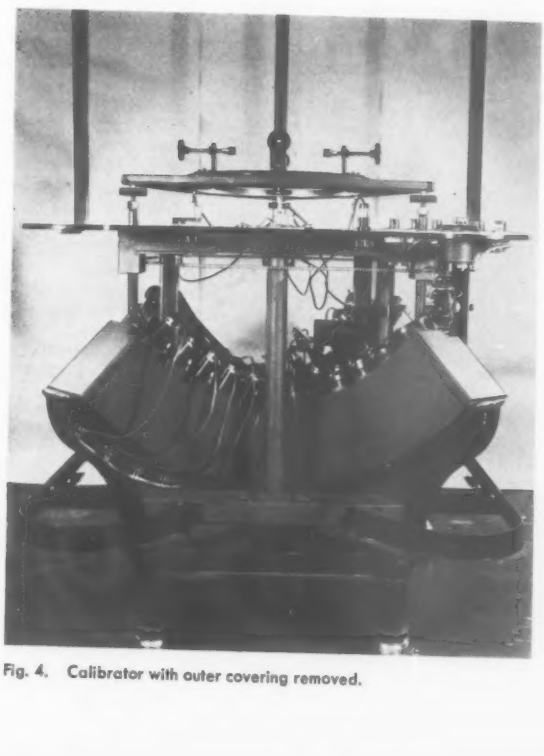

Fig. 4. Calibrator with outer covering removed.

is stress-relieved prior to and subsequent to rough machining.

Although the neutral density filters approximately balance the cosine fourth-power illumination loss, minor variations are achieved with the zone rheostats. The exposure timer, located in the center of the panel, is continuously variable from approximately 2½ sec to 5 min. The timer is graduated in 5-sec intervals but can be set within 1 sec.

The lamp control panel contains 25 rheostats, one for each of the collimator lamps. This arrangement allows individual lamp adjustment within each zone. If a lamp burns out, a new lamp can be installed and balanced with the remaining lamps of the zone. The constant voltage transformer and power supply are isolated from the Camera Calibrator by placing them directly on the floor beneath the instrument. The electrical requirement is 110 v, 60 cycles, single-phase ac.

The data code projector accommodates a writing space ¼ in. in diameter. The data are projected in the vicinity of the first zone so that an identification number can be exposed on the negative of the camera under test.

Figure 4 shows the Camera Calibrator, Model III, with the outer covering removed. The symmetrical array of 25 collimators is supported on Meehanite stress-relieved castings. The small crank raises or lowers the camera stage to position the front nodal point of the camera lens at the intersection of the collimator axes. Four adjustable lamps located just below the camera stage (top of figure) illuminate the fiducial marks or the focal-plane frame.

The autocollimator (top portion of Fig. 1) is aligned with the central collimator by actuating the autocollimator leveling head until the autocollimator cross lines bisect the center cross of the central collimator. The camera under test is clamped into position so that the lens is placed within the center of all the collimated bundles. A plane-parallel mirror is placed on the focal plane of the camera. The camera-stage leveling screws are adjusted until the image of the projected and reflected cross lines of the autocollimator are superimposed on the actual reticle cross lines. This autocollimating procedure establishes a relationship of perpendicularity between the focal plane and the collimated beam of the central collimator. The image of the center cross of the central collimator on the negative of the camera under test is the location of the principal point when the lens is free of decentration. In the event that an elegant calibration solution is required and one does not wish to assume that the decentration behaves as a thin prism, the center cross can be used initially as a close approximation for the location of the principal point.

The Camera Calibrator is calibrated by means of a Wild T-2 theodolite that has been modified for reading angles when the theodolite is supported in a horizontal position. The targets of each collimator are adjusted radially and tangentially until the interval between collimators is 7½° and the two banks of collimators are perpendicular to each other.

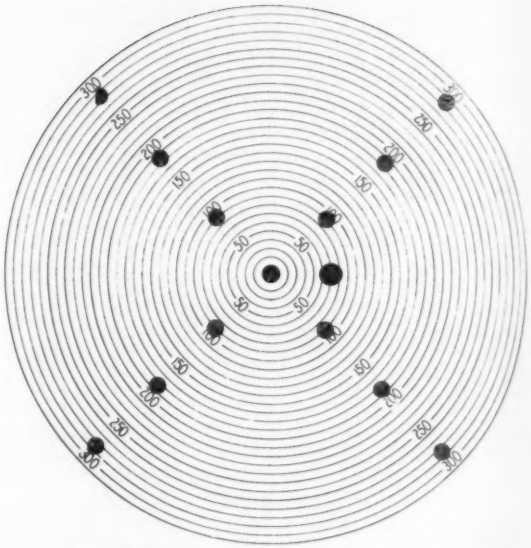
300
250
200
150
100
50
50
50

• Book and Journal Reviews

Tables of Blackbody Radiation Functions

MARK PIVOVONSKY AND MAX R. NAGEL, AND THE STAFF OF THE HARVARD UNIVERSITY COMPUTATION LABORATORY, Macmillan, New York, 1961, *xlii* + 481 pp., 8½ by 11 in., $12.50

It is explained in the introduction that this monumental tabulation of Planck's radiation law and related functions, occupying 481 pages of tables and 42 pages of introductory, descriptive, and bibliographic matter, was primarily designed for use in the development of artificial light sources to be used in photometry, photographic sensitometry, and physiological-optical research. The plans of the undertaking were sent for comment to experts in observatories and research organizations. As a result of the response, the scope of the tables was broadened to include, in a set of tables useful in a wide variety of radiometric applications, including those in spectroscopy and astrophysics, data beyond the spectral and temperature ranges normally appropriate to photographic sensitometry and colorimetry.

The tables are constructed to minimize, as far as possible within a manageable volume, the necessity of extrapolations and secondary calculations. The intervals in wavelength and temperature are based on the importance, in the specific application, of such factors as the spectral sensitivity of photographic materials and of the eye, or the temperatures attainable and the accuracy of their measurement in given temperature ranges.

The longest of the tables lists, as functions of wavelength over the range 200 to 1200 mμ and of temperature over the range 800° to 40,000°K, (a) the spectral radiance of a blackbody in watt cm^{-3} $steradian^{-1}$, (b) the relative radiance of the blackbody at a given wavelength to that at wavelength 560 mμ, the reference wavelength in many colorimetric and physiological-optical investigations, and (c) the fraction of the total radiance which is emitted in the spectral region between wavelength zero and a given wavelength, useful in calculations of the energy emitted within a given wavelength band. Another table gives the same data over the spectral range from 1.1 to 1000 μ and the temperature range 20° to 13,000°K. There are tables of spectral radiance functions as functions of the product λT, of total radiance, of maximum spectral radiance, and of the wavelength of maximum radiance, as functions of the temperature in the range 1000° to 10,000°K, and there are tables, useful in spectroscopy and astrophysics, of radiation functions expressed in terms of wave number and the reciprocal of the temperature. In addition to tables of luminance and of the chromaticity coordinates of the blackbody as a function of temperature in the range 800° to 40,000°K, there are auxiliary tables of colorimetric and physiological-optical interest, data on the spectral emissivity of tungsten ribbon, and, to diminish the danger of obsolescence of the tables as a result of changes in the numerical values of the radiation functions with changes in the values of the fundamental physical constants on which the tables are based, there are tables of functions related to these changes, from which corrections in Planck's equation can be made.

Particularly valuable to the novice and the occasional user of the tables are fully worked out examples of their use in many specific applications.

The format of the tables is excellent—the individual entries are easily read, and the paper and binding appear good and resistant to wear. A few slips in the introductory section were found; the authors of the section of Radiometry in the American Institute of Physics Handbook, referred to on p. *xl*, are M. M. Reynolds, R. J. Corruccini, M. M. Fulk, and R. M. Burley; on p. *xxiii*, the triple point of water should be given as 273.16°.

This volume truly fills a long-felt want, and the over-all time that can be saved with its aid is incalculable. It needs no great prescience to predict that these Tables will become indispensible to all seriously concerned with radiometric, photometric, colorimetric, photographic-sensitometric and physiological-optical investigations.—*William West, Eastman Kodak Company, Rochester, N.Y.*

Color Problems in the Graphic Arts

Symposium of the Inter-Society Color Council

1959, 148 pp., $2.00, paper cover. Order from Inter-Society Color Council, c/o W. L. Rhodes, Rochester Institute of Technology, Rochester 8, N.Y.

This collection of articles, originally presented at the 25th Annual Meeting of the Inter-Society Color Council in the spring of 1956, contains, in addition to a foreword and introduction, 10 articles on color in the graphic arts. These are: "Color Printing Methods in Graphic Arts," by M. C. Rogers; "Tone Reproduction in Graphic Arts Processes," by W. L. Rhodes; "The Scanner in Color Reproduction," by V. C. Hall and J. G. Jordan; "Color Problems in the Pressroom," by G. H. Dalsemer; "Paper Controls in the Graphic Arts," by J. H. Kronenberg; "Color Matching and Control of Printing Inks," by C. R. Conquergood; "Printing Controls at the Press," by D. Smith; "Lighting for Color Control," by W. B. Reese; "Use of Color Systems in Graphic Arts," by C. E. Foss; and "The Role of the Publisher in Color Problems," by F. E. Church. Many of the problems dealt with in the symposium, while described with particular reference to the graphic arts, are problems of interest in color photography. Unfortunately, one of the originally presented papers which was of particular interest to photographic scientists and engineers ("Color Correction in Photomechanical Reproduction," by W. Clark) is not included in the published volume because of reproduction difficulties. In general, the papers are not highly technical but present, in a concise manner, a general description of the problems enumerated above.—*C. J. Bartleson, Eastman Kodak Company, Rochester, N. Y.*

Small-Scale Preparation of Fine-Grain (Colloidal) Photographic Emulsions

B. H. CRAWFORD. Notes on Applied Science No. 20 (National Physical Laboratory, Great Britain), Her Majesty's Stationery Office, London, 1960, 13 pp., 1s 6d

Details are given of the preparation on a laboratory scale of ultrafine-grain emulsions. Extremely high-resolving powers can be obtained, sufficient to give brilliant Lippmann-Ives interference colors, which means a resolving power of better than 5000 lines/mm.

Directory of Industrial Research Laboratories in New York State, 1960

The New York State Department of Commerce, 112 State St., Albany 7, N.Y., has announced publication of the 1960 Directory of Industrial Research Laboratories in New York State. The 280-page directory lists over 1,000 laboratories, and is available on request.

A typical listing includes: the name and address of the laboratory and of the parent company, the name of the research director and other executives, the size and kind of research staff, and the fields of activity. In addition to the listings, which are divided into three sections, there is also a Subject Index of Research Activity and a new feature, the Geographic Appendix. Of particular interest to SPSE members are the many listings of laboratories under Photography, Photogrammetry, Photomicrography, etc. Included under these listings are photo equipments, emulsions, photosensitive materials, etc. — *Frank Smith, 21 Butler Pl., Brooklyn, N.Y.*

The Optical Industry Directory

The Optical Publishing Co., Lenox, Mass., 1961, paper cover, 200 pp., $7.50

Published by the Optical Publishing Co., this is the seventh annual directory of American importers, designers, manufacturers, and distributers of optical instruments. The listings are categorized under 350 item groupings. A revised lens appendix brings up to date the information on a thousand commercially available lenses for photographic and optical instrumentation. Previous editions were reviewed in *P S & E*, **3:** 305 (1959) and **4:** 359 (1960).

Infrared Physics

Volume 1, Number 1, March 1961, 104 pp.

This new journal, published by Pergamon Press Ltd., New York and Oxford, is being established as an international forum for the publication of research papers and critical surveys concerned with infrared theory, experiment, and instrumentation as applied to infrared detection and transmission and to problems of atmospheric, meteorological, geophysical, astrophysical, and space research. The Board of Editors consists of W. K. Weihe (U. S. Army), S. Passman (Rand Corp.), N. Migeotte (Université de Liège), and T. S. Moss (Royal Aircraft Establishment).

Zhurnal Nauchnoĭ i Prikladnoĭ Fotografii i Kinematografii

Vol. 6, No. 2, March-April 1961 (in Russian)

Résumés by S. C. Goddard

An Investigation of the Hardening of a Color Positive Film during Processing

N. I. Kirillov, N. I. Ermolaeva, L. K. Krupenin, and N. E. Kirillova, pp. 81–86

Hardening of an Agfa (Wolfen) color positive film before processing was compared with hardening produced by a hardening fixing solution, processing being of the NIKFI type (*Uspekhi Nauch. Fotografii*, **4:** 155 (1955)). In addition to melting temperatures (actually temperatures at which one layer begins to slide on the layer under it), the influence of hardening on the spectral absorptions of the dyes and on sensitometric properties of the film was studied. Both forms of hardening gave a satisfactory rise in melting temperature with no significant effect on photographic properties; preliminary hardening gave the better results, but the use of a hardening fixing bath during processing is simpler.

The Action of Slow Electrons on Photographic Emulsions: II—The Change in the Relation between Density and Electron Energy in the Aging of X-Ray Films

V. V. Krachko, pp. 87–91

Part I (*Zhur. Nauch. i Priklad. Fotografii i Kinematografii*, **5:** 34 (1960)) showed that 2× [presumably a Russian type], Agfa Laue, and Agfa Texo radiographic films were sensitive to electrons with energies down to 2 ev, and that, among other findings, the curve of density against the energy of the electrons shows a minimum at 12 ev. Experiments on naturally aged films have now shown a range of maxima and minima of density at energies of 7.5, 11.5, 26, and 35 ev, with a $\pm 10\%$ variation. Within the experimental error, these values coincide with ionization potentials of free atoms and ions of bromine and silver. Sensitization of aged films (Agfa Laue) with triethanolamine does not alter the positions of the maxima and minima, but leads to a considerable increase in density for 20 and 35 ev. Triethanolamine-sensitized MR (NIKFI) film showed a boundary to sensitivity at 36 ev.

The Sensitization Spectra of Dicarbocyanine Dyes

E. B. Lifshits and S. V. Natanson, pp. 92–96, 2 plates

Spectral sensitization spectra have been obtained for a negative silver iodobromide emulsion (3 mole % AgI) sensitized with symmetrical and unsymmetrical carbocyanine dyes. Wedge spectra and absorption curves are reproduced. The dicarbocyanines studied showed a marked tendency to the formation of J-aggregates on the silver halide surface, as well as to enter into the H-state. Hence the dicarbocyanines do not differ in principle, in respect of absorption spectra in emulsion layers and sensitization spectra, from the corresponding dyes with a shorter polymethine chain.

A Study of the Temperature Dependence of Photographic Development: VII—The Dependence of the Activation Energy on the Exposure and the Length of Development

V. I. Sheberstov, pp. 97–101

An ammoniacal silver iodobromide emulsion (2 mole % AgI) was divided into portions given different times of digestion. The activation energy (E) of development of these emulsions was determined for a range of exposures and times of development. The data tabulated show that for development to small densities E_i (image development) generally falls, and often gradually rises again with longer development. For fog development, E_f rises with increase in time of development, except for the emulsion given a long (10-hr) digestion, for which E_f fell for short development times. Increase in exposure causes E to fall. The changes in E are in general such as might be expected from the knowledge that different classes of grains begin to develop at different times, but further elaboration is required to explain all the results. E falls with increased time of digestion up to 6 hr, but rises again for 10-hr digestion. This is ascribed to the desensitization of emulsion grains with prolonged digestion. The significance of the results for the understanding of the mechanism is discussed.

The Determination of the Accuracy of Quantitative Interpretation of a Motion-Picture Film

A. A. KUKIBNYĬ, pp. 102–107

In the quantitative interpretation of the frames of a motion-picture film, it is not possible to avoid either the smoothing out of the calculated results in space and time or errors in observation of the magnitude being measured. By means of an analytical mathematical method, an estimation can be made of the accuracy of the results of calculation of magnitudes, depending on the assumed smoothing out in time and space and the errors of observation of linear magnitudes. The length of the time interval taken for averaging has an influence on the accuracy of the treatment of the results of the investigation: the smaller the period of averaging, the higher the accuracy of the calculation of the magnitudes to be determined. Errors due to smoothing-out in space are reduced in the case in which the sighting plane is a plane of symmetry of the motions of the bodies, and the planes of their motions are not significantly inclined to the sighting plane of the objective of the motion-picture camera. — (*Translation of author's abstract*)

The Optical Sensitization of the Internal Photoelectric Effect in Silver Bromide by Organic Dyes

I. A. AKIMOV AND A. N. TERENIN, pp. 108–116

Experiments are reported which show that the photocurrent in silver bromide is carried by electrons in a perfect crystal, but by positive holes when lattice imperfections are introduced. The contact potentials of semiconductors and dyes have been measured against palladium by a method described earlier by the authors, and the results are tabulated for layers of silver bromide and thallium iodide and for various dyes. Work functions and electron affinities have been deduced from the data. Contact potentials are influenced by light, and are shown to be sensitive to light of wavelengths lying in the absorption region of the dye. Absorption spectra and absorption integrals have been obtained for Rhodamine B and 1,1′-diethyl-3,3,3′,3′,-tetramethylindocarbocyanine iodide in solution and adsorbed on silver halide sols.

The results are taken to confirm generally held ideas on the mechanism of the sensitization of the internal photoeffects, the results being more readily explicable by the transfer of energy from the dye to the semiconductor than by the transfer of electrons.

The Formulation of Compensating Developers

S. G. BOGDANOV, pp. 117–124

The oxidation-reduction conditions existing in compensating developers are analysed from a theoretical point of view and the behavior of an experimental developer and the Kodak developers D-19 and D-76 are studied experimentally. It is concluded that developers intended to give high emulsion speed with development to a comparatively low gamma should possess a small redox buffer capacity, a high negative redox potential and, as far as possible, a low concentration of potassium bromide. The more positive the redox potential, the smaller should be the bromide content. The thickness of the emulsion layer being processed also needs to be taken into account: the thinner the layer and the smaller its photometric equivalent, the smaller should be the redox buffer capacity of the developer.

Points in the Kinetics of Color Development

V. I. USPENSKIĬ AND N. I. RODIONOVA, pp. 125–129

When a leuco-base is formed as the dye-intermediate in color development of gelatin silver bromide layers containing nondiffusing color couplers, linear relations are found between the density or gamma of the dye image and the duration of development for all concentrations of the couplers, including relatively small concentrations. The growth of silver density is expressed, as usual, by a curve with a gradually decreasing gradient. The explanation given for this type of kinetics of development of a color image is that no lowering of the covering power of the dyes occurs on prolonged development, whereas the photometric equivalent of the silver alters in the appropriate manner. For couplers which do not give rise to leuco-bases during the formation of the dye, the kinetics of development of the dye image show for most cases a slowing-down with prolongation of development, and in this respect are similar to the kinetics of black-and-white development. — (*Based on authors' abstract*)

The Theory of the Threshold Characteristics of Photographic Apparatus: IV—The Reproduction of Detail in the Form of Separate Streaks of any Width and of any Contrast with the Field by Means of a Combination of an Optical System and a Photographic Layer

L. P. MOROZ, pp. 130–138

Equations are obtained which allow solutions of the problem of finding the necessary [threshold] values of the parameters which characterize the optical system of the apparatus and the grainy layer [image receiver], and the parameters which characterize the subject; and also of the problem of compensating for changes in some parameters by changes in the others. A suggestion is made for a method of evaluating the quality of apparatus working on the principle of optical image formation. — (*Translation of author's abstract*)

The Influence of Polyethyleneglycols on the Speed of Photographic Emulsions

A. M. CHURAEVA AND A. I. RYBNIKOVA, pp. 139–140

Polyethyleneglycols were prepared with the general formula $HO(CH_2CH_2O)_nH$ (n = 3 to 100) and molecular weights ranging from 150 to 4420, and were added to a high-speed gold-sensitized ammoniacal emulsion, spectrally sensitized with a 5,5′-disubstituted 9-ethylthiacarbocyanine, just before coating. The speed of the emulsion increased markedly as n passed through the region 10–20, and continued to rise as n increased. The presence of the polyethyleneglycols also increased the rate of development; the maximum speed was the same as for a control emulsion, but was reached in a shorter time of development. Studies on a digestion series show that the polymers only affect the speed when the emulsion has not been digested to its optimum speed. The action of polyethyleneglycols is explained by their adsorption to the silver halide grains with displacement of the gelatin.

The Reciprocity-Failure Phenomenon in the Photographic Action of Gamma Radiation

A. L. KARTUZHANSKIĬ, pp. 141–142

Reciprocity-failure curves have been obtained for a lantern-slide plate and an electron-recording plate ex-

posed to β- and γ-radiation from a Co-60 wedge source. The γ-radiation produced a much more marked reciprocity failure than the β-radiation, agreeing with the supposition that the cause of the reciprocity failure is latent-image fading.

The Mechanism of Aging of Infrared Materials

A. S. KHEĬNMAN, pp. 142–143

The work reported in *Zhur. Nauch. i Prikl. Fotografii i Kinematografii*, 5:297 (1960), has been continued. A number of new observations are discussed and are held to confirm the earlier conclusions (changes in sensitivity are to be explained as due to the formation of desensitizers by the oxidation of the sensitizing dye), or at least not to be in contradiction with them.

The Problem of the Choice of the Optimum Parameters in Stereocinematography

N. A. OVSYANNIKOVA AND B. T. IVANOV (Scientific Discussion), pp. 144–145

Answer to the article by N. A. Ovsyannikova and B. T. Ivanov, "The Problem of the Choice of the Optimum Parameters in Stereocinematography"

A. N. SHATSKAYA (Scientific Discussion), pp. 146–148

Nature of the Latent Image Formed by the Action of Light and Charged Particles

K. S. BOGOMOLOV (Review), pp. 149–153

Soviet-Produced Photographic Papers for Printing Documents and Text

M. I. SHOR (Review), pp. 154–159

Trudy Vsesoyuznoĭ Nauchno-Issledovatel'skogo Kinofotoinstituta

No. 35 (1960) (in Russian)

Abstracts translated from Teknika Kino i Televideniya by S. C. Goddard

The Influence of the Gelatin on the Kinetics of Digestion of Photographic Emulsions

V. A. BEKUNOV, pp. 5–13

The influence of gelatins on the kinetics of digestion (chemical ripening) of a photographic emulsion, and also the difference between the gelatins, may be expressed quantitatively by means of the content of sulfur sensitizers, the degree of restraining of the digestion, and the magnitude of the apparent activation energy of digestion.

The Estimation of the Quality and Classification of Gelatin for Its Photographic Properties According to GOST 317-52

V. A. BEKUNOV, pp. 14–28

The principles on which the photographic section of the standard GOST 317-52 on photographic gelatin are based, and the results of an investigation, are presented. The estimation of the quality of gelatins according to the standard is based entirely on the effect of the gelatins on the digestion of a photographic emulsion. An appendix gives a photographic method of testing gelatins.

The Principles of Establishing the Composition of Gelatins

V. A. BEKUNOV, pp. 31–40

The basic principles for establishing the composition of gelatins for the production of photographic emulsions are reviewed, taking into account the evaluation and classification of gelatins for their photographic properties according to the standard GOST 317-52. The aim of the work described was to assist workers in the industry to select gelatins by the characteristics given in the standard for different methods and stages of emulsion making.

The Connection between the Structure and Adsorption of Surface-Active Substances

S. M. LEVI AND O. K. SMIRNOV, pp. 41–53

The use of surface-active substances as wetting agents in emulsion coating is discussed. The experimentally obtained relations between certain adsorption and technological properties and the structure of surface-active agents is discussed for the alkenylsuccinic and alkylphosphinic acids, which are agents of interest to the photographic industry.

The Sedimentation of Photographic Emulsions with the Aid of Inclined Plates

V. L. ZELIKMAN, V. A. DMITRIEVA, AND E. B. KONDRAT'EVA, pp. 54–59

Reported are the results of an investigation of the sedimentation of the photographic emulsion and its use as a method of separating the solid phase of the emulsion after ripening. The construction of the SP-3 prototype laboratory plate sedimenter for the separation of the solid phase of silver halide emulsions is described. The use of a sedimenter of this construction permits a considerable reduction in the area of the tank used to collect the precipitate and allows a number of consecutive sedimentation cycles (7–10 cycles) to be carried out without any intermediate cleaning of the plates.

Reversible Aggregation of an Ultrafine-Grain Emulsion

V. L. ZELIKMAN AND V. A. DMITRIEVA, pp. 60–63

A procedure is described for isolating the solid phase by sedimentation or centrifuging in the preparation of highly dispersed silver bromide emulsions by the reversible aggregation method. Emulsions which have undergone reversible aggregation exhibit normal properties in regard to photographic characteristics, optical sensitization, and keeping qualities.

The Use of a Doctor Blade in Coating Emulsion Layers

B. V. DERYAGIN AND S. M. LEVI, pp. 64–69

Described are: theoretical principles for the use of a doctor blade in coating layers; the construction of a new model of blade; and the results of experimental emulsion coatings at different speeds and with different distances of the blade from the coating trough. The use of doctor blades gives new technical possibilities for thin-layer coating and the coating of normal-viscosity emulsions at increased speeds.

Abstracts of remaining papers, pp. 70–125, from Trudy Vsesoyuz. Nauch.-Issledovatel. Kinofotoinst., *No. 35 (1960), will appear in the next issue of* Photographic Science and Engineering.

PHOTOGRAPHIC SCIENCE AND ENGINEERING
Volume 5, Number 5, September-October 1961

• New Products and Developments

FRANK SMITH

• Cameras and Accessories

Camera-Gard Photographic Protection System

Gard Electronics, Inc., 111 Eighth Ave., New York 11, N.Y., has developed a 16mm microfilm camera which simultaneously photographs a person standing in front of the unit and a dated, coded document placed vertically on the stand, on a single frame of 16mm microfilm, using available light.

The unit has been used to photograph visitors to restricted areas in industrial plants and government installations, as well as to photograph persons cashing checks.

• Illumination

Unilectron Synchronized Submicrosecond Light-Pulse Generator

Unilectron, Inc., Cambridge, Mass., has announced a flash point-source which provides a single high-intensity light pulse with a duration as short as 0.3 μsec.

Fields of application include schlieren and shadowgraph photography, carrier life testing of semiconductors, and ballistic range photography. Four models provide energy levels from 2 to 20 joules, with durations from 0.3 to 1 μsec. Source size ranges from 0.015 to 0.060 in. diameter, depending upon energy level. The light-pulse output can be synchronized with a hypervelocity event, and the opening of Unilectron's "Nanosecond Kerr Cell Shutter."

A synchronizing output pulse, in time phase with the light pulse, is also provided to activate an external device such as a chronograph.

The unit is housed in a cylinder 5 in. in diameter by 12½ in., which acts as a radio-frequency shield, and allows removal of the interior section without disturbing the critical alignment of the point-source.

• Optics

Bausch & Lomb Lens for General Electric X-Ray System

Bausch & Lomb, Inc., Rochester 2, N.Y., has designed a 90mm $f/1.0$ lens for use in General Electric's Fluoricon X-Ray Image Intensifier. This fluoroscopic system uses mirror magnification, closed-circuit television, and motion pictures, to present x-ray images to the diagnostician. The lens picks up the image from a phosphor screen rather than directly from the x-rays, and is designed to photograph in the region of 550 mμ. The five-element design produces greatly increased light transmission and uniformity of screen illumination. One of the features of this lens is the high degree of aberrational correction obtained without resorting to aspheric surfaces.

Although the information contained in this section is compiled from sources believed to be reliable, the author cannot assume responsibility for its accuracy. Publication of the information here is not to be construed as an endorsement or recommendation of the product or equipment described.

• Projection

Minnesota Mining & Mfg. Co. Portable Overhead Projector

An overhead projector which combines portability with all the features of a full-sized standard model has been announced by Minnesota Mining and Manufacturing Co., 900 Bush Ave., St. Paul 6. The projector folds into a single self-contained unit which serves as its own carrying case. The lens and all operating components fold away, affording protection against scratching or rough handling.

The aperture on the projection stage is 10 by 10 in. It is equipped with a 500-w projection lamp and a 14-in. $f/3.5$ lens, weighs 30 lb, and is 14 by 22 by 10 in.

• Radiography

Field Emission Corp. Model 210 Flexitron Flash X-Ray Unit

Field Emission Corp., McMinnville, Ore., has announced a small flash x-ray unit which weighs only 40 lb and occupies less than a cubic foot of space. Despite its small size, the unit has a peak power of 140 million w, and an exposure time of 0.03 μsec. The x-ray tube is housed in a hand-held pistol grip about the size of a 45 automatic, and is connected by a cable to the power source. Thus the bulky tube-support structures of conventional x-ray systems are avoided. Because of the very short exposure time, sharp radiographs are obtained in spite of possible motion of the operator's hand.

The model 210 Flexitron is one of several higher-voltage flash x-ray units which are an outgrowth of basic research on the field-emission electron source at Linfield Research Institute, which is also located in McMinnville.

• Reproduction and Copying

Recordak Reader-Printer

A microfilm reader which automatically makes paper prints of documents on microfilm has been announced by Recordak Corp., 415 Madison Ave., New York 17. The unit operates with 16mm or 35mm film in roll form, in aperture cards, or in card-size film jackets.

Images are enlarged up to clear and sharp readability on the self-contained 11- by 11-in. screen, and the operator merely pushes a button to make within 45 sec a print of the microfilm record projected on the screen.

A variety of lenses is available to provide prints up to 87% of original size, irrespective of the reduction ratio at which the documents are microfilmed. Prints 8½ by 11 in. are delivered cut to size, squeegee dry, from roll paper contained within the reader. The unit can be operated and loaded in normal room light.

Thermo-Fax Visual Communications System

A system which enables a plastic transparency to be made from almost any document in less than 10 sec in

normal light, and projected in a fully lighted room using the Thermo-Fax overhead projector, has been announced by Minnesota Mining and Manufacturing Co., 900 Bush Ave., St. Paul 6.

To make a transparency for projection, the transparency and original document are inserted in a Thermo-Fax copying machine. The image is made in about 4 sec. The process is completely dry; no chemicals or solutions are needed. Originals may be opaque, transparent, or translucent, and may be printed on one or both sides.

The transparencies are permanent and durable and can be filed away for future use. New data can be added to old transparencies by running them through the copying machine at any time.

• Sensitive Materials

Anscochrome FPC-132

Ansco Div., General Aniline and Film Corp., Binghamton, N.Y., has released basic information on the special color film used to photograph Lt. Commander Alan B. Shepard during his space flight in the dimly-lighted Mercury Capsule on May 5, 1961. The 16mm film which was developed specially for the space program is claimed to be the fastest color film yet produced.

The film is daylight type (6000°K), but may be used with tungsten illumination in special cases. Like other color films, the speed of FPC-132 is considerably reduced by the filters required when it is used under artificial light. For this reason, Ansco recommends the use of Super Anscochrome Tungsten type under these conditions.

The FPC-132 film is of moderate grain size, and gradation is similar to that of Super Anscochrome. Resolution is between 45 and 55 lines/mm. Although the film is presently rated at a minimum of ASA 200, Ansco's experiments have indicated that a rating up to ASA 500 is acceptable because of the film's good latitude, without the necessity of forced processing. The film's wide latitude permits exposure variations of $\pm\frac{1}{2}$ stop for full color quality, and up to ± 1 stop for applications where data acquisition is the requirement.

• Miscellaneous

Optical Converter for Three-Dimensional Television

A Stereo-Television Kit which optically converts industrial television to three-dimensional capabilities has been developed by Stereotronics Corp., 1717 N. Highland Ave., Los Angeles. In operation, the scene is viewed by the Stereo-Captor through two physically displaced, adjustable mirror systems which produce two separate images side-by-side on the face of the camera tube. A split Stereo-Screen, with each half polarized at right angles to the other, covers the face of the television monitor. The two images are viewed through polarized stereo-glasses as a single object in three dimensions.

The interobjective distance of 85 mm heightens depth perception for applications such as handling of dangerous materials, environmental studies, and student viewing of medical operations.

Itek Laboratories' "Hermes" Precision Film Reader

Itek Laboratories, Lexington 73, Mass., has announced a film reader designed for the semiautomatic conversion of photographic data to digital form. Measuring three views in sequence from a single platen, the reader provides an accurate and economical method of obtaining quantitative data from photographic films.

The instrument was designed for the analysis of photographs of nuclear tracks in bubble chambers. With minor adaptations, the reader can be used for the reduction of photographic data in other fields, such as astronomy and satellite or missile tracking. Applications can be found wherever precise measurements of the coordinates of lines or points are required from photographic emulsions.

The reader makes measurements as it automatically scans a line or series of points on a photographic emulsion. These measurements are initially read into a buffer storage, from which they can be transferred to punched cards or perforated tape.

A detailed brochure describing the instrument may be obtained from E. D. Phillips, Itek Laboratories, a Division of Itek Corp., 10 Maguire Rd., Lexington 73, Mass.

General Dynamics/Electronics Projection Display for Air Traffic Control

A prototype S-C 2000 Bright Display, for use in air traffic surveillance and control, has been delivered to MITRE Corp. by General Dynamics/Electronics, Information Technology Div., San Diego, Calif. The unit utilizes a small dry processor to store information displayed on the face of a Charactron shaped-beam tube at rates up to 40,000 characters/sec. Less than 2 sec after reception of the data, the information is projected on the screen of the console or on a large theatre-type screen for viewing by a group.

Maps may be displayed concurrently with radar targets and their identifying symbols. In air traffic control, the maps will assist operators in geographic orientation of targets.

Seven-color displays can be produced, giving color differentiation of targets or other information. Data can also be viewed as white against black or black against white.

Westinghouse Ultraviolet-Sensitive Electron Tube

An ultraviolet-sensitive electronic-imaging tube for use in space vehicles has been developed by scientists at the Westinghouse Research Laboratories. Called the Uvicon, the tube was developed for the Astrophysical Observatory of the Smithsonian Institution, Cambridge, Mass., for the Observatory's Project Celescope. Project Celescope is one of several experiments planned for the National Aeronautics and Space Administration's Orbiting Astronomical Observatory program. NASA has announced that the first of the orbiting observatories is planned for 1963.

In operation, the Uvicon tube receives an ultraviolet image through a special lithium fluoride window. The back surface of the window is coated with a material that releases electrons when the ultraviolet image strikes it. These electrons are accelerated by 15,000 v toward the rear end of the tube, where they strike a thin film or target. The impact of the electrons on the target causes it to take on an amplified electrical charge in the exact pattern of the ultraviolet image. The next step is to read off this charge by scanning the rear surface of the target with an electron beam, to produce an electrical signal which can be amplified and broadcast. The overall technique is known as electron-bombardment-induced conductivity.

The Society of Photographic Scientists and Engineers

Box 1609 • Main Post Office • Washington, D.C.

OFFICERS

President	STEVEN LEVINOS, Ansco-Ozalid, Binghamton, N.Y.
First Vice-President	C. E. IVES, Research Laboratories, Eastman Kodak Company, Rochester 4, N.Y.
Western Area Vice-President	JACK C. URBAN, Urban Engineering Co., 6717 Melrose Ave., Hollywood 38, Calif.
Eastern Area Vice-President	WILLIAM S. SHOEMAKER, Rochester Institute of Technology, 65 Plymouth Ave. South, Rochester 8, N.Y.
Conference Vice-President	IRA R. KOHLMAN, LogEtronics Inc., 500 East Monroe Ave., Alexandria, Va.
Science and Engineering Vice-President	FORDYCE M. BROWN, Photomechanisms, Inc., Huntington Station, L.I., N.Y.
Editorial Vice-President	R. CLARK JONES, Polaroid Corporation, 730 Main Street, Cambridge 39, Mass.
Financial Vice-President	ROBERT S. QUACKENBUSH, JR., R.Adm., 2412 North Quincy St., Arlington, Va.
Secretary-Treasurer	FRANCIS J. HEYDEN, S.J., Georgetown College Observatory, Washington 7, D.C.
Executive Secretary	EDWARD S. COBB, Box 1609, Main Post Office, Washington, D.C.

CHAPTERS *and* CHAPTER OFFICERS

Binghamton, New York	*President*	FRANCIS H. GERHARDT, 771 River Rd., Chenango Bridge, N.Y.
	Secretary	CHARLES M. WHITTEMORE, 3122 Malverne Rd. Endwell, N.Y.
Boston, Massachusetts	*President*	JOHN B. TAYLOR, 290 Davis Rd., Bedford, Mass.
	Secretary	ROBERT J. KOHLER, Itek Corp., 10 Maguire Rd., Lexington, Mass.
Chicago, Illinois	*President*	JOSEPH HARANT, 4838 W. 24th St., Cicero 50, Ill.
	Secretary	JOSEPH G. SMAJO, Vogue Wright Studios, 469 E. Ohio St., Chicago 11, Ill.
Cleveland, Ohio	*President*	ROGER FERRYMAN, Metal Photo Corp., 6811 Superior Ave., Cleveland 3, Ohio
	Secretary	JOHN J. SPROSTY, Preformed Line Products Co., 5310 St. Clair Ave., Cleveland 3, Ohio
Monmouth, New Jersey	*President*	D. L. CASTELLINI, 98 Leland Terrace, New Shrewsbury, N.J.
	Secretary	MISS MARILYN LEVY, 100 McLaren St., Red Bank, N.J
New York, New York	*President*	HENRY CROIX, Industrial Photo Products, Inc., 86 Worth St., New York 13, N.Y.
	Secretary	REUBEN SIEGEL, 1776 Union St., Brooklyn 13, N.Y.
Northern California	*President*	J. KENNETH CORNELL, 2331 Ross Rd., Palo Alto, Calif.
	Secretary	JAMES B. BELL, Jr., Ansco, 206 Utah Ave., South San Francisco, Calif.
Rochester, New York	*President*	JOHN D. HAYES, Bausch & Lomb, Inc., St. Paul St., Rochester 2, N.Y.
	Secretary	WOODLIEF THOMAS, JR., Color Technology Division, Eastman Kodak Company, Rochester 4, N.Y.
Southern California	*President*	GEORGE W. BOEMLER, 22632 Collins St., Woodland Hills, Calif.
	Secretary	GEORGE FUKASAWA, 18809 Citrus Edge, Azusa, Calif.
Washington, D.C.	*President*	CALVIN S. McCAMY, 5004 Bangor Dr., Kensington, Md.
	Secretary	WALTER E. SHEA, Eastman Kodak Company, 1000 Connecticut Ave., N.W., Washington 6, D.C.

Sustaining Members / Society of Photographic Scientists and Engineers

Ansco Division, General Aniline & Film Corporation
Binghamton, New York

Atkinson Laboratory, Incorporated
Hollywood 38, California

Atlantic Gelatin, Div. General Foods Corporation
Woburn, Massachusetts

Bausch & Lomb Incorporated
Rochester 2, New York

Bell & Howell Company
Chicago 45, Illinois

Bulova Watch Company, Inc., Photographic Division
Woodside 77, New York

Burke & James, Incorporated
Chicago 4, Illinois

Byron Motion Pictures, Incorporated
Washington 7, D.C.

Chicago Aerial Industries, Incorporated
Barrington, Illinois

Consolidated Film Industries
Hollywood 38, California

DeJur-Amsco Corporation
Long Island City 1, New York

E. I. du Pont de Nemours & Company
Parlin, New Jersey

Eastman Kodak Company
Rochester 4, New York

Edgerton, Germeshausen & Grier, Incorporated
Boston 15, Massachusetts

Elgeet Optical Company, Incorporated
Rochester 6, New York

Fairchild Camera & Instrument Corporation
Syosset, Long Island, New York

FMA, Incorporated
El Segundo, California

The FR Corporation
New York 51, New York

General Electric Company
Schenectady, New York

General Film Laboratories
Hollywood 28, California

Graflex, Incorporated
Rochester, 3, New York

W. & L. E. Gurley
Troy, New York

Hardale Associates
New York 22, New York

Hi-Speed Equipment, Incorporated
Waltham 54, Massachusetts

Houston Fearless Corporation
Los Angeles 64, California

Charles A. Hulcher Company, Incorporated
Hampton, Virginia

Philip A. Hunt Company
Palisades Park, New Jersey

Hycon Manufacturing Company
Monrovia, California

Itek Laboratories, Division of Itek Corporation
Lexington 73, Massachusetts

The Kalart Company, Incorporated
Plainville, Connecticut

Kollmorgen Corporation
Northampton, Massachusetts

LogEtronics Incorporated
Alexandria, Virginia

J. A. Maurer, Incorporated
Long Island City 1, New York

The Morse Instrument Company
Hudson, Ohio

North American Aviation, Incorporated
Los Angeles 45, California

Pako Corporation
Minneapolis 40, Minnesota

The Pavelle Corporation
New York 20, New York

Photogrammetry, Incorporated
Rockville, Maryland

Photomechanisms, Incorporated
Huntington Station, Long Island, New York

Polaroid Corporation
Cambridge 39, Massachusetts

Rolor Industrial Corporation
New York 17, New York

Simmon Brothers, Incorporated
Long Island City 1, New York

Wollensak Optical Company
Rochester 21, New York

Xerox Corporation
Rochester 3, New York

Zoomar, Incorporated
Glen Cove, New York